AD_____

Award Number: W81XWH-11-1-0510

TITLE: Early Detection of Ovarian Cancer by Molecular Targeted Ultrasound Imaging Together with Serum Markers of Tumor-Associated Nuclear Change and Angiogenesis

PRINCIPAL INVESTIGATOR: Animesh Barua, Ph.D.

CONTRACTING ORGANIZATION: Rush University Medical Center
Chicago, IL 60612

REPORT DATE: March 2014

TYPE OF REPORT: Final

PREPARED FOR: U.S. Army Medical Research and Materiel Command
Fort Detrick, Maryland 21702-5012

DISTRIBUTION STATEMENT: Approved for Public Release;
Distribution Unlimited

The views, opinions and/or findings contained in this report are those of the author(s) and should not be construed as an official Department of the Army position, policy or decision unless so designated by other documentation.

REPORT DOCUMENTATION PAGE

Form Approved
OMB No. 0704-0188

Public reporting burden for this collection of information is estimated to average 1 hour per response, including the time for reviewing instructions, searching existing data sources, gathering and maintaining the data needed, and completing and reviewing this collection of information. Send comments regarding this burden estimate or any other aspect of this collection of information, including suggestions for reducing this burden to Department of Defense, Washington Headquarters Services, Directorate for Information Operations and Reports (0704-0188), 1215 Jefferson Davis Highway, Suite 1204, Arlington, VA 22202-4302. Respondents should be aware that notwithstanding any other provision of law, no person shall be subject to any penalty for failing to comply with a collection of information if it does not display a currently valid OMB control number. **PLEASE DO NOT RETURN YOUR FORM TO THE ABOVE ADDRESS.**

1. REPORT DATE	2. REPORT TYPE	3. DATES COVERED
March 2014	Final	30 September 2011 - 29 December 2013

4. TITLE AND SUBTITLE
Early Detection of Ovarian Cancer by Molecular Targeted Ultrasound Imaging Together with Serum Markers of Tumor-Associated Nuclear Change and Angiogenesis

5a. CONTRACT NUMBER

5b. GRANT NUMBER
W81XWH-11-1-0510

5c. PROGRAM ELEMENT NUMBER

6. AUTHOR(S)
Animesh Barua, Ph.D.

E-Mail: Animesh_Barua@rush.edu

5d. PROJECT NUMBER

5e. TASK NUMBER

5f. WORK UNIT NUMBER

7. PERFORMING ORGANIZATION NAME(S) AND ADDRESS(ES)
Rush University Medical Center,
Chicago, IL 60612

8. PERFORMING ORGANIZATION REPORT NUMBER

9. SPONSORING / MONITORING AGENCY NAME(S) AND ADDRESS(ES)
U.S. Army Medical Research and Materiel Command
Fort Detrick, Maryland 21702-5012

10. SPONSOR/MONITOR'S ACRONYM(S)

11. SPONSOR/MONITOR'S REPORT NUMBER(S)

12. DISTRIBUTION / AVAILABILITY STATEMENT
Approved for Public Release; Distribution Unlimited

13. SUPPLEMENTARY NOTES

14. ABSTRACT:
Overall goal of this study was to examine the feasibility of vascular endothelial growth factor receptor -2 (VEGFR-2)-targeted ultrasound molecular imaging for the detection of spontaneous ovarian cancer (OVCA) at early stage in association with serum anti-nuclear matrix protein (anti-NMP) antibodies (a marker of ovarian malignant transformation) and serum IL-16 levels (a marker of ovarian tumor-associated neoangiogenesis, TAN). This goal was realized by two specific aims. The results of this study showed that VEGFR-2-targeted ultrasound molecular imaging agent bound with its target expressed by ovarian tumors and enhanced the signal intensity of ultrasound imaging. This study also showed that serum prevalence of anti-NMP antibodies and levels of IL-16 increased in association with ovarian malignant transformation and OVCA development. Furthermore, tumor-associated serum IL-16 levels were elevated even before the formation of a solid tumor mass in the ovary. VEGFR-2-targeted molecular ultrasound imaging together with serum anti-NMP antibodies and IL-16 levels, improved early detection of OVCA and detected ovarian tumors when it is limited to a part of the ovary. Thus VEGFR-2-targeted imaging agents showed potential to be a feasible imaging agent for early OVCA detection. Additionally, laying hens offer a feasible preclinical model to develop OVCA-preventive anti-angiogenic therapeutics targeting VEGFR-2 expressed by tumor associated microvessels.

15. SUBJECT TERMS :
Ovarian cancer, Early detection, Ultrasound molecular imaging, VEGFR-2, animal model

16. SECURITY CLASSIFICATION OF:			17. LIMITATION OF ABSTRACT	18. NUMBER OF PAGES	19a. NAME OF RESPONSIBLE PERSON
a. REPORT	b. ABSTRACT	c. THIS PAGE			USAMRMC
U	U	U	UU	85	19b. TELEPHONE NUMBER *(include area code)*

Table of Contents

Page

INTRODUCTION:

Ovarian cancer (OVCA) is the leading cause of death of women due to gynecological cancers[1]. While the survival rates of OVCA patients are remarkably high if the disease is detected at early stage (>80%), most cases of OVCA are diagnosed at late stages when the likelihood of successful therapy is very low[2]. Non-specificity of symptoms at early stage and the lack of an effective and specific early detection test make early detection of OVCA very difficult. Serum levels of CA-125 and traditional transvaginal ultrasound (TVUS) scanning are the currently available tests for the detection of OVCA. A combination of CA-125 and TVUS scanning failed to effectively detect OVCA at early stage as circulating levels of CA-125 are non-specific to early OVCA and traditional TVUS scanning cannot detect early OVCA related changes in the ovary[3]. ***Thus a fresh approach is needed***. Malignant nuclear transformation and tumor associated neoangiogenesis (TAN) are two of the earliest events in tumor initiation and development. During malignant transformation, the nuclei of cells undergo profound morphological changes in size and shape together with rearrangements in nuclear matrix proteins (NMPs). As a result, NMPs are shed into the circulation, in response to which the immune system produces anti-NMP antibodies. These NMPs and their corresponding anti-NMP antibodies are tissue specific[4]. Malignant nuclear transformation is followed by ovarian TAN. Development of angiogenic microvessels is the characteristic feature of ovarian TAN. These microvessels express vascular endothelial growth factor receptor-2 (VEGFR-2) which is an accepted marker of angiogenesis. Serum anti-NMP antibodies and VEGFR-2 expressed by TAN vessels in the ovary represent potential markers for early ovarian tumor related changes. Thus, serum anti-NMP antibodies and VEGFR-2 can be detected by serum analysis and by *in vivo* imaging, respectively, if an *in vivo* imaging probe can be developed. Although traditional Doppler ultrasound (DUS) scanning detects ovarian vascular structures, its limited resolution cannot detect early stage OVCA related ovarian TAN vessels. Our long term goal is to improve the detectability of ovarian TAN vessels at early stage OVCA by contrast enhanced VEGFR-2-targeted ultrasound molecular imaging. Due to the difficulty in identifying patients with early stage OVCA, we used laying hen model of spontaneous OVCA [5, 6] in this study.

BODY: the research accomplishments associated with each task outlined in the approved Statement of Work (SOW).

The overall ***hypothesis*** of this project is that *early stage OVCA lesions can be detected in laying hens using VEGFR-2 targeted contrast enhanced ultrasound imaging in association with anti-NMP antibodies and serum levels of IL-16.* This hypothesis was tested by two specific aims: 1) Molecular targeted-ultrasound imaging will differentiate hens with early stage OVCA from hens with normal ovaries. 2) VEGFR-2-targeted ultrasound acoustic indices (AI) and TAN indices (TI) established in Aim 1 will detect ovarian TAN in hens with anti-NMP antibodies.

1. **Task 1. Molecular targeted-ultrasound imaging of hen ovarian tumors and tumor associated neoangiogenesis (TAN)**

1a. Scanning of 150 hens to detect ovarian tumor associated abnormalities.

i) Molecular imaging probes containing VEGFR-2-targeted microbubbles were supplied by Targeson, Inc., San Diego, CA.

ii) Detection of ovarian tumors by molecular imaging using molecular probes containing VEGFR-2-targeted microbubbles with gray scale ultrasound scanning;

iii) Detection of ovarian tumor associated microvessels (TAN vessels) by contrast enhanced Doppler ultrasound (DUS) imaging.

iv) Blood was collected from the brachial vein of each hen before ultrasound scan, serum was separated and aliquots were stored at -80^{0}C until further use;

v) Following ultrasound scanning, hens were sacrificed, presence of OVCA and its stages were diagnosed, ovaries with or without tumors and other relevant tissues were harvested, processed for paraffin, frozen, proteomic and molecular biological studies.

1b. Ovarian histopathology and immunohistochemical studies

i) Histopathological diagnosis of OVCA: representative paraffin sections of 5μm thick from ovaries with or without gross tumors were made, stained with hematoxylin & eosin and examined under a light microscope. Presence of ovarian carcinoma on the sections and their histological types were determined.

ii) Paraffin sections were examined for immunohistochemical determination of VEGFR-2 and smooth muscle actin (SMA) expressing angiogenic microvessels using anti-chicken VEGFR2 and anti-SMA antibodies. Similarly, immunopositive CD8 T cell and IL-16 expressing cells/vessels were determined in frozen sections by anti-Chicken CD8 and anti-chicken IL-16 antibodies.

iii) Immunostained sections were examined, the frequencies of immunopositive CD 8+ T and IL-16 cells were determined, correlation between the frequencies of immunopositive cells (markers of ovarian TAN) and tumor stages and tumor sub-types was determined.

1c. Biochemical and molecular biological as well as processing of archived ultrasound imaging data.

i) Serum prevalence of anti-NMP antibodies and circulatory levels of IL-16 in hens with or without ovarian tumors were determined by immunoassay.

ii) Gene expression of IL-16 by normal and tumor bearing hen ovarian tissues was determined by semi-quantitative RT-PCR using chicken IL-16 primers.

iii) Archived pre- and post-targeted ultrasound images were reviewed and analyzed off-line and contrast parameters or imaging indices detective of early stage OVCA were determined with reference to gross and histopathological observations.

iv) Correlation among the molecular targeted imaging parameters and serum anti-NMP antibody status as well as IL-16 levels detective of OVCA at early stage were examined.

Task 1 milestone: Indices for early stage OVCA comprising molecular targeted ultrasound imaging parameters in association with serum anti-NMP antibodies and IL-16 levels were established.

1.1. Detailed Reports on the Accomplishments related to Task 1 (Year-1 of the project life):

Task 1 included the implementation of specific aim 1:

Specific Aim 1: Molecular targeted-ultrasound imaging will differentiate hens with early stage OVCA from hens with normal ovaries.

Animals:

150 White Leghorn hens (3-year old) with low egg laying rates, (<125eggs/year) and 40 hens with normal egg laying rates (>250eggs/year) were selected from a flock of laying hens. In the first study, an additional 20 hens were selected and divided into two groups (10 hens each) and injected with non-targeted microbubbles or Optison^{TM} and compared with those injected with VEGFR-2 targeted microbubbles. The binding specificity of VEGFR-2-targeted microbubbles was determined and a dose of 10uL/kg body weight was found to be optimal. In the subsequent study, selected hens were injected with 10uL/kg body weight of VEGFR-2-targeted microbubbles via the left brachial vein. All selected hens were reared under identical environmental conditions and provided with food and water *ad libitum*.

Serum collection: Blood from all hens was collected prior to ultrasound imaging and sera were obtained and aliquots were stored at -80 °C for later use.

Molecular (VEGFR-2)-targeted contrast enhanced imaging: *Sonography and Image Analysis*

Pre-targeted imaging: Ultrasound imaging was performed before the injection of VEGFR-2-targeted microbubbles with the mechanical set up reported previously [7, 8]. Briefly, all hens were scanned using an instrument equipped with a 5- to 7.5-MHz endovaginal transducer (MicroMaxx; SonoSite, Inc, Bothell, WA). Following immobilization of each hen, the transducer was inserted transvaginally and 2-dimensional (2D) transvaginal gray scale and pulsed Doppler sonographies were performed. Ovarian morphology was examined by gray scale sonography while ovarian vasculature was examined by DUS imaging. DUS imaging indices including the resistive index (RI: [systolic velocity – diastolic velocity]/systolic velocity) and the pulsatility index (PI: [systolic velocity – diastolic velocity]/mean) were automatically calculated from at least two separate images from the same ovary.The lower RI and PI values were used for analysis. All images were processed and digitally archived.

VEGFR-2 targeted imaging:

VEGFR-2-Targeted imaging was performed following the injection of ovarian VEGFR-2-targeted microbubbles in a similar manner as described earlier [9, 10] and the same pre-targeted area was included in imaging according to the instruction of the manufacturer of the targeted agent and earlier report [7, 9, 10].

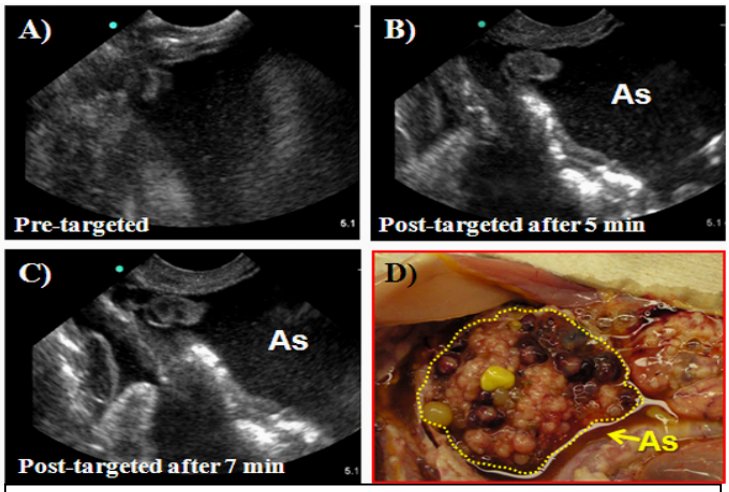

Figure 1. ***Proof-of- principle***: VEGFR-2-targeted imaging agents enhanced ultrasound imaging signals from their targets in the ovary. A) Pre-contrast gray scale ultrasound image of a hen ovary suspected to have tumor. Intensity of the signals from the tissue is very low. B) Gray scale image of the same ovary 5min after the injection of VEGRF-2 targeted imaging agent. Compared with pre-targeted, signal intensity from the tissue was enhanced remarkably (appears like a white triangular-shaped island of solid mass). C) Gray scale image of the same ovary 7min after the injection of targeted imaging agent showing larger tumor mass with enhanced signal intensity. D) Gross ovarian tumor (dotted line) in the hen scanned in A-C confirming the prediction of targeted ultrasound molecular imaging. As = ascitic fluid.

Within 5-7 min from the arrival, targeted microbubbles were accumulated at the target sites and unbound free microbubbles were washed out. All images were archived digitally in a still format as well as in real-time clips (15 minutes for each hen). The effects of targeted microbubbles were visually evaluated online during the scanning examination and off-line afterward by reviewing the archived still images and video clips. The time of contrast agent arrival (interval in seconds from administration of the contrast agent to its visual observation [in seconds]) in the ovaries with or without tumor was recorded in real time. After review of the complete clip, the region of interest (ROI) was selected. The average image intensity (in pixel values) over a ROI encompassing the tumor was calculated using a computer assisted software (Microsuite^{TM} version Five, Olympus America, Inc., Canter Valley, PA) and compared with the intensity of the pre-targeted imaging of the same ROI. The pixel intensities of ROI predictive of OVCA were determined. In addition, RI and PI values from post-targeted imaging were calculated.

Result: Representative molecular targeted ultrasonograms of a suspected ovarian tumor in a hen before and after the injection of VEGFR-2-targeted microbubbles are shown in **Figure 1** (Gray scale, showing tumor). Large preovulatory follicles together with several small growing follicles were seen during the ultrasound imaging in normal ovaries in healthy hens (n = 20 selected hens). Compared with pre-targeted scanning, VEGFR-2-targeted imaging enhanced the visualization of solid masses in the ovaries of 26 hens on gray scale and these hens were "suspected to have

ovarian malignant tumors" (**Figure 1A-D**). Overall, in contrast to the pre-targeted scan, the pixel intensities of the signals from normal ovaries or ovaries with tumor increased significantly after the injection of VEGFR-2-targeted microbubbles. The mean signal intensity of VEGFR-2-targeted ovarian sonograms for healthy hens was 60352.00 ± 21259.33 (mean ± SD) pixels and it was significantly higher in hens in which tumor masses limited to a part of the ovaries (early stage) 104479.80 ± 28295.62 (mean ± SD) pixels. The signal intensities increased further in hens with large solid ovarian masses accompanied with profuse ascites and predicted to have late stage OVCA, 112989 ± 13373.19 (mean ± SD) pixels. Blood vessels were detected in the ovarian stroma by color Doppler ultrasound imaging. The mean pre-targeted RI values for hens with normal, with small or large ovarian masses were 0.58 ± 0.12, 0.56 ± 0.11and 0.40 ± 0.04, respectively. The RI values were found to be decreased in all hens to 0.47 ± 0.12 (normal), 0.43 ± 0.08 (early stage) and 0.33 ± 0.05 (late stage), respectively, in post-targeted color Doppler ultrasound imaging. Similar patterns were also observed for PI values.

Ovarian histopathology and immunohistochemical studies:

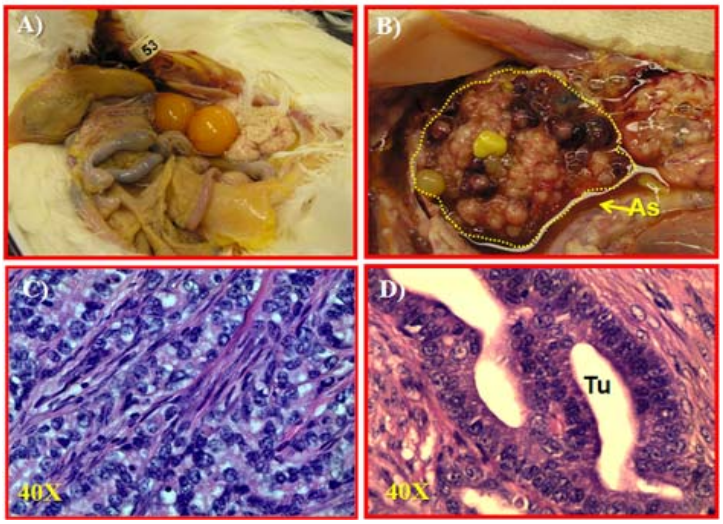

Figure 2. Confirmation of predictions of ovarian malignant tumors by VEGFR-2-targeted ultrasound molecular imaging. A) A normal ovary in an old laying hen with low egg laying rates. The ovary had two developing pre-ovulatory follicles as opposed to 5-6 follicles seen in a younger laying hen with normal egg laying rates. B) An ovarian tumor at late stage in a laying hen. The tumor appears like a cauliflower. C-D) Examples of histological types of malignant ovarian tumors in hens detected in this study. C) Serous ovarian tumor appears like a sheet of malignant cells with pleomorphic nuclei surrounded by fibromuscular layer. D) An endometrioid ovarian tumor showing back to back tumor glands (Tu) resembling those seen in endometrium with a single layer of epithelial cells and sharp luminal lining. Dotted line shows the tumor. Tu= tumor40X.

Following VEGFR-2-targeted imaging, all hens were euthanized and sonographic predictions were confirmed by gross examination of hens at necropsy. Gross morphology including the presence of ovarian follicles, atrophied ovaries and oviducts, presence of solid tumor mass in the ovary, extent of tumor metastasis, stages of OVCA and accompanying ascites, was recorded. Normal ovaries and ovaries with tumor together with other relevant tissues including oviducts were harvested and processed for paraffin, frozen, proteomic and molecular biological studies. Ovarian tumors and their types were confirmed by routine histological examination with hematoxylin-eosin staining (**Figure 2A-D**). Staging of ovarian tumors was performed as reported previously [6]. As predicted by sonographic examinations, late stage OVCA (n = 18 hens including 7 serous, 9 endometrioid, 2 mucinous) was accompanied with moderate to profuse ascites and metastasized to peritoneal and abdominal organs. In early stage OVCA (n = 8 including 3 serous, 4 endometrioid, 1mucinous) tumors were limited to the ovary with no or very little ascites. In addition, histological examinations confirmed the presence of microscopic ovarian carcinoma in 6 hens (3 serous and 3 endometrioid) that had no detectable ovarian mass during VEGFR-2-targeted imaging as well as at gross examination. Thus the total number of hens with early stage OVCA was (8 + 6) = 14.

Immunohistochemical detection of ovarian tumor associated neo-angiogenic (TAN) markers:
Sections of normal ovaries or ovaries with tumor were immunostained for the detection of VEGFR-2+, SMA+, IL-16+ and CD8+ T cells using specific antibodies and the frequencies of the immunopositive vessels or cells were counted and analyzed as reported previously[11-13]. Differences in the frequency of immunopositive microvessels or cells between normal and hens with OVCA were considered significant when the $P < 0.05$.

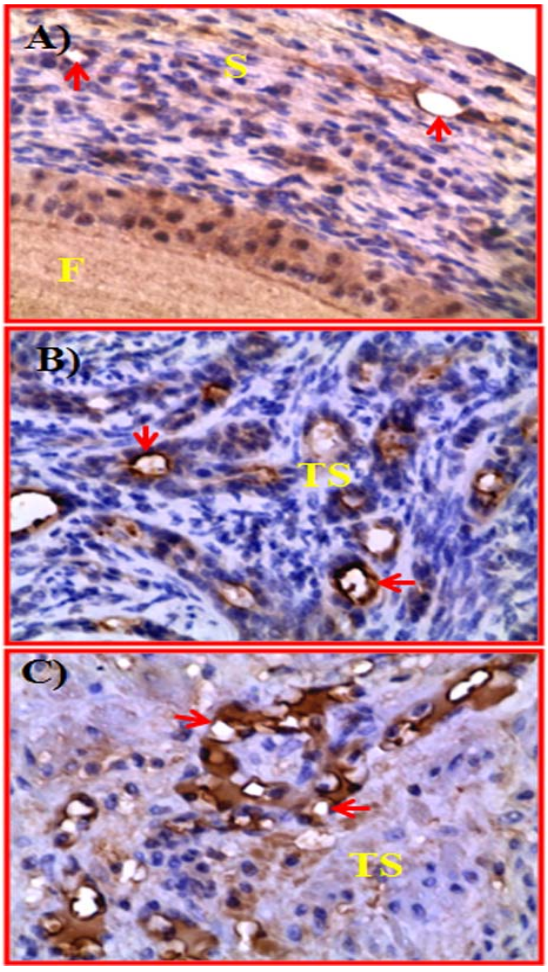

Figure 3. Detection of VEGFR-2 expressing microvessels in a normal ovary or ovaries with tumors in hens by immunohistochemistry. Sections were immunostained with anti-VEGRF-2 antibodies. Microvessels expressing VEGFR-2 appeared to be immature and leaky with incomplete or discontinous smooth muscle layers. Arrows show examples of VEGFR-2-expressing microvessels. A) Very few VEGFR-2 expressing microvessels are seen in the stroma of normal ovary. B-C) Compared with normal ovary (A), more VEGFR-2 expressing microvessels are seen in the stroma of the ovaries with tumor at early (B) and late (C) stages of OVCA. F = stromal follicle, S = stroma, TS = tumor stroma. 40X.

Results: *Morphology of TAN vessels:* VEGFR-2 or SMA-expressing neoangiogenic microvessels were immature and appeared to be leaky with a discontinuous smooth muscle layer surrounding them. *Expression of VEGFR-2 and SMA by TAN vessels:* VEGFR-2 or SMA expressing microvessels were localized at the spaces between tumor glands (tumor vicinity, **Figure 3B-C**). Occasionally ovarian tumor epithelia were also found positive for VEGFR-2 expression. The frequencies of VEGFR-2 expressing microvessels were significantly ($P<0.05$) greater in hens with early stage OVCA (mean $\pm$ SD= 12.8 $\pm$ 2.28 in 20,000μm^2 of tumor tissue) than in normal hens (3.12 $\pm$ 0.94 in 20,000μm^2 of ovarian stromal tissue) and increased further in hens with late stage of OVCA (18.33 $\pm$ 2.38 in 20,000μm^2 of tumor tissue) (**Figure 4**). Similar patterns of changes in the frequencies of SMA-expressing microvessels were also observed. Differences in the frequencies of VEGFR-2 and SMA-expressing microvessels were not observed among different histological sub-types of malignant ovarian tumors in hens. These results support the predictions of VEGFR-2 targeted imaging that VEGFR-2 expressing ovarian

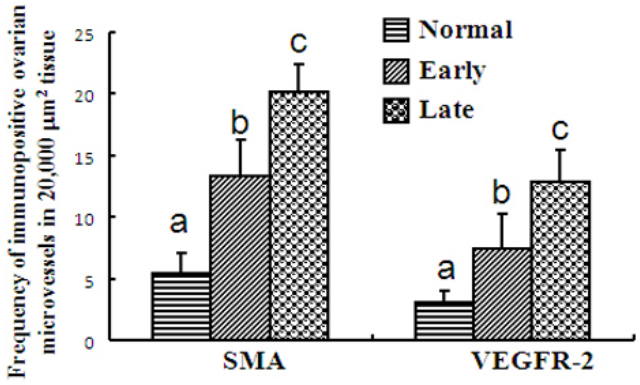

Figure 4. Increase in the frequencies of SMA and VEGFR-2 expressing microvessels in normal ovaries or ovaries with tumors in hens in association with ovarian tumor development and progression. Values are expressed as mean $\pm$ SD. Compared with normal ovaries (n = 15 hens), the frequencies of SMA and VEGFR-2-expressing microvessels were significantly greater in hens with early stage of ovarian cancer (OVCA, n = 14) ($P<0.01$) and increased further in hens with late stage OVCA (n = 18) ($P<0.01$). Patterns of changes in the frequency of SMA-expressing cells are similar to that of VEGFR-2-expressing vessels. Bars with different letters within the same marker group are significantly different.

tumor associated microvessels can be detected *in vivo* and may be used as an imaging probe for the early detection of OVCA.

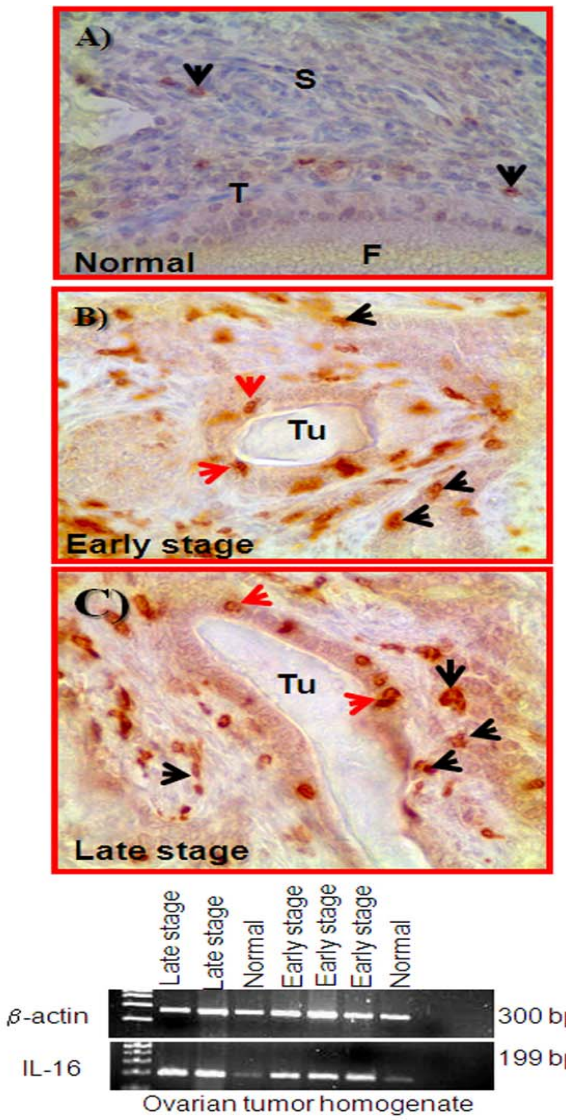

Figure 5. *Upper panel*: Localization of IL-16 expressing cells in the stroma of a normal ovary or ovaries with tumors in hens by immuno-histochemistry. Cells expressing IL-16 are round or irregular shaped and seen in the normal ovarian or tumor stroma (arrows show the examples of IL-16+cells). A) Very few positive cells are seen in the stroma of normal ovary. B-C) IL-16 expression in early (B) and late (C) stages of OVCA in hens. A number of epithelial cells of the tumor also expressed IL-16 (red arrows). Compared with normal (A), more IL-16+ cells are seen in the stroma of the ovaries with tumor. S = ovarian stroma, Tu = tumor gland, 40X. T = theca layer of follicle (F).
Lower panel: IL-16 gene expression: Compared with weak expression by normal ovaries, strong expression of IL-16 mRNA was observed in homogenates from early and late stage OVCA.

Detection of IL-16+ and CD8+ T cells: IL-16 is a chemoattractant and pro-angiogenic cytokine produced by a variety of cells including CD8 T cells. In normal ovaries, very few IL-16-expressing cells were seen in the ovarian stroma and the follicular theca. In contrast, many IL-16 expressing cells were localized in hens with OVCA (**Figure 5**). The population of IL-16-expressing cells was significantly (P<0.05) higher in hens with early stage OVCA (mean + SD= 16.30 ± 3.39in 20,000μm^2 of tumor tissue) than in normal hens (4.86 ± 0.95 in 20,000μm^2 of ovarian stromal tissue) and increased further in hens with late stage of OVCA (20.27 ± 4.58 in 20,000μm^2 of tumor tissue) (**Figure 6**).

CD8+ T cells were localized in the ovarian stroma and the theca layers of the stroma follicles while in ovaries with tumors they were localized in the tumor stroma as well as in close proximity to the tumor glands. A significantly higher frequency of CD8+ T cells was observed in hens with ovarian tumors than in hens with normal ovaries (**Figure 6**). The frequency of CD8+ T cells was 6 .00 ± 1.60 in 20,000μm^2 of ovarian stromal tissue (mean ± SD) in normal ovaries and increased significantly (P<0.05) in hens with early stage (mean ± SD= 24.92 + 6.69 in 20,000 μm^2 of tumor tissue) and late stages (27.07 + 4.52 in 20,000μm^2 of tumor tissue) of OVCA (**Figure 6**). The changes in the frequency of IL-16 positive cells were

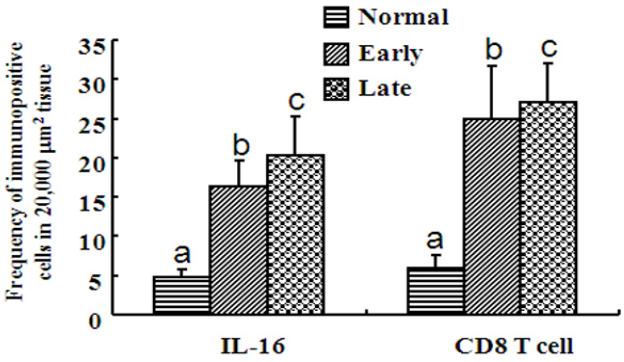

Figure 6. Changes in the frequencies of IL-16 expressing and CD8+ T cells in normal ovaries or ovaries with tumors in hens in association with ovarian tumor development and progression. Values are expressed as mean ± SD. Compared with normal ovaries (n = 15 hens), the frequencies of IL-16 expressing cells and CD8+ T cells were significantly greater in hens with early stage OVCA (n=14) (P<0.01) and increased further in hens with late stage OVCA (n=18) (P<0.05). Patterns of changes in the frequency of IL-16 expressing cells are positively correlated with that of CD8+ T cells. Bars with different letters within the same marker group are significantly different.

positively correlated with the changes in the frequency of CD8+ T cells as the tumor develops and progressed to late stages.

Thus the results of the immunohistochemical studies suggest that the frequencies of IL-16 expressing cells and their precursor (CD8+ T cells) increased in association with tumor development and progression.

Biochemical and molecular biological detection of malignant nuclear transformation and tumor associated neoangiogenesis:

Serum prevalence of anti-NMP antibodies: Nuclear matrix proteins were extracted from normal ovaries and ovaries with tumors as reported previously [4]. 96-well plates were coated with NMPs and the immunoreactivities of serum samples from each hen against the coated normal or ovarian tumor NMPs were determined by immunoassay as reported earlier[14]. Each serum sample was assayed in duplicate and the plates were read at 405nm in an ELISA plate reader (Softmax Pro, version 1.2.0, software; Molecular Devices, Sunnyvale, CA). Serum from young healthy hens with fully functional ovaries was used as negative control (established in a previous study) for the presence of anti-NMP antibodies. Serum with optical density (OD) values higher than the control mean + 2SD (cut-off value) were considered positive for the presence of anti-NMP antibodies.

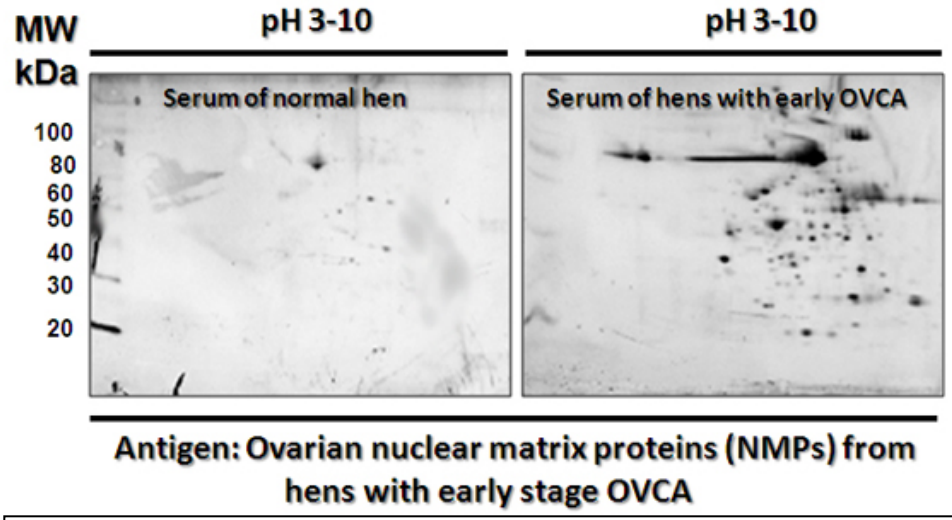

Figure 7. Immunoproteomic (2 dimensional Western blotting, 2D-WB) detection of anti-nuclear matrix protein (NMP) antibodies in the serum of hens with or without ovarian tumors. NMPs from hens with ovarian tumors were blotted in membranes and reacted with the serum of normal or OVCA hens. Compared with normal serum (left panel), OVCA serum reacted specifically against the ovarian tumor NMPs (most reactive antigens are seen approximately at 20-50kD) from OVCA hens.

All hens (n = 32) with OVCA were positive for anti-NMP antibodies while 5 normal hens (7.6%) hens were found positive for anti-NMP antibodies. Immunoreactivity observed in the immunoassay and OVCA specificity of the serum anti-NMP antibodies were tested by 2 dimensional Western blotting (2D-WB) as reported earlier[14]. Serum positive for anti-NMP antibodies from OVCA hens reacted specifically against NMPs from ovarian tumors (**Figure 7**) while very few immunoreactive spots were observed for hens with normal ovaries.

Serum IL-16 levels: IL-16 levels in serum were determined by Chicken IL-16 Vetset^{TM} ELISA Kit (Kingfisher Biotech, St. Paul, MN) pre-coated with anti-Chicken IL-16 antibodies and chicken IL-16 as standards as per the manufacturer's instructions reported earlier[12].The absorbance for each well was recorded by reading the plates at 405nm in a plate reader (Thermomax; Molecular Devices, Sunnyvale, CA). A standard curve was generated by plotting the optical density (OD) values of the standards against their concentrations. Serum IL-16 levels were determined with reference to the standard curve as per manufacturer's instruction using a software program (Softmax Pro, version 1.2.0, software; Molecular Devices, Sunnyvale, CA). All standards and serum samples were run in duplicate.

The mean concentration of serum IL-16 was 230.73 ± 47.01 pg/mL (mean ± SD) in normal hens. Compared with normal hens, the mean concentration of serum IL-16 was significantly higher ($P < 0.0002$) in hens with early (428.36 ± 136.53 pg/mL) and late stages (534.92 ± 204.62 pg/mL) of OVCA (**Figure 8**). However, the differences in serum IL-16 levels were not significant between the early and late stages OVCA as well as among the different histological subtypes of OVCA.

IL-16 mRNA expression by normal ovaries or ovaries with tumor in hens: IL-16 gene expression was assessed by semi-quantitative RT-PCR as reported previously[12, 15] using chicken-specific IL-16 primers designed by Oligoperfect Designer software (Invitrogen, Carlsbad, CA) with the IL-16 sequence from the NCBI (GeneBank: NM_204352.3). The forward primer was 5-TCTCTGCTTTCCCCTGAA-GA and the reverse primer was 5-GTCCATTGGGAAACACCT-TG located between exons 4 and 6. β-actin was used as the endogenous control with a forward primer of TGCGTGACATCAAGGAGAAG and a reverse primer of ATGCCAGGGTACATTGTGGT. The expected base pair size for the IL-16 amplicon was 199 bp and for β-actin was 300 bp. PCR amplicons were visualized in a 3% agarose gel (Pierce/Thermo Fisher, Rockford, IL USA) in TAE buffer and stained with ethidium bromide. The image was captured using a ChemiDoc XRS system (Bio-Rad, Hercules, CA).

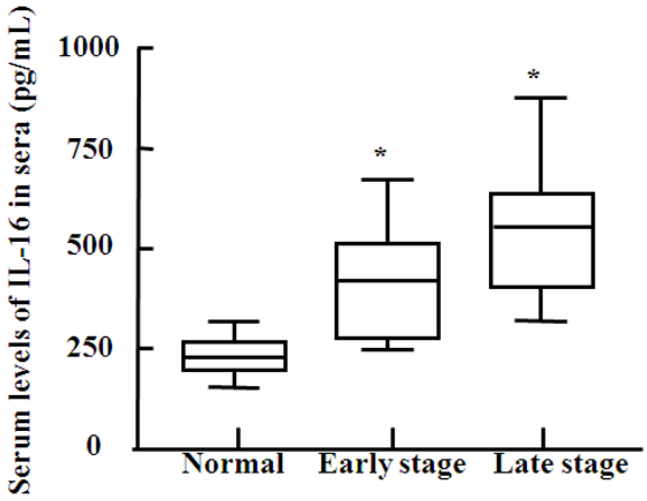

Figure 8. Circulating levels of IL-16 (pg/mL) in hens with or without ovarian cancer (OVCA) displayed as box and whiskers. The median, range (whiskers), and 25th to 75th percentiles (box) are shown. Serum samples from normal hens were used as experimental controls. Compared with normal hens (n = 66), serum IL-16 levels was significantly greater ($P<0.0002$) in hens with early (n = 14) and late (n = 18) stages of OVCA. * denotes significant differences in the serum IL-16 levels between normal hens and hens with OVCA.

IL-16 mRNA expression was weak for ovarian homogenates from normal hens. In contrast, hens with ovarian tumors showed a strong amplification signal for IL-16 (**Figure 5**) and differences were not observed in IL-16 mRNA expression among different histological subtypes of OVCA. Thus, IL-16 mRNA expression confirmed the observed variations in serum IL-16 levels and ovarian expression of IL-16 among normal and OVCA hens.

Ovarian TAN Index (TI): The patterns of tumor associated changes in the frequencies of VEGFR-2 expressing microvessels were found to be similar in OVCA hens irrespective of tumor sub-types. A tumor associated neoangiogenic index indicative of OVCA with reference to histopathology was calculated as: TI = Number of VEGFR-2-expressing microvessels in [tumor ovaries/normal ovaries]. Compared with normal hens, the mean TI for early stage and late stage OVCA was significantly higher (4.26 vs 1.00, $P <0.01$) and (6.26 vs 1.00, $P < 0.01$), respectively. Considering the TI values for normal as 1 (number of VEGFR-2-expressing vessels in normal hens/ number of VEGFR-2-expressing vessels in normal hens), these TI values are higher than 2X of TI of normal hens. In addition, the population of VEGFR-2-expressing microvessels in hens with early stage OVCA (mean + SD = 12.8 + 2.28 in 20,000 μm^2 area) is greater than the 2 X mean of normal hens + 2SD (= 2 X 3.12 + 2X0.94 = 8.12). Thus, it is assumed that the TI for early stage OVCA shown above (4.26) will effectively identify ovarian TAN in early stage OVCA. Moreover, TI was inversely associated with Doppler indices from OVCA hens (the higher the TI, the lower the RI and PI) indicating that development of ovarian TAN is associated with an increase in blood

flow to the tumor tissue. Overall, diagnostic indices for early detection of OVCA were established in specific aim 1 with reference to histopathology and ovarian expression of TAN markers which are as follows:

a. Ultrasound signal intensities (pixel values) diagnostic of early stage OVCA from VEGFR-2-targeted molecular imaging: 10,500 pixels or higher
b. Doppler indices diagnostic of early stage OVCA from VEGFR-2 targeted ultrasound molecular imaging: RI = 0.44 or lower
c. Serum IL-16 level: Diagnostic levels of serum IL-16 for early stage OVCA = 450 pg/mL or higher based on corresponding histopathological diagnosis of ovarian tumors.

KEY RESEARCH ACCOMPLISHMENTS DURING YEAR-1 (SPECIFIC AIM 1):

- Confirmed the binding of targeted imaging agents to the tissue marker of ovarian tumor associated neoangiogenesis (microvessels expressing VEGFR-2) in a preclinical model of spontaneous ovarian cancer.
- Enhancement of OVCA detectability of traditional ultrasound scanning by VEGFR-2-targeted molecular imaging agents.
- Ultrasound prediction of tumor related overexpression of ovarian VEGFR-2 confirmed by immunohistochemical detection.
- OVCA diagnostic level of serum IL-16, a novel marker of tumor associated neoangiogenesis at early stage was determined by an immunoassay.
- Immunoproteomics, immunoassay and gene expression study suggest that ovarian tumor epithelium may be a source of serum IL-16 in this animal model.
- Furthermore, specific aim 1 also showed that serum anti-NMP antibodies were associated with the early ovarian tumor development.

2. Task 2. VEGFR-2-targeted ultrasound molecular imaging indices established in specific aim 1 will detect ovarian tumors at early stage in hens with circulatory anti-NMP antibodies.

2a. Selection and prospective monitoring of hens:

1. ***Selection of hens:*** Hens with low egg laying rates were examined for the presence of serum anti-NMPs by ELISA and ovarian abnormal morphology by VEGFR-2-targeted ultrasound molecular imaging indices established in Task 1. Hens with (n=50) and without (n=50) circulating anti-NMP antibodies and without any ovarian abnormality (detectable by VEGFR-2-targeted ultrasound molecular imaging) were selected.
2. All selected hens including with or without serum anti-NMP antibodies were monitored prospectively.

2b. Prospective monitoring of hens by contrast enhanced VEGFR-2-targeted ultrasound molecular imaging for the detection of ovarian tumor or tumor associated neo-angiogenesis at early stage:

1. All hens were monitored prospectively at 15 weeks intervals using the imaging indices established in Task 1.

2. Serum samples were collected at each scan to examine the prevalence of anti-NMP antibodies and the levels of circulatory IL-16.
3. Hens predicted to have early stage ovarian cancer by targeted imaging were sacrificed immediately after diagnosis, gross morphology was recorded, ovarian tissues were collected and processed for routine histology for microscopic examination for tumor lesions and their sub-types as well as for immunohistochemical and proteomic studies.
4. Ovarian sections were examined for the expression of molecular markers of TAN including VEGFR-2 and IL-16.
5. Immunohistochemical expression of VEGFR-2 expression was confirmed by immunoblotting.
6. To determine the period between the initiation of ovarian malignant lesions/microscopic carcinoma (as indicated by the prevalence of serum anti-NMP antibodies) to a solid tissue mass limited to a part of the ovary and detectable by VEGFR-2-targeted imaging, hens were monitored prospectively up to 56 weeks.

Task 2 milestone: Efficacy of VEGFR-2-targeted imaging agents for the detection of OVCA at early stage was tested and its predictive value was established.

2.1. Detailed Reports on the Accomplishments in Year-2 of the project life:

Specific Aim 2: VEGFR-2-targeted ultrasound molecular imaging indices and TAN (tumor associated neo-angiogenesis) indices established in specific aim 1 will detect ovarian tumors and ovarian TAN in anti-NMP antibody positive hens.

Animals:

3-4years old hens with low egg laying rates (<125 eggs/year) were selected from a flock of White Leghorn laying hens. Hens were further screened for the presence of serum anti-NMP antibodies and 50 hens with and 50 hens without anti-NMP antibodies were selected for prospective monitoring with VEGFR-2-targeted ultrasound molecular imaging for the detection of ovarian tumors at early stage using imaging indices established in Specific Aim 1. Hens were maintained under standard poultry husbandry practices and provided with food and water *ad libitum*.

Serum: Blood from all selected hens were collected at each scan, serum samples were separated and stored at -80^{o}C to determine the prevalence of anti-NMP antibodies and IL-16 levels by immunoassay.

Contrast enhanced VEGFR-2-targeted ultrasound molecular imaging and image analysis:

Pre-targeted traditional ultrasound imaging: Hens were examined by traditional transvaginal ultrasound (TVUS) imaging prior to the injection of VEGFR-2-targeted microbubbles using mechanical set up as reported earlier [7, 8]. Briefly, hens were humanely held by an assistant and imaged using an instrument equipped with a 5- to 7.5-MHz endovaginal transducer (MicroMaxx; SonoSite, Inc, Bothell, WA). Following immobilization of each hen, the transducer was inserted transvaginally and 2-dimensional (2D) transvaginal gray scale and pulsed Doppler sonographies were performed as reported earlier [7, 8]. Ovarian morphology was examined by gray scale sonography while ovarian vasculature was examined by Doppler ultrasound (DUS) imaging. DUS imaging indices including the resistive index (RI: [systolic velocity – diastolic velocity]/systolic velocity) and the pulsatility index (PI: [systolic velocity – diastolic velocity]/mean) were automatically calculated from at least two separate images from the same ovary as reported earlier [7, 8]. The lower RI and PI values were used for analysis. All images were processed, digitally archived and reviewed off-line later.

VEGFR-2-targeted imaging:

Contrast enhanced VEGFR-2-targeted ultrasound molecular imaging was performed immediately after pre-targeted imaging as reported earlier [9, 10]. Hens were injected with VEGFR-2-targeted microbubbles in a similar manner as described earlier [9, 10]. The same pre-targeted areas as well as relevant surrounding areas were imaged according to the instruction of the manufacturer of the targeted imaging agent and earlier report [7, 9, 10]. Within 5-7 min from the arrival, targeted microbubbles were accumulated at the target sites and unbound free microbubbles were washed out. All images were archived digitally in a still format as well as in real-time clips (15 minutes for each hen). The effects of targeted microbubbles were visually evaluated online during scanning and off-line afterward by reviewing the archived still images and video clips. The time of targeted imaging agent arrival (interval in seconds from administration of the contrast agent to its visual observation [in seconds]) in the ovaries with or without tumor was recorded in real time. After review of the complete clip, the region of interest (ROI) was selected. The average image intensity (in pixel values) over a ROI encompassing the tumor or a normal ovarian stroma was calculated using a computer assisted software (Microsuite^{TM} version Five, Olympus America, Inc., Canter Valley, PA) and diagnosed either to have early OVCA or normal based on the signal intensities established in specific aim 1. In addition, RI and PI values from post-targeted imaging were calculated.

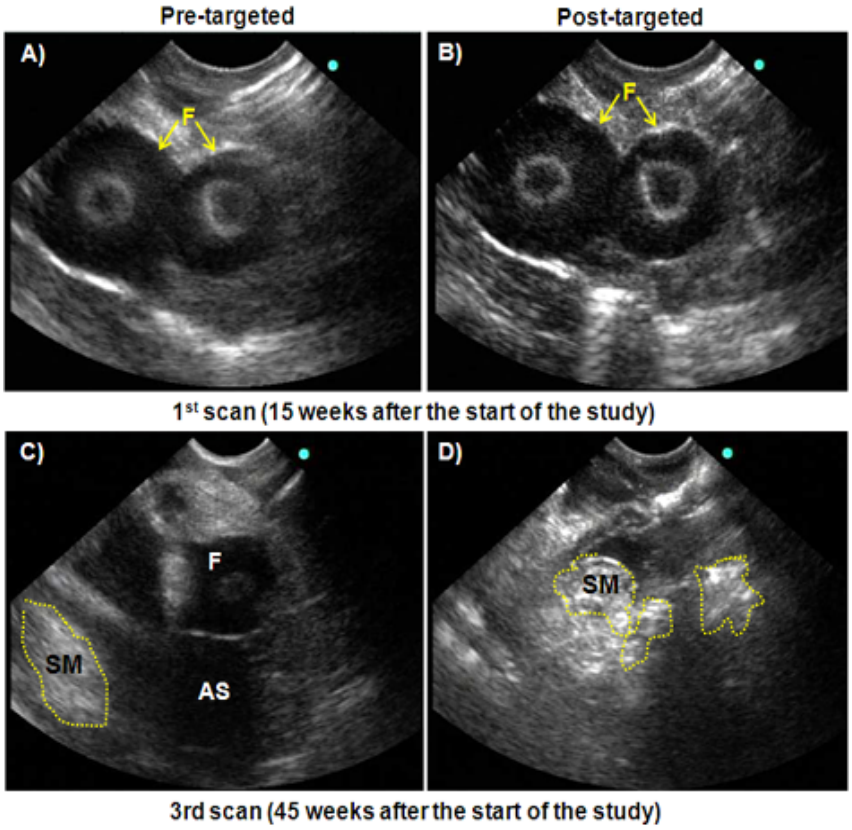

Figure 9. Prospective monitoring of hens to detect early changes associated with ovarian tumor development using VEGFR-2-targeted ultrasound molecular imaging agents. ***Top panel***: This hen was selected to have circulatory anti-NMP antibodies without any solid mass detectable by targeted ultrasound imaging. A-B) At 15 weeks after the start of the prospective monitoring, two developing preovulatory follicles (F) are seen in the ovary. The ovary appeared normal and compared with pre-targeted (A), remarkable increase in the signal intensity was not recorded during post-targeted imaging (B). ***Bottom panel***: The same ovary shown in top panel was scanned at 45 weeks after the start of the study. Pre-targeted sonogram (C) showed a suspected solid mass (SM) in a part of the ovary with little to moderate ascites (AS) and a developing preovulatory follicle (F). Post-targeted scan (D) showed significant enhancement in signal intensity from areas of solid mass (yellow dotted circles).

Gross morphology and histopathology: All hens were euthanized following the diagnosis of ovarian tumors or ovarian TAN by contrast enhanced VEGFR-2-targeted ultrasound molecular imaging.

Abnormal ovarian presentation including presence of ovarian solid mass with or without accompanied ascites as well as tumor metastasis (if any) to other organs was determined from gross observation after euthanasia, as reported earlier [6]. Tissues were processed for routine staining to determine histological sub-types of ovarian tumors as well as immunohistochemical and immunoblotting studies as reported previously [6].

Immunoassay and Immunoblotting: Serum prevalence of anti-NMP antibodies and IL-16 levels were determined by ELISA and confirmed by Western blotting as reported earlier [10, 12, 14].

Immunohistochemistry: Paraffin and frozen sections of ovarian tumors were examined for the detection of VEGFR-2- and IL-16-expressing cells using anti-chicken VEGFR-2 and anti-IL-16 primary antibodies as reported earlier [10, 12]. The frequencies of VEGFR-2-expressing microvessels or IL-16-expressing cells were counted and analyzed as reported previously [10, 12]

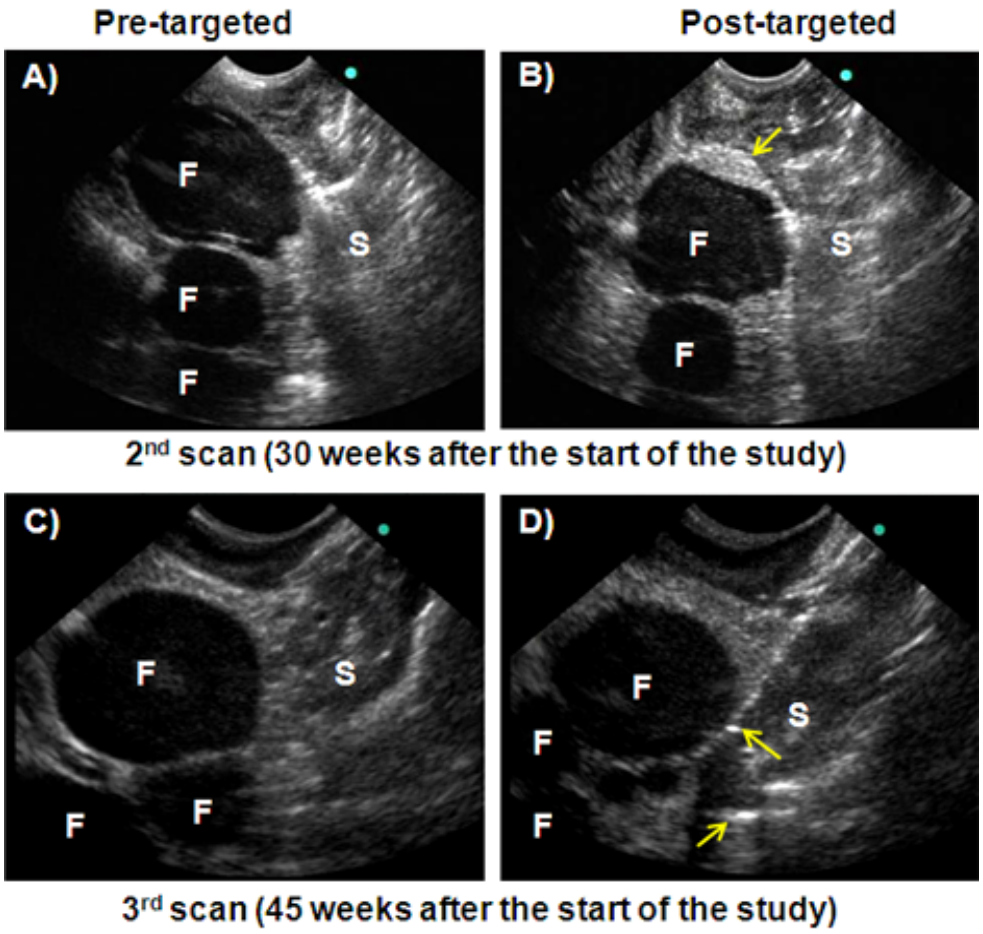

Figure 10. Prospective monitoring a hen without circulatory anti-NMP antibodies by VEGFR-2-targeted molecular imaging agents. ***Top panel***: A-B) At 30 weeks after the start of the prospective monitoring, sonograms revealed the ovary appeared normal containing 2-3 small and large developing follicles (*F*). Although intensity of signals increased alongside of the follicular wall (vascular areas) (arrow), compared with pre-targeted (A), remarkable increase in the signal intensity from ovarian stroma was not recorded during post-targeted imaging (B). ***Bottom panel***: The same ovary shown in top panel was scanned at 45 weeks after the start of the study. The ovary remained normal at 45 weeks and no abnormality was detected in targeted imaging. S= stroma. Arrows are the examples of potential blood vessels bound with the imaging agents.

Results: Changes in ovarian morphology relative to malignant transformation during the prospective monitoring detected by contrast enhanced VEGFR-2-targeted ultrasound molecular imaging are shown in **Figure 9**.

Detection of changes in ovarian morphology in hens with serum anti-NMP antibodies by prospective monitoring with VEGFR-2 targeted ultrasound imaging: All hens with circulating anti-NMP antibodies at initial scan had one or two developing large follicles without any detectable abnormalities in ovarian morphology. At 1st scan (15 weeks after the initial scan), similar to initial scan, all hens showed developing preovulatory follicles without any distinguishable abnormality including the presence of solid mass in the ovary. Serum IL-16 levels were lower and Doppler indices were higher than those diagnostic of OVCA established in specific aim 1. At 2nd scan (30 weeks after the initial scan) although serum IL-16 levels increased in 15 hens with anti-NMP antibodies, no detectable changes in ovarian morphology was found during targeted scan. At 3rd scan (45 weeks from initial scan) additional 12 hens had increased serum IL-16 levels and all these hens (total 12+15 =27 of 50 hens had imaging intensities higher than that diagnostic of OVCA established in specific aim 1. Targeted imaging predicted a small solid tissue mass limited to a part of

their ovaries in 15 hens. In addition, 12 hens had multiple solid tissue masses accompanied with profuse ascites with imaging intensities higher than diagnostic levels established in specific aim 1. These tumor-like changes in the ovaries were associated with remarkable decrease in Doppler indices which were lower than those established in specific aim 1 for the diagnosis of early OVCA. All of these hens were euthanized. Furthermore, of 23 remaining hens, 6 hens showed increase in serum IL-16 levels at 3rd scan for the first time but had imaging signal intensity lower than that of diagnostic levels and these hens together with remaining 17 hens with normal IL-16 levels were monitored further up to 56 weeks. Two of these 6 hens were found to have imaging indices higher than the diagnostic levels established in specific aim 1 at final scan at 56 weeks and these 2 hens were predicted to have early OVCA. However, no detectable changes were observed in remaining 4 of these 6 hens. Furthermore, 2 additional hens had increased serum IL-16 levels at final scan (56 weeks) with no detectable change in ovarian imaging intensity. Thus a total of 6 hens had increased serum IL-16 levels with imaging signal intensity lower than that of diagnostic levels.

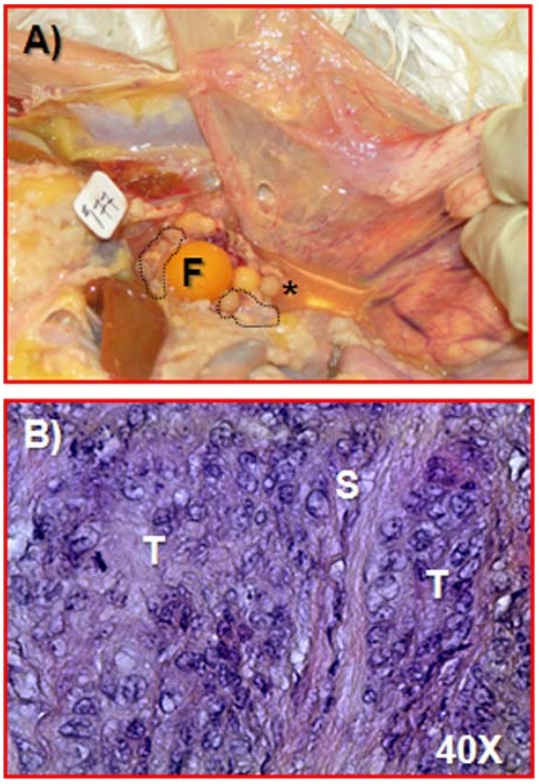

Figure 11. Gross and microscopic presentations of a hen ovary diagnosed to have ovarian tumor at early stage by VEGFR-2-targeted ultrasound molecular imaging shown in *figure 9*. A) As predicted during imaging, small solid masses (black dotted circles) were limited to parts of the ovary confirming early stage OVCA accompanied with little ascites (*****) and a developing preovulatory follicle (*F*). B) Routine staining confirmed the tumor (T) was of serous sub-type containing malignant cells with large pleomorphic nuclei surrounded by a sheath of fibromuscular layer in the stroma (S). 40X.

Prospective imaging of hens without serum anti-NMP antibodies: No significant changes were observed in ovarian morphology of hens without circulating anti-NMP antibodies (**Figure 10**). Subsequent immunoassay showed neither the prevalence of anti-NMP antibodies nor a significant increase in their serum IL-16 levels in "hens without anti-NMP antibody group" at 1st to 2nd scan (30 weeks from the start of the prospective study). At 3rd scan (45 weeks from the start of the study), anti-NMP antibodies were detected for the first time in 4 hens and at final scan (56 weeks) 1 additional hen found positive for serum anti-NMP antibodies.

Gross presentations and histopathological examinations of hens predicted to have ovarian tumors or ovarian TAN:

Following the diagnosis of suspected ovarian tumors by the VEGFR-2-targeted ultrasound molecular imaging, all hens were euthanized and gross morphology of ovaries were recorded and compared with the predictions of targeted imaging. Gross morphology including the presence of solid tumor mass in the ovary, extent of tumor metastasis and stages of OVCA as well as accompanying ascites was recorded. Ovaries with tumor and other relevant tissues including oviducts were harvested and processed for paraffin, frozen, proteomic and molecular biological studies. Histological sub-types of ovarian tumors were confirmed by routine histological examination with hematoxylin-eosin staining (**Figure 11**) as reported earlier [6]. As suggested by targeted ultrasound imaging, 15 hens had early stage OVCA (including 7 serous, 5 endometrioid, 3 mucinous) and tumors were limited to the ovary with no or very little ascites. In late stage OVCA (n = 12 hens including 4 serous, 4 endometrioid, 3 mucinous and 1 sero-mucinous mixed) was accompanied with moderate to profuse ascites and metastasized to peritoneal and abdominal organs.

Furthermore, of 23 remaining hens, 8 hens that showed increase in serum IL-16 levels for the first time at 3rd scan (6 hens) and at final scan (2 hen). 2 of these 8 had small tumor mass in a part of the ovary as predicted by the targeted imaging. 1 of these 2 had serous while the other one was a mucinous OVCA. The remaining 6 of these 8 hens had microscopic carcinoma (3 serous, 2 endometrioid and 1 mucinous) detected by histopathology. (**Figure 12B-C**) Five hens of "*hens without anti-NMP antibodies*" group those had anti-NMP antibodies for the first time at 3rd scan (45 weeks from the start of the study) and 1 at final scan (56 weeks) had preneoplastic lesions detected by hematoxylin and eosin staining (**Figure 12B**).

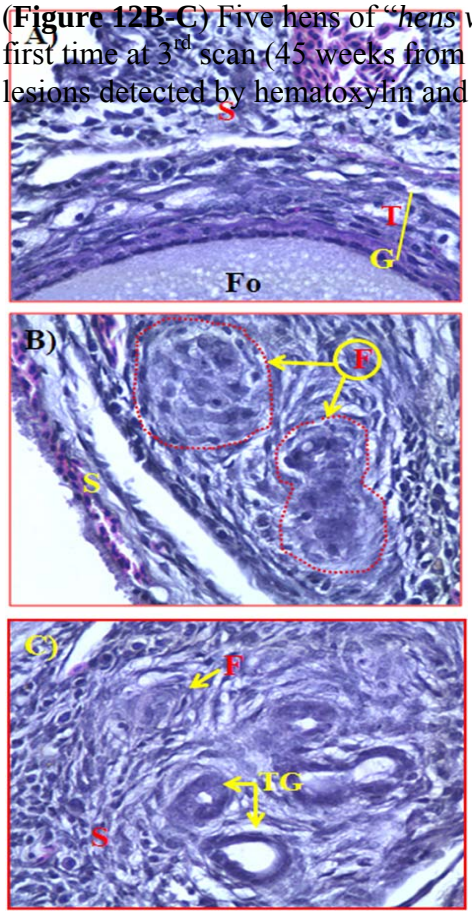

Figure12. Malignant transformation in the ovary of hens with serum anti-NMP antibodies observed in prospective monitoring. A) Section of normal ovary from a hen without serum anti-NMP-antibodies. An embedded cortical follicle is seen in the stroma. B) Ovarian section of a hen with serum anti-NMP antibodies showing preneoplastic focal lesions (F). C) Ovarian section of a hen with serum anti-NMP antibodies showing microscopic tumor lesion. No solid tumor mass was detected at euthanasia. Fo=follicle,G=granulosa cell layer, S= stroma, T= theca layer of follicle, TG= tumor gland. 40x.

Thus overall, 29 (12+15+2) of 50 hens with anti-NMP antibodies developed ovarian solid mass detectable by targeted imaging and 6 with microscopic carcinomas. Targeted imaging detected ovarian cancer in 29 hens of 35 OVCA cases (approximately 83%) and failed to detect microscopic carcinomas. However, this study confirmed that serum IL-16 levels increased even before the tumor forms a solid tissue mass (microscopic carcinoma).

Immunohistochemical expression of VEGFR-2:

Enhanced imaging intensity from VEGFR-2-targeted ultrasound molecular imaging as well as establishment of tumor associated neo-angiogenesis was confirmed by immunohistochemical localization of VEGFR-2. As reported earlier [10, 11], microvessels expressing VEGFR-2 were localized at the spaces between tumor glands (tumor vicinity, **Figure 13** ***top panel***). Malignant cells were also occasionally expressed VEGFR-2. The frequencies of VEGFR-2 expressing microvessels in hens with early stage OVCA were higher than those of diagnostic levels established in specific aim 1. The frequencies of VEGFR-2-expressing microvessels increased further as the tumor progressed to late stages. Differences in the frequencies of VEGFR-2 expressing microvessels were not observed among different histological sub-types of ovarian tumors. Increase in the population of ovarian VEGFR-2 expressing microvessels in association with tumor progression supported the increase in VEGFR-2-targeted imaging signal intensities in hens with late stage OVCA than hens with early stages.

Immunoblotting study detected VEGFR-2 protein of approx 55 kDa by ovarian tumors at early and late stages (**Figure 13,** ***bottom panel***). Compared with early stage, strong immunoreactive bands were observed for VEGFR-2 in ovarian tumors at late stage further confirming the increased expression as well as higher imaging signal intensities in hens with late stage OVCA than early stage OVCA.

Thus, VEGFR-2-targeted molecular imaging agent enhances the detectability of ovarian tumors by transvaginal ultrasound imaging and represents a potential *in vivo* imaging probe for early detection of OVCA.

Detection of serum IL-16 levels and expression by ovarian tumors:

Serum levels of IL-16 were determined using Chicken IL-16 Vetset™ ELISA Kit (Kingfisher Biotech, St. Paul, MN) pre-coated with anti-Chicken IL-16 antibodies and chicken IL-16 as standards as per the manufacturer's instructions reported earlier and as reported previously [12]. The mean concentration of serum IL-16 in hens with early stage OVCA was higher than those of diagnostic levels established in specific aim 1 and increased further in hens at late stages of OVCA. However, the differences in serum IL-16 levels were not significant between the early and late stages OVCA as well as among the different histological subtypes of OVCA.

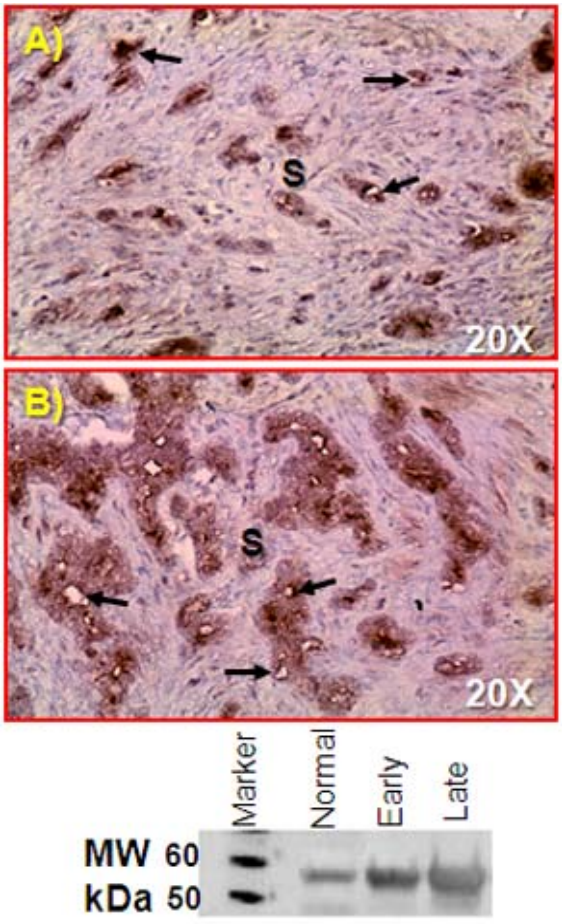

Figure 13. ***Top panel:*** A-B) Detection of VEGFR-2 expressing microvessels in ovarian tumors in hens. Immunopositive VEGFR-2 expressing microvessels were localized in the stroma (S) of ovaries with tumor at early stage (A) shown in *figure 11* as well as at late stage of OVCA (B). Compared with early stage, more VEGFR-2 expressing microvessels are seen in late stage OVCA. 20X.
Bottom panel: Tissue expression of VEGFR-2 by normal and ovarian tumors at early and late stages. Western blotting showed increased expression of VEGFR-2 protein in association with OVCA development and progression. These results together with immunohistochemical detection support increased signal intensity due to binding of targeted agents with the increased number of VEGFR-2-expressing microvessels in tumors. 20X

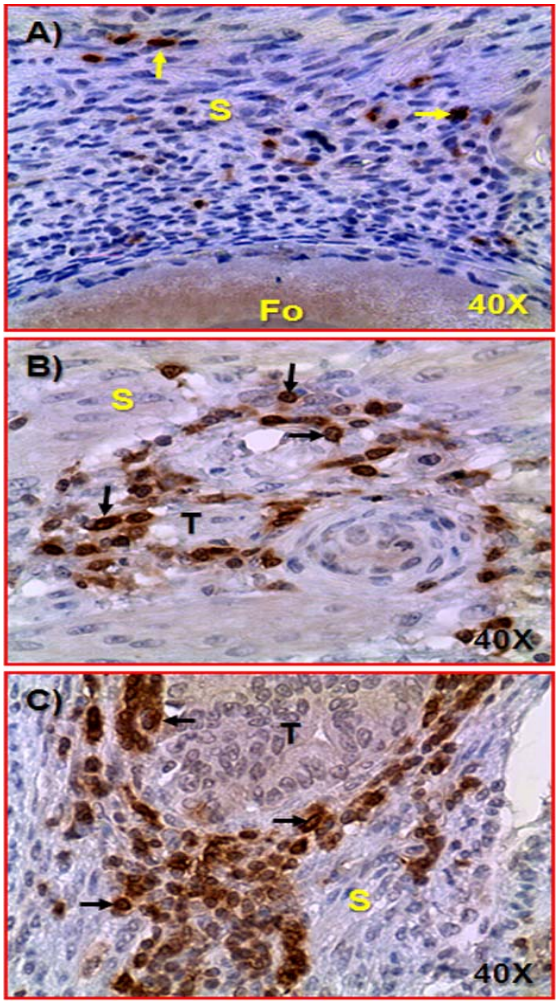

Figure 14. Changes in IL-16 expression in association with ovarian cancer (OVCA) development and progression. A) Section of a normal ovary showing very few immunostained IL-16-expressing cells in the stroma (S). B) section from an ovarian tumor at early stage of OVCA. Compared to normal, more IL-16-expressing cells seen in the stroma surrounding the tumor (T). C) section of an ovarian tumor at late stage. Many IL-16-expressing cells are seen in the stroma surrounding the tumor (T). Arrows indicate the examples of IL-16-expressing cells. 40X.

IL-16 was expressed by both the stromal cells including immune-cell like cells in the tumor stroma as well as occasionally by the ovarian malignant cells (**Figure 14**). A higher frequency of IL-16-expressing cells than those of diagnostic levels established in specific aim 1 was observed in hens with early stage OVCA and increased further in hens with late stage of OVCA.

These results suggest that increase in the frequency of IL-16 expressing cells in association with tumor initiation and progression may be a reason for the increase in serum IL-16 levels as the tumor progressed to later stages.

***Prevalence of serum anti-NMP antibodies in hens during prospective monitoring*:** All serum samples collected at different scan intervals were tested for the prevalence of anti-NMP antibodies using NMPs from archived normal or ovarian tumors collected from hens diagnosed for OVCA during prospective monitoring. The procedures for NMP collection and immunoassay were reported earlier [4, 10, 14]. Briefly, 96-well ELISA plates (NUNC) were coated with either tumor or normal ovarian NMPs and the immunoreactivities of serum samples from each hen collected at different scanning intervals were tested against the coated normal or ovarian tumor NMPs. Each serum sample was assayed in duplicate and the plates were read at 405nm in an ELISA plate reader (Softmax Pro, version 1.2.0, software; Molecular Devices, Sunnyvale, CA). Serum from young healthy hens with fully functional ovaries was used as negative control (established in earlier studies) for the presence of anti-NMP antibodies. Serum with optical density (OD) values higher than the control mean + 2SD (cut-off value) were considered positive for the presence of anti-NMP antibodies.

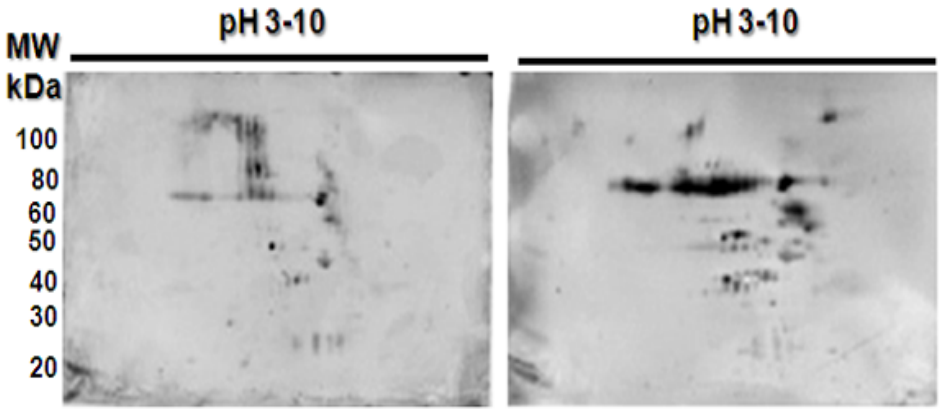

Figure 15. Immunoproteomic confirmation of prevalence of anti-NMP antibodies in sera of hens with ovarian malignant lesions. Tumor serum reacted specifically against tumor NMPs (of 30-100kDa sizes). Compared with heterogenous NMPs (left panel), serum reacted against more NMPs of homogenous tumor. These results confirmed the production of anti-NMP antibodies in response to a developing tumor.

All hens in "*hens **with** anti-NMP antibodies*" group remained positive for anti-NMP antibodies at all scans including those diagnosed with OVCA. In contrast, neither the prevalence of anti-NMP antibodies nor a significant increase in serum IL-16 levels was detected in "*hens **without** anti-NMP antibody group*" at 1st to 2nd scan (30 weeks from the start of the prospective study). Anti-NMP antibodies were detected for the first time in 4 hens at 3rd scan (45 weeks from the start of the study), and in 1 hen at final scan, however, neither serum IL-16 levels nor a tumor related changes in their ovarian morphology were detected by targeted ultrasound imaging at finalscan.

Representative serum samples with positive reactivity against normal or tumor NMPs were analyzed by immunoproteomic study (2 dimensional -Western blotting, 2D-WB) to confirm immunoreactivities observed in ELISA.

Immunoreactive NMPs of different sizes (approx. 30-100kDa) were detected by 2D-WB (**Figure 15**) confirming the results of ELISA for the prevalence of anti-NMP antibodies in serum. Thus, these results suggest that NMPs are shed in serum during malignant transformation in the ovary and can be used to aid the early detection of ovarian cancer.

KEY RESEARCH ACCOMPLISHMENTS DURING YEAR-2 (SPECIFIC AIM 2):

- Further confirmation of the enhancement in ovarian tumor detection at early stage by VEGFR-2-targeted molecular imaging agents.
- Serum anti-NMP antibodies were found to be a useful surrogate marker for the early detection of OVCA by VEGFR-2-targeted imaging.
- Compared with normal ovaries, increased frequency of VEGFR-2-expressing microvessels detected by immunohistochemistry supported the increased signal intensities due to the binding of VEGFR-2-targeted imaging agents with their targets expressed by the tumor associated microvessels.
- Serum prevalence of anti-NMP antibodies as well as serum IL-16 levels increases even befroe the tumor becomes detectable by targeted imaging. This information will lead to the suitability of these markers for a screening protocol to detect early stage OVCA in the clinics.

3. **OVERALL KEY ACCOMPLISHMENTS REPORTABLE OUTCOMES:**

- Established for the first time that VEGFR-2-targeted ultrasound imaging agents bind with spontaneous ovarian tumor associated neoangiogenesis microvessels expressing VEGFR-2 in a preclinical animal model.
- Binding of VEGFR-2 targeted molecular imaging agents with tumor associated microvessels enhanced the OVCA detection limit of traditional ultrasound scanning.
- VEGFR-2-targeted ultrasound molecular imaging agents detected ovarian cancer at early stage when the tumor mass is limited to a part of the ovary (appended in pages 25-55 and 78-79).
- Serum anti-NMP antibodies were associated with ovarian malignant transformation.
- Serum anti-NMP antibodies were found to be a useful surrogate marker for the early detection of OVCA by VEGFR-2-targeted imaging.
- Ovarian tumor epithelium may be a source of serum IL-16, a novel marker of tumor associated neoangiogenesis and is associated with ovarian tumor development and progression (appended in pages 55-64).
- Prevalence of anti-NMP antibodies and IL-16 levels in serum increases when the tumor still microscopic and before the formation of solid mass in a part of the ovary (first detectable by targeted imaging). This information will lead to the suitability of these markers for a screening protocol leading to the scanning by VEGFR-2-targeted ultrasound molecular imaging to detect early stage OVCA in clinics.
- Additionally, this study showed that tumor progression was associated with suppression of NK cell immunity (appended in pages 65-77).

4. LIMITATIONS/CAVEATS OF THE STUDY:

This study detected ovarian cancer at early stage when the tumor forms a solid mass and limited to a part of the ovary. As hypothesized, the expression of VEGFR-2 by tumor associated neoangiogenic vessels in these tumors was detected by VEGFR-2-targeted molecular ultrasound imaging agents. However, this study failed to detect ovarian microscopic carcinoma which did not form any detectable solid tumor mass. One of the reasons of this failure might be due to the lack of an established tumor associated neo-angiogenesis in these microscopic tumors. Thus, VEGFR-2-targeted molecular imaging requires establishment of tumor associated neoangiogenesis to detect ovarian cnacer at early stage. However, this limitation can be overcome by using additional markers of malignant transformation including anti-NMP antibodies and serum IL-16 proteins partly secreted by the developing ovarian tumors.

5. TRANSLATIONAL RELEVANCE OF THE FINDINGS OF THE STUDY:

Difficulty of identification and access to patients at early stage ovarian cancer are the two significant barriers to study molecular changes associated with ovarian cancer development and to establish an early detection test. Thus the lack of an effective early detection test remains one of the main causes contributing to the high case to death ratio of OVCA patients. Ultrasound imaging is a safe, effective and non-invasive in vivo imaging modality for the detection of OVCA provided its resolution can be improved. Current study showed that the laying hen is a feasible preclinical model of studying the improvement of OVCA detection by ultrasound imaging using molecular targeted imaging agents. In this study neither a deleterious effect nor a toxic response indicative of abnormal physiology during or after the injection of VEGFR-2-targeted imaging agents was recorded. As the laying hen shares similar ovarian physiology, similar features of spontaneous OVCA and their histological types together with expression of similar molecular markers, results of this study may form the foundation for a clinical study. As this study used ultrasound imaging system similar to those used in clinics, results of the current study can be translated to clinic with minimum modification. Furthermore, this model can be effective and feasible for the development of novel anti-angiogenic therapeutics within a short time.

6. OVERALL REPORTABLE OUTCOMES DURING THE PROJECT LIFE (YEAR1 – YEAR 2):

Manuscript: Submitted or Published

1. Barua A, Yellapa A, Bahr JM, Machado SA, Bitterman P, Basu S, Sharma S and Abramowicz JS (2014). VEGFR2-targeted ultrasound imaging agent enhances the detection of ovarian tumors at early stage in laying hens, a preclinical model of spontaneous ovarian cancer. Submitted to *Ultrasounic Imaging* (under review) (appended in pages 25-54).

2. Yellapa A, Bitterman P, Sharma S, Guirguis AS, Bahr JM, Basu S, Abramowicz JS, Barua A (2013). Interleukin 16 expression changes in association with ovarian malignant transformation. *Am J Obstet Gynecol*. 2013 Dec 28. pii: S0002-9378(13)02286-2. doi: 10.1016/j.ajog.2013.12.041. [Epub ahead of print]. PMID: 24380743. (appended in pages 55-64)

3. Barua A, Bradaric MJ, Bitterman P, Abramowicz JS, Sharma S, Basu S, Lopez H, Bahr JM. Dietary supplementation of Ashwagandha (Withania somnifera, Dunal) enhances NK cell function in ovarian

tumors in the laying hen model of spontaneous ovarian cancer. *Am J Reprod Immunol*. 2013; 70(6):538-50. doi: 10.1111/aji.12172. Epub 2013 Nov 5. PMID: 24188693. (appended in pages 65-77).

Meeting presentations: Abstract published and presented:

1. Barua A, Qureshi T, Bitterman P, Bahr JM, Basu S, Edassery SL, Abramowicz JS, (2012) Molecular targeted imaging of vascular endothelial growth factor receptor (VEGFR)-2 and anti-NMP autoantibodies detect ovarian tumor at early stage. American Association for Cancer Research annual meeting, 2012; March 3[1st] to April [4th], 2012, McCormick Place, Chicago, IL. Abstract ID# 2455; http://cancerres.aacrjournals.org/cgi/content/meeting_abstract/72/8_MeetingAbstracts/2455 (Appended in pages 78-79).
2. Alongkronrusmee D, Bitterman P, Abramowicz JS, Bahr JM, Basu S, Grasso S, Sharma S, Rotmensch J and Barua. A (2013). "GRP78 in association with VEGFR-2 detects early stage ovarian cancer." In: Proceedings of the 104th Annual Meeting of the American Association for Cancer Research; 2013 Apr 6-10; Washington, DC. Philadelphia (PA): AACR; *Cancer Res* 2013; 73(8 Suppl): Abstract nr 4642. doi:10.1158/1538-7445.AM2013-4642 http://cancerres.aacrjournals.org/cgi/content/meeting_abstract/73/8_MeetingAbstracts/4642 (appended in pages 80-81).
3. Yellapa A, Bitterman P, Abramowicz JS, Bahr JM, Sharma S, Basu S, Barua A (2013). Association of interleukin 16 with early metastasis of ovarian tumors. Presented in the meeting on Advances in Ovarian Cancer Research, American Association for Cancer Research, September 18-21, 2013, Miami, Florida, Abstract Number #136197_2 (appended in pages 82-85).

7. OVERALL CONCLUSIONS:

This study examined the feasibility of VEGFR-2-targeted ultrasound molecular agents in detecting ovarian cancer at early stage in a preclinical model of spontaneous ovarian cancer, the laying hens. The results of this study showed that VEGFR-2-targeted ultrasound molecular imaging agent bound with its target expressed by ovarian tumors and enhanced the signal intensity of ultrasound imaging. This study also showed that serum prevalence of anti-NMP antibodies and levels of IL-16 increased in association with ovarian malignant transformation and OVCA development. Furthermore, tumor-associated serum IL-16 levels were elevated even before the formation of a solid tumor mass in the ovary. VEGFR-2-targeted molecular ultrasound imaging together with serum anti-NMP antibodies and IL-16 levels, improved early detection of OVCA and detected ovarian tumors when it is limited to a part of the ovary. Thus VEGFR-2-targeted imaging agents showed potential to be a feasible imaging agent for early OVCA detection in clinics. Additionally, laying hens offer a feasible preclinical model to develop OVCA-preventive anti-angiogenic therapeutics targeting VEGFR-2-expressed by tumor associated microvessels**.**

REFERENCES:

[1] Siegel, R., D. Naishadham and A. Jemal (2013). "Cancer statistics, 2013." CA Cancer J Clin **63**(1): 11-30.
[2] Ries, L. A. (1993). "Ovarian cancer. Survival and treatment differences by age." Cancer **71**(2 Suppl): 524-9.
[3] Moore, R. G., S. MacLaughlan and R. C. Bast, Jr. (2010). "Current state of biomarker development for clinical application in epithelial ovarian cancer." Gynecol Oncol **116**(2): 240-5.
[4] Yu, E., H. Lee, W. Oh, B. Yu, H. Moon and I. Lee (1999). "Morphological and biochemical analysis of anti-nuclear matrix protein antibodies in human sera." J Korean Med Sci **14**(1): 27-33.
[5] Vanderhyden, B. C., T. J. Shaw and J. F. Ethier (2003). "Animal models of ovarian cancer." Reprod Biol Endocrinol **1**: 67.
[6] Barua, A., P. Bitterman, J. S. Abramowicz, A. L. Dirks, J. M. Bahr, D. B. Hales, M. J. Bradaric, S. L. Edassery, J. Rotmensch and J. L. Luborsky (2009). "Histopathology of ovarian tumors in laying hens: a preclinical model of human ovarian cancer." Int J Gynecol Cancer **19**(4): 531-9.
[7] Barua, A., J. S. Abramowicz, J. M. Bahr, P. Bitterman, A. Dirks, K. A. Holub, E. Sheiner, M. J. Bradaric, S. L. Edassery and J. L. Luborsky (2007). "Detection of ovarian tumors in chicken by sonography: a step toward early diagnosis in humans?" J Ultrasound Med **26**(7): 909-19.
[8] Barua, A., P. Bitterman, J. M. Bahr, S. Basu, E. Sheiner, M. J. Bradaric, D. B. Hales, J. L. Luborsky and J. S. Abramowicz (2011). "Contrast-enhanced sonography depicts spontaneous ovarian cancer at early stages in a preclinical animal model." J Ultrasound Med **30**(3): 333-45.
[9] Anderson, C. R., J. J. Rychak, M. Backer, J. Backer, K. Ley and A. L. Klibanov (2010). "scVEGF microbubble ultrasound contrast agents: a novel probe for ultrasound molecular imaging of tumor angiogenesis." Invest Radiol **45**(10): 579-85.
[10] Barua A, Qureshi T, Bitterman P, Bahr JM, Basu S, Edassery SL and Abramowicz JS (2012). "Molecular targeted imaging of vascular endothelial growth factor receptor (VEGFR)-2 and anti-NMP autoantibodies detect ovarian tumor at early stage." In: Proceedings of the 103rd Annual Meeting of the American Association for Cancer Research; 2012 Mar 31-Apr 4; Chicago, IL. Philadelphia (PA): AACR; Cancer Res 2012; 72(8 Suppl): Abstract nr 2455. Doi:1538-7445.AM2012-2455
[11] Barua, A., P. Bitterman, J. M. Bahr, M. J. Bradaric, D. B. Hales, J. L. Luborsky and J. S. Abramowicz (2010). "Detection of tumor-associated neoangiogenesis by Doppler ultrasonography during early-stage ovarian cancer in laying hens: a preclinical model of human spontaneous ovarian cancer." J Ultrasound Med **29**(2): 173-82.
[12] Yellapa, A., J. M. Bahr, P. Bitterman, J. S. Abramowicz, S. L. Edassery, K. Penumatsa, S. Basu, J. Rotmensch and A. Barua (2012). "Association of interleukin 16 with the development of ovarian tumor and tumor-associated neoangiogenesis in laying hen model of spontaneous ovarian cancer." Int J Gynecol Cancer **22**(2): 199-207.
[13] Barua, A., Y. Yoshimura and T. Tamura (1998). "Effects of ageing and oestrogen on the localization of immunoglobulin-containing cells in the chicken ovary." J Reprod Fertil **114**(1): 11-6.

[14] Barua, A., S. L. Edassery, P. Bitterman, J. S. Abramowicz, A. L. Dirks, J. M. Bahr, D. B. Hales, M. J. Bradaric and J. L. Luborsky (2009). "Prevalence of antitumor antibodies in laying hen model of human ovarian cancer." Int J Gynecol Cancer **19**(4): 500-7.
[15] Hong, Y. H., H. S. Lillehoj, S. H. Lee, R. A. Dalloul and E. P. Lillehoj (2006). "Analysis of chicken cytokine and chemokine gene expression following Eimeria acervulina and Eimeria tenella infections." Vet Immunol Immunopathol **114**(3-4): 209-23.

Ultrasonic Imaging

VEGFR2-targeted ultrasound imaging agent enhances the detection of ovarian tumors at early stage in laying hens, a preclinical model of spontaneous ovarian cancer

Journal:	*Ultrasonic Imaging*
Manuscript ID:	Draft
Manuscript Type:	Technical Article
Date Submitted by the Author:	n/a
Complete List of Authors:	Barua, Animesh; Rush University Medical Center, Pharmacology, Obstetrics and Gynecology, Pathology Yellapa, Aparna; Rush University, Pharmacology Bahr, Janice; University of Illinois at Urbana-Champaign, Animal Sciences Machado, Sergio; University of Illinois at Urbana-Champaign, Animal Sciences Bitterman, Pincas; Rush University Medical Center, Pathology, Obstetrics and Gynecology Basu, Sanjib; Rush University Medical Center, Preventive Medicine (Biostatistics) Sharma, Sameer; Franciscan St. Margaret Health, Gynecological Oncology Abramowicz, Jacques; Wayne State University, Obstetrics and Gynecology
Keywords:	Ovarian cancer, Early detection, Ultrasound imaging, VEGFR2-targeted imaging agent, Laying hen model

Abstract:	Tumor-associated neoangiogenesis (TAN) is an early event in ovarian cancer (OVCA) development. Increased expression of vascular endothelial growth factor receptor 2 (VEGFR2) by TAN vessels presents a potential target for early detection by ultrasound imaging. The goal of this study was to examine the suitability of VEGFR2-targeted ultrasound imaging agents in detecting spontaneous OVCA in laying hens. Effects of VEGFR2-targeted imaging agents in enhancing ultrasound signal intensity from spontaneous ovarian tumors in hens was examined in a cross sectional study. Enhancement in signal intensity was determined before and after injection of VEGFR2-targeted imaging agents. All ultrasound images were digitally stored and analyzed offline. Following scanning, ovarian tissues were collected and processed for histology and detection of VEGFR2-expressing microvessels. Enhancement in visualization of ovarian morphology was detected by gray scale imaging following injection of VEGFR2-targeted imaging agents. Compared with pre-targeted, targeted imaging enhanced signal intensities significantly ($P < 0.001$) irrespective of the pathological status of ovaries. In contrast to normal hens, ultrasound signal intensity was significantly ($P < 0.001$) higher in hens with early stage OVCA and increased further in hens with late stage OVCA. Higher signal intensities in hens with OVCA was positively correlated with increased ($P<0.001$) frequencies of VEGFR2-expressing microvessels. The results of this study

	suggest that VEGFR2-targeted imaging agents enhance the visualization of spontaneous ovarian tumors in hens at early and late stages of OVCA. The laying hen may be a suitable model to test new imaging agents and develop targeted therapeutics.

SCHOLARONE™
Manuscripts

For Peer Review

VEGFR2-targeted ultrasound imaging agent enhances the detection of ovarian tumors at early stage in laying hens, a preclinical model of spontaneous ovarian cancer

Animesh Barua[1, 2, 3], Aparna Yellapa[1], Janice M Bahr[4], Sergio A Machado[4], Pincas Bitterman[2, 3], Sanjib Basu[5], Sameer Sharma[1, 2] and Jacques S Abramowicz[2, 5]

Departments of [1]Pharmacology, [2]Obstetrics and Gynecology, [3]Pathology, [5]Preventive Medicine (Biostatistics), Rush University Medical Center; [4]Department of Animal Sciences, University of Illinois at Urbana-Champaign, Illinois; [5]Department of Obstetrics and Gynecology, Wayne State University, Detroit, MI

For Peer Review

Short Title: VEGFR2- targeted imaging of ovarian tumors

Correspondence to:
Animesh Barua, Ph.D.
Laboratory for Translational Research on Ovarian Cancer,
Department of Pharmacology
Room # 410, Cohn Building,
Rush University Medical Center
1735 W. Harrison St., Chicago IL 60612
Tel. 312-942-6666
Fax: 312-563-3552
Animesh_Barua@rush.edu

Key words- Ovarian cancer; early detection; ultrasound imaging; VEGFR2-targeted imaging agent; laying hen model

Acknowledgements and support:

This study was supported by the Department of Defense pilot award # W81XWH-11-1-0510 on ovarian cancer. We thank Chet and Pam Utterback and Doug Hilgendorf, staff of the University of Illinois at Urbana-Champaign Poultry Research Farm, for maintenance of the hens. We also thank Heather Lopez, research Assistant, Department of Animal Sciences, University of Illinois at Urbana-Champaign, for helping in hen tissue collection.

ABSTRACT: Tumor-associated neoangiogenesis (TAN) is an early event in ovarian cancer (OVCA) development. Increased expression of vascular endothelial growth factor receptor 2 (VEGFR2) by TAN vessels presents a potential target for early detection by ultrasound imaging. The goal of this study was to examine the suitability of VEGFR2-targeted ultrasound imaging agents in detecting spontaneous OVCA in laying hens. Effects of VEGFR2-targeted imaging agents in enhancing ultrasound signal intensity from spontaneous ovarian tumors in hens was examined in a cross sectional study. Enhancement in signal intensity was determined before and after injection of VEGFR2-targeted imaging agents. All ultrasound images were digitally stored and analyzed offline. Following scanning, ovarian tissues were collected and processed for histology and detection of VEGFR2-expressing microvessels. Enhancement in visualization of ovarian morphology was detected by gray scale imaging following injection of VEGFR2-targeted imaging agents. Compared with pre-targeted, targeted imaging enhanced signal intensities significantly (P <0.001) irrespective of the pathological status of ovaries. In contrast to normal hens, ultrasound signal intensity was significantly (P <0.001) higher in hens with early stage OVCA and increased further in hens with late stage OVCA. Higher signal intensities in hens with OVCA was positively correlated with increased (P<0.001) frequencies of VEGFR2-expressing microvessels. The results of this study suggest that VEGFR2-targeted imaging agents enhance the visualization of spontaneous ovarian tumors in hens at early and late stages of OVCA. The laying hen may be a suitable model to test new imaging agents and develop targeted therapeutics.

For Peer Review

INTRODUCTION

Owing to its high case to death ratio, ovarian cancer (OVCA) ranks as the second lethal malignancy of women, after breast cancer. The global rate of OVCA death per year is approximately 140, 200 women and that of the USA is approximately 15,000[1, 2]. While 90% OVCA cases can be cured if diagnosed at early stage, OVCA in most cases are detected at late stages due to the lack of an early detection test. Thus early detection of OVCA is critical. Extensive studies have been performed to establish serum based marker(s) but none of them have met success in clinics due to their lack of specificity and/or sensitivity. Thus, a non-invasive imaging method for early detection of OVCA is urgently needed which will also add to the specificity and sensitivity of these serum based markers. Although traditional transvaginal ultrasound (TVUS) imaging is the currently preferred method for non-invasive imaging of ovarian abnormality, due to its limited resolution, it lacks the required sensitivity for detecting early OVCA[3]. Establishment of ovarian tumor related imaging target(s) as well as development of imaging probes to detect this target(s) are essential to improve current OVCA detection levels by TVUS imaging.

Malignant nuclear transformation followed by tumor-associated neoangiogenesis (TAN) are early events in ovarian tumor development. TAN, a process of formation of new vessels from the existing ones is a hallmark of tumor progression[4, 5]. Tumor requires TAN for their flow of nutrition and growth; therefore, ovarian TAN vessels present potential targets for early detection of OVCA. Imaging agents capable of detecting molecular markers expressed by TAN vessels non-invasively would be the desirable tool for early detection of OVCA. Several molecular markers associated with ovarian TAN have been well characterized and vascular endothelial growth factor receptor 2(VEGFR2) is one of them. VEGFR2 is a receptor tyrosine kinase,

together with its ligand VEGF, stimulates growth and proliferation of vascular endothelial cells and enhances their permeability[6, 7]. Extensive studies both on ovarian and non-ovarian solid tumors have shown over expression of VEGFR2 during tumor-associated neoangiognesis[8]. Moreover, inhibitions of VEGFR2 activation have been shown to reduce tumor growth and monoclonal antibodies targeting VEGFR2 are approved by the United States Food and Drug Administration (FDA) for the treatment of cancer patients[9, 10]. Thus VEGFR2 not only represents a target for early detection of OVCA, but may also be helpful for monitoring the efficacy of anti-angiogenic therapies if a suitable imaging probe to detect VEGFR2 can be developed.

Contrast agents have been introduced to enhance the visualization of tumor vasculature by different imaging modalities including TVUS[11-15]. VEGFR2-targeted molecular imaging agents for the detection of tumors have been developed and successfully tested. However, very few reports are available on the detection of OVCA using VEGFR2-targeted molecular imaging and most of these reports are based either on the induced tumor model in rodents or patients with late stage OVCA[16-19]. Understandably, identification and access to patients with early stage OVCA are the main barriers to test the efficacy of these imaging agents in detecting spontaneous OVCA at early stage. Rodents do not develop OVCA spontaneously and induced tumors in rodents are different from spontaneous OVCA in their histopathology[20]. Spontaneous incidence of OVCA with histopathology and expression of several molecular markers similar to humans have been reported in laying hens[20-27]. We adapted TVUS imaging method for the detection of ovarian tumors in hens[28-30]. Thus the laying hen is a highly innovative model to test the suitability of VEGFR2-targeted imaging probes for the detection of spontaneous OVCA at an early stage by non-invasive *in vivo* TVUS imaging. The goal of this study was to examine whether VEGFR2-targeted imaging probes enhance the visualization of sponatneous ovarian

tumors in laying hens, a preclinical model of OVCA. Enhancement of visualization of spontaneous ovarian tumors was examined in an exploratory study.

MATERIALS and METHODS

Animals

A flock of 150 commercial strains of White Leghorn laying hens (*Gallus domesticus*, approximately 4-years old) were reared under standard poultry care and management and provided with feed and water *ad libitum*. The egg-laying rates (an indicator of ovarian function; a low egg-laying rate indicates decreased rate of ovulation as well as reduced ovarian function) of the hens were recorded on a daily basis. The normal rate of egg laying by a commercial laying hen is more than 250 eggs per year, and less than 50% of the normal laying rate is considered a low egg-laying rate[28]. Fifty two hens with low or irregular egg-laying rates and those that stopped laying with no large preovulatory follicle, with or without solid mass in the ovary and abdominal distention (a sign of possible ovarian tumor-associated ascites) were selected by traditional TVUS from the flock for VEGFR2-targeted TVUS imaging. The incidence of ovarian cancer in laying hens of this age group was reported to be approximately 15% to 20% and is associated with low or complete cessation of egg laying[20, 21, 28.] All procedures were performed according to Institutional Animal Care and Use Committee approved protocol.

VEGFR2- targeted imaging probes

VEGFR2- targeted TVUS imaging of hen ovaries was performed using Visistar® VEGFR2 Targeted Ultrasound Contrast Agent (VS-102, Targeson, Inc San Diego, CA). Visistar ®

For Peer Review

VEGFR2 is indicated for ultrasound molecular imaging of tumor angiogenesis, targeted specifically to the VEGFR2 receptors expressed by the endothelial cells of blood vessels. The agent remains acoustically active for upto15 minutes. Visistar® VEGFR2 is a microsphere ultrasound contrast agent containing a single-chain VEGF-based targeting ligand. Visistar® VEGFR2 is known to bind to VEGFR2 found on angiogenic vascular endothelium. Agents are administered as an intravenous bolus injection. Microbubbles preparation, ligand conjugation, characterization of labeled microbubbles and their binding specificity of tumor endothelium has been reported earlier[31].

Ultrasonography

Pre-targeted traditional ultrasound imaging

Ultraonography was performed in a continuous pattern before, during and after the injection of targeted imaging probes as reported previously with little modification[28, 30]. All hens were scanned using an instrument equipped with a 1 to 7.5-MHz transvaginal transducer (MicroMaxx; SonoSite, Inc, Bothell, WA). Hens were immobilized and gently restrained by an assistant. Transmission gel was applied to the surface of the transducer, covered by a probe cover and to ensure uninterrupted conductance of the sound waves, gel was reapplied to the covered probe. The transducer was inserted approximately at a 30° angle to the body, 3 to 5 cm into the vagina and 2-dimensional (2D) transvaginal gray scale and pulsed Doppler sonography were performed. Young egg-laying hens (as the ovaries of these hens contain more developing follicles compared to old hens) were used as standard controls for mechanical adjustment to reveal and characterize the fully functional normal ovaries of hens. The area of a tumor to be imaged was determined

For Peer Review

according to 3 conditions as reported previously[30]: (a) the whole tumor, if possible, should be seen on the image; (b) the sectional plane should contain the solid part (wall, septa, and papillae) of the tumor; and (c) the most vascularized area was selected. For normal ovaries, ovaries without any detectable tumor, and atrophic ovaries, the region surrounding the ovary was scanned, and the transducer was swept through the entire area for complete scanning of the ovary. Gray scale morphologic evaluation of the ovarian mass was performed with attention to the number of preovulatory follicles, the presence of abnormal-looking follicles, septations, papillary projections or solid areas, and echogenicity. After morphologic evaluation, color Doppler mode was activated for identification of vascular color signals. Once a vessel was identified on color Doppler imaging, pulsed Doppler was activated to obtain a flow velocity waveform. The resistive index and the pulsatility index were automatically calculated from at least 2 consecutive samples (2 separate images from the same ovary) and recorded. All images were processed and digitally archived.

Injection of VEGFR2-targeted imaging agents and post-targeted ultrasound imaging

Targeted imaging was performed according to the manufacturer's instructions as reported earlier[31] with modification. A preliminary experiment was conducted with VEGFR2-targeted or isotype control microbubbles using 10 animals containing fully functional ovaries to adjust the mechanical setup and determine the optimum dosage of microbubbles. The dose of 10 μL/kg body weight was found optimal for better resolution in the preliminary experiment. Targeted microbubbles were prepared before injection according to the manufacturer's directions. Briefly, the vial containing the microbubble suspension was inverted and gently rotated to resuspend the microspheres completely. The suspension was transferred from the vial by an injection syringe

For Peer Review

with a 19-gauge needle to a angiocatheter (small-vein infusion set, female luer, 12-in tubing, 25-gauge needle; Kawasumi Laboratories, Tampa, FL) containing 100 μL of 0.9% sodium chloride previously inserted into the left wing vein (brachial vein) of the hen and followed by the reloading of 100 μL of a 0.9% sodium chloride solution. The loading of the sodium chloride solution before and after injection of microbubbles helped maintain the vascular patency and airtight condition, in addition to flushing the bubbles from the hen's circulation.

The area imaged during pre-targeted imaging was imaged again after targeted microbubble injection. Targeted imaging were performed at a lower mechanical index 5min after the injection of microbubbles containing targeted agents to allow binding and retention of targeted microbubbles in the tumor as well as washing-out of unbound microbubbles. Then a destructive pulse with high mechanical index was delivered and images were taken again. The difference in signal intensity between the images 5min after injection at a low mechanical index and images after the delivery of destructive pulse confirms that the signal acquired after targeted microbubble injection was from microbubbles-bounded target tissue. All images were archived digitally in a still format as well as real-time clips (up to 15 minutes for each hen) on single-sided recordable digital video disks (DVD+R format; Maxell Corporation of America, Fair Lawn, NJ) readable on a personal computer.

Evaluation of the Effects of VEGFR2-Targeted Microbubbles

The effect of targeted microbubbles was evaluated visually during the examination and the enhancement of microvessel detection by targeted imaging was assessed afterward from reviewing the archived video clips. After review of the complete clips, the region of interest

For Peer Review

(ROI) was selected by drawing on the ovarian stroma of normal hens or on the area containing solid tissue mass in OVCA hens. In normal hens, areas containing large developing follicles were avoided during the selection of ROIs. The signal intensity of the selected area was measured in pixel values using a computer-assisted software program (MicroSuite version 5; Olympus Corporation, Tokyo, Japan). The intensity of the ROI (sum of the pixel values within the region of interest) was measured from the pre-targeted and targeted image. The net contrast enhancement ($CE = C_t - C_{pt}$) was determined and the CE ratio (CER) was calculated using the following equation: $CER = (C_t - C_{pt})/C_{pt} \times 100\%$ where C_{pt} = pixel intensities from ROI of pre-targeted image and C_t = pixel intensities from ROI of targeted image. As mentioned above Ct is the difference between the intensity of signals from images taken at lower mechanical index 5min after injection of targeted agents and after the delivery of a destructive pulse at high mechanical index.

Ovarian gross morphologic evaluation

All hens were euthanized after targeted imaging and examined for the presence of a solid mass in the ovary and any other organs, ascitic fluid, preovulatory follicles, and atrophy of the ovary, as reported previously[21]. Gross observation was compared with the sonographic evaluations and photographed. A normally functional ovary had viable preovulatory follicles (more detailed information on hen ovarian physiology has been published elsewhere[21, 28]), whereas no large follicles or visible lesions were found in normal hens that stopped egg laying. Tumor staging was performed according to the gross metastatic status, as reported previously[21]. Briefly, early OVCA was characterized by detectable formation of solid tumor limited to the ovary. Late stages

For Peer Review

of OVCA were characterized by tumor metastasis to distant organs with moderate to extensive ascites.

Histologic evaluation and immunohistochemical detection of ovarian microvessels

Representative portions of a solid ovarian mass or the whole ovary (in cases of atrophic or grossly normal-appearing ovaries) were divided into several blocks, processed for paraffin or frozen sections, and stained with hematoxylin-eosin. Microscopic tumor (if present) in any part of the ovary was detected by routine histologic examination with hematoxylin-eosin staining, and tumor types were determined by light microscopy, as reported previously[21].

After histopathologic examination, paraffin sections (4 μm thick) of normal and malignant ovaries of all stages and types were processed for routine immunohistochemistry to assess the tumor-associated microvessel density using rabbit anti-chicken VEGFR2 polyclonal antibodies. The frequencies of VEGFR2-expressing microvessels were determined from the vicinity of tumor or ovarian stroma of normal hens (excluding the follicular areas), as reported earlier[29, 32] using a light microscope attached to digital imaging stereological software (MicroSuite version 5; Olympus Corporation) with little modification. Briefly, immunostained slides were examined at low-power magnification (x10 objective and x10 ocular) to identify the areas of maximum neovascularization of the tumor. Vessels with thick, regular, and complete muscular walls as well as vessels with large lumina were excluded from the count, as reported previously[29]. In each section, the 5 most vascular areas were chosen. The number of microvessels in a 20,000-μm^2 area was counted at an x40 objective and x10 ocular magnification. The averages of these sections were expressed as the number of immunopositive microvessels in a

For Peer Review

20,000-μm^2 area of a normal or tumorous ovary. Tumor histologic and immunohistochemical observations were compared to the sonographic predictions.

Statistical Analysis

Descriptive statistics for imaging parameters were determined, and statistical analysis was performed in SPSS version 15 (SPSS Inc, Chicago, IL The differences in the net ultrasound signal intensities and the frequencies of VEGFR2-expressing microvessels among normal hens or hens with early and late stage OVCA were analyzed by the two-sample *t* test. The association between the net ultrasound signal intensity and the frequency VEGFR2-expressing microvessels was examined by Pearson coefficient of correlations. $P < 0.05$ was considered significant. All reported *P* values are 2 sided.

RESULTS

Evaluation of non-invasive targeted ultrasound imaging

On pre-targeted and targeted imaging, multiple preovulatory follicles and small growing stromal follicles were observed in normal hens with functional ovaries. Compared to pre-targeted ovaries, visualization of solid ovarian masses with or without projected septa and papillary structures, accompanying ascites, or both were enhanced remarkably in the ovaries of 26 hens. Of these 26 hens, 18 had solid masses in the ovary together with profuse ascites and were predicted to have late-stage OVCA (**Figure 1**). In the remaining 8 hens, solid masses were limited to a part of the ovary with no or little ascites, and they were provisionally categorized as early-stage OVCA (**Figures 2**). All hens were euthanized following VEGFR2-targeted imaging

For Peer Review

and sonographic predictions as well as stages of the tumor were confirmed by gross examination of hens at necropsy (**Figures 1-2**).

Gross morphology including the presence of ovarian follicles, atrophied ovaries and oviducts, presence of solid tumor mass in the ovary, extent of tumor metastasis, stages of OVCA and accompanying ascites, was recorded. Ovarian tumors and their types were confirmed by routine histological examination with hematoxylin-eosin staining (**Figures 1-2**). Staging of ovarian tumors was performed as reported previously[21]. As predicted by sonographic examinations, late stage OVCA (n = 18 hens including 7 serous, 9 endometrioid, 2 mucinous) was accompanied with moderate to profuse ascites and metastasized to peritoneal and abdominal organs. In early stage OVCA (n = 8 including 3 serous, 4 endometrioid, 1mucinous), tumors were limited to the ovary with no or very little ascites. In addition, histological examinations confirmed the presence of microscopic ovarian carcinoma in 6 hens (3 serous and 3 endometrioid) that had no detectable ovarian mass during VEGFR-2 targeted gray scale scan as well as at gross.

Overall, in contrast to the pre-targeted scan, the pixel intensities of the signals from normal ovaries or ovaries with tumor increased significantly after the injection of VEGFR2-targeted microbubbles (**Figure 3A**). The average net enhancement of signal intensity due to VEGFR2-targeted imaging for low laying healthy hens was 805700.61 $\pm$ 296220.42 pixels (n = 20, mean $\pm$ SD) (22.92 % over the pre-targeted) and it was significantly (P<0.0001) higher in hens with tumor masses limited to a part of the ovaries (early stage, n = 8, 1382219.22 $\pm$ 584123.62 pixels) (34.78% over the pre-targeted) (**Figure 3B**). The net signal intensity enhanced further (P<0.0001) in hens with large solid ovarian masses accompanied with profuse ascites (late stage, n = 18, 2028421.08 $\pm$ 723585.62 pixels) (39.13% over the pre-targeted) (**Figure 3B**).

For Peer Review

Pre-and post-targeted ultrasound signal intensities were not found to be significantly different among different histological sub-types of ovarian tumors.

Immunohistochemical detection of VEGFR2-expressing ovarian tumor associated neo-angiogenic microvessels

Paraffin sections of normal ovaries or ovaries with tumor were immunostained for the detection of VEGFR2-expressing microvessels using anti-VEGFR2 antibodies as primary antibodies mentioned above. VEGFR2-expressing microvessels were detected in both normal ovaries and ovaries with tumor (**Figure 4**A-C). In normal ovaries, very few VEGFR2-expressing microvessels were seen in the follicular theca and the ovarian stroma (**Figure 4**A). Immunoreactive microvessels expressing VEGFR2 were localized at the spaces between tumor glands (vicinity of the tumor, **Figure 4B-C**). Compared with normal ovary, many VEGFR2-expressing microvessels were localized in the vicinity of the tumor in hens with OVCA. Occasionally, ovarian tumor epithelia were also found positive for VEGFR-2 expression. The frequencies of VEGFR2-expressing microvessels were significantly (P<0.0001) greater in hens with early stage OVCA (mean $\pm$ SD= 13.48 $\pm$ 0.52 in 20,000μm^2 of tumor tissue) than in normal hens (3.12 $\pm$ 0.59 in 20,000μm^2 of ovarian stromal tissue) and increased further (P<0.0001) in hens with late stage of OVCA (18.33 $\pm$ 1.57 in 20,000μm^2 of tumor tissue) (**Figure 5**). Differences in the frequencies of VEGFR2-expressing microvessels were not observed among different histological sub-types of malignant ovarian tumors in hens.

Increases in signal intensities due to VEGFR2-targeted imaging were positively correlated with the frequencies of VEGFR2-expressing microvessels in ovarian tumors at early stage (r = 0.46) and late stage (r = 0.70). These results support the predictions of VEGFR2-

For Peer Review

targeted imaging that enhanced signal intensity due to the VEGFR2-targeted imaging in hens with tumors were due to the increased tumor associated microvessels in their ovaries.

DISCUSSION

This is the first study on the suitability of VEGFR2-targeted imaging probes on the enhancement of *in vivo* visualization of ovarian tumors in a preclinical model of spontaneous ovarian cancer. The results of this study demonstrated that VEGFR2-targeted imaging probes bound with their targets in spontaneous ovarian tumors at early and late stages in hens and enhanced ultrasound signal intensities from these tumors.

Tumor-associated neo-angiogenesis is an early event in ovarian tumor development and presents a potential target for *in vivo* imaging to detect OVCA at early stage[4, 5, 29]. VEGFR2 is an established marker of angiogenic microvessels which is expressed in low levels in quiescent endothelial cells and highly up-regulated during angiogenesis[6]. Over expression of VEGFR2 by the angiogenic endothelium in solid tumors offers a molecular target for the delivery of imaging agents directly to the tumor vasculature[16, 18]. Previous studies have reported the binding of VEGFR2-targeted imaging agents with their targets in induced tumors in rodents[16-19] and this study demonstrated the bindings of VEGFR2-targeted imaging agents with their targets in spontaneous ovarian tumors in hens. In the present study, compared with pre-targeted, VEGFR2-targeted ultrasound imaging agents increased the visualization of ovarian vasculature in tumor bearing ovaries. As expected, compared with pre-targeted signal, the enhancement of ultrasound signals increased significantly following the injection of VEGFR2-targeted imaging agents in hens with large solid tumor mass even detectable by non-targeted gray scale TVUS. These

For Peer Review

observations suggest a proof-of-principle that VEGFR2-targeted imaging agents can also enhance the detection of spontaneous ovarian tumors in hens as reported for induced tumors in rodents [16, 19].

In addition to the enhancement of ultrasound signals from large solid ovarian masses, VEGFR2-targeted ultrasound imaging detected ovarian tumors when the tumor was limited to a part of the ovary. Pre-targeted gray scale imaging signals from these early stage ovarian tumors were inclusive. However, compared with pre-targeted imaging, VEGFR2-targeted imaging enhanced ultrasound signal intensity significantly from these hens. On the other hand, VEGFR2-targeted imaging probes failed to enhance the signal intensity from hens with microscopic tumors suggesting that VEGFR2-targeted imaging may detect early stage OVCA when the tumor protrudes from the stroma (forming a small mass)[7, 6] but not the microscopic ones (embedded in the stroma).

In this study, ultrasound predictions of tumor associated neoangiogenesis were tested by immunohistochemical localization of VEGFR2-expressing microvessels in ovaries with tumors at early and late stages. Compared with normal ovaries, significant increase in the frequencies of ovarian tumor associated microvessels in early and late stage OVCA confirms the predictions of ultrasound signal intensities detected by VEGFR2-targted microvessels. Similar observations were also reported following injection of VEGFR2-targeted imaging agents in induced tumors in rodents [16-18]. The intensities of VEGFR2-targeted ultrasound imaging from hens with early and late stage OVCA was positively correlated with frequencies of ovarian angiogenic microvessels suggesting that increased ultrasound signal intensity was due to the increased frequency of

For Peer Review

microvessels in these hens. Thus VEGFR2-targeted imaging agent enhanced the detection of spontaneous ovarian tumors in hens by binding with their targets in the tumors.

From translational aspects, the results observed in the present study have several unique features. *First*, most of the previous studies used rodent models with induced tumors. In contrast, this study used domestic hens, the only widely available and easily accessible spontaneous model of OVCA. Rodents do not develop spontaneous OVCA and the histopathology of induced OVCA is different than that of spontaneous OVCA. Moreover, anatomical differences in the location of induced rodent models (subcutaneous tumor) compared with deeper tissue like the ovary may also affect on the transduction of ultrasound signals as well as the behavior of contrast agents. Thus information on the binding ability and detection of spontaneous OVCA by VEGFR2-targeted imaging agents is essential. *Second* and perhaps most importantly, poultry farms are available in most places making the hens easy to access to test and develop targeted imaging agents as well as anti-angiogenic drugs for the detection and treatment of spontaneous OVCA. Moreover, because of lower cost of hens, this model also offers testing toxicological studies of any newly developed imaging agent or therapeutic in a cost-effective way. Currently, studies with hens are ongoing in which animals are being monitored prospectively with VEGFR2-targeted microbubbles together with serum markers to detect spontaneous ovarian tumor development at relatively earlier stages. This study has also some limitations. One of the main concerns of using VEGFR2-targeted imaging agent is its specificity for tumor specific microvessels as the angiogenesis (in developing follicles) is a common phenomenon in the ovaries of women of reproductive age. However, as observed in this study, the morphology of developing ovarian follicles is very distinct and can be easily detected during gray scale

For Peer Review

sonography and excluded from the analysis. Additionally, we did not use animals with benign ovarian tumors. Small sample size specially the number of hens with ovarian tumors may also be a limitation of this study.

In conclusion, the results of this study suggest that the VEGFR2-targeted imaging probes bind with their targets expressed by the spontaneous ovarian tumors in hens and enhance the visualization of tumors at early and late stages. Our results also suggest that laying hens offer a new platform for testing and development of new imaging agents and targeted anti-angiogenic therapeutics.

REFERENCES

1. American, CS (2013). Cancer Facts & Figures 2013 http://www.cancer.org/research/cancerfactsstatistics/cancerfactsfigures2013/index.

2. Siegel R, Naishadham D, Jemal A. CA Cancer J Clin. 2013; 63:11-30

3. Buys SS, Partridge E, Black A, Johnson CC, Lamerato L, Isaacs C, Reding DJ, Greenlee RT, Yokochi LA, Kessel B, Crawford ED, Church TR, Andriole GL, Weissfeld JL, Fouad MN, Chia D, O'Brien B, Ragard LR, Clapp JD, Rathmell, Riley TL, Hartge P, Pinsky PF, Zhu CS, Izmirlian G, Kramer BS, Miller AB, Xu JL, Prorok PC, Gohagan JK, Berg CD. Effect of screening on ovarian cancer mortality: the Prostate, Lung, Colorectal and Ovarian (PLCO) Cancer Screening Randomized Controlled Trial. JAMA, 2011; **305**: 2295-2303.

4. Folkman J. What is the evidence that tumors are angiogenesis dependent? J Natl Cancer Inst. 1990; **82**: 4-6.

For Peer Review

5. Ramakrishnan S, Subramanian IV, Yokoyama Y, Geller M. Angiogenesis in normal and neoplastic ovaries. Angiogenesis. 2005; **8**: 169-182.

6. Hicklin DJ, Ellis LM. Role of the vascular endothelial growth factor pathway in tumor growth and angiogenesis. J Clin Oncol. 2005; **23**: 1011-1027.

7. Folkman J. "Angiogenesis." Annu Rev Med. 2006; **57**: 1-18.

8. Cao Y, Arbiser J, D'Amato RJ, D'Amore PA, Ingber DE, Kerbel R, Klagsbrun M, Lim S, Moses MA, Zetter B, Dvorak H, Langer R. "Forty-year journey of angiogenesis translational research." Sci Transl Med. 2011; **3**: 114rv3.

9. Escudier B, Eisen T, Stadler WM, Szczylik C, Oudard S, Siebels M, Negrier S, Chevreau C, Solska E, Desai AA, Rolland F, Demkow T, Hutson TE, Gore M, Freeman S, Schwartz B, Shan M, Simantov R, Bukowski RM. Sorafenib in advanced clear-cell renal-cell carcinoma. N Engl J Med. 2007; **356**: 125-134.

10. Motzer RJ, Hutson TE, Tomczak P, Michaelson MD, Bukowski RM, Rixe O, Oudard S, Negrier S, Szczylik C, Kim ST, Chen I, Bycott PW, Baum CM and Figlin RA (2007). Sunitinib versus interferon alfa in metastatic renal-cell carcinoma. N Engl J Med, 2007; **356**: 115-124.

11. Abramowicz, JS. Ultrasonographic contrast media: has the time come in obstetrics and gynecology? J Ultrasound Med. 2005; **24**: 517-531.

12. Dutta S, Wang FQ, Fleischer AC, Fishman DA. New frontiers for ovarian cancer risk evaluation: proteomics and contrast-enhanced ultrasound. AJR Am J Roentgenol. 2010; **194**: 349-354.

13. Fleischer AC, Lyshchik A, Andreotti RF, Hwang M, Jones 3rd HW, Fishman DA. Advances in sonographic detection of ovarian cancer: depiction of tumor neovascularity with microbubbles. Am J Roentgenol. 2010; **194**: 343-348.

For Peer Review

14. Fleischer AC, Lyshchik A, Jones 3rd HW, Crispens MA, Andreotti RF, Williams PK, Fishman DA. Diagnostic parameters to differentiate benign from malignant ovarian masses with contrast-enhanced transvaginal sonography. J Ultrasound Med. 2009; **28**: 1273-1280.

15. Fleischer AC, Lyshchik A, Jones Jr HW, Crispens M, Loveless M, Andreotti RF, Williams PK, Fishman DA. Contrast-enhanced transvaginal sonography of benign versus malignant ovarian masses: preliminary findings. J Ultrasound Med. 2008; 27: 1011-1008; quiz 1019-1021.

16. Lee DA, Lyshchik A, Huamani J, Hallahan DE, Fleischer AC. Relationship between retention of a vascular endothelial growth factor receptor 2 (VEGFR2)-targeted ultrasonographic contrast agent and the level of VEGFR2 expression in an in vivo breast cancer model. J Ultrasound Med, 2008; **27**: 855-866.

17. Lyshchik A, Fleischer AC, Huamani J, Hallahan DE, Brissova M, Gore JC. Molecular imaging of vascular endothelial growth factor receptor 2 expression using targeted contrast-enhanced high-frequency ultrasonography. J Ultrasound Med.2007; **26**: 1575-1586.

18. Willmann JK, Paulmurugan R, Chen K, Gheysens O, Rodriguez-Porcel M, Lutz AM, Chen IY, Chen X, Gambhir SS. US imaging of tumor angiogenesis with microbubbles targeted to vascular endothelial growth factor receptor type 2 in mice. Radiology. 2008; **246**: 508-518.

19. Willmann JK, Lutz AM, Paulmurugan R, Patel MR, Chu P, Rosenberg J, Gambhir SS. Dual-targeted contrast agent for US assessment of tumor angiogenesis in vivo. Radiology. 2008; **248**: 936-944.

20. Rodriguez-Burford C, Barnes MN, Berry W, Partridge EE, Grizzle WE. Immunohistochemical expression of molecular markers in an avian model: a potential model for preclinical evaluation of agents for ovarian cancer chemoprevention. Gynecol Oncol. 2001; **81**: 373-379.

For Peer Review

21.Barua A, Bitterman P, Abramowicz JS, Dirks AL, Bahr JM, Hales DB, Bradaric MJ, Edassery SL, Rotmensch J, Luborsky. Histopathology of ovarian tumors in laying hens: a preclinical model of human ovarian cancer. Int J Gynecol Cancer. 2009; **19**: 531-539.

22. Fredrickson TN. "Ovarian tumors of the hen. Environ Health Perspect. 1987; **73**: 35-51.

23. Jackson E, Anderson K, Ashwell C, Petitte J, Mozdziak PE. CA125 expression in spontaneous ovarian adenocarcinomas from laying hens. Gynecol Oncol. 2007; **104**: 192-198.

24. Stammer K, Edassery SL, Barua A, Bitterman P, Bahr JM, Hales DB, Luborsky JL. Selenium-Binding Protein 1 expression in ovaries and ovarian tumors in the laying hen, a spontaneous model of human ovarian cancer. Gynecol Oncol. 2008; **109**: 115-121.

25. Giles JR, HL Shivaprasad, Johnson PA. Ovarian tumor expression of an oviductal protein in the hen: a model for human serous ovarian adenocarcinoma. Gynecol Oncol. 2004; 95: 530-533.

26. Khan MF, Bahr JM, Yellapa Y, Bitterman P, Abramowicz JS, Edassery SL, Basu S, Rotmensch J, Barua A. "Expression of Leukocyte Inhibitory Immunoglobulin-like Transcript 3 Receptors by Ovarian Tumors in Laying Hen Model of Spontaneous Ovarian Cancer." Transl Oncol. 2012; **5**: 85-91.

27. Yellapa A, Bahr JM, Bitterman P, Abramowicz JS, Edassery SL, Penumatsa K, Basu s, Rotmensch J, Barua A. Association of interleukin 16 with the development of ovarian tumor and tumor-associated neoangiogenesis in laying hen model of spontaneous ovarian cancer. Int J Gynecol Cancer. 2012; **22**: 199-207.

28. Barua A, Abramowicz JS, Bahr JM, Bitterman P, Dirks A, Holub KA, Sheiner E, Bradaric MJ, Edassery SL, Luborsky JL. Detection of ovarian tumors in chicken by sonography: a step toward early diagnosis in humans? J Ultrasound Med.2007; **26**: 909-919.

For Peer Review

29. Barua A, Bitterman P, Bahr JM, Bradaric MJ, Hales DB, Luborsky JL, Abramowicz JS. Detection of tumor-associated neoangiogenesis by Doppler ultrasonography during early-stage ovarian cancer in laying hens: a preclinical model of human spontaneous ovarian cancer. J Ultrasound Med. 2010; **29**: 173-182.

30. Barua A, Bitterman P, Bahr JM, Basu S, Sheiner E, Bradaric MJ, Hales DB, Luborsky JL, Abramowicz JS. Contrast-enhanced sonography depicts spontaneous ovarian cancer at early stages in a preclinical animal model. J Ultrasound Med, 2011; **30**: 333-345.

31. Anderson CR, Rychak JJ, Backer M, Backer J, Ley K, Klibanov AL. scVEGF microbubble ultrasound contrast agents: a novel probe for ultrasound molecular imaging of tumor angiogenesis. Invest Radiol. 2010; **45**: 579-585.

32. Barua A, Yellapa A, Bahr JM, Abramowicz JS, Edassery SL, Basu S, Rotmensch J, Bitterman P. Expression of death receptor 6 by ovarian tumors in laying hens, a preclinical model of spontaneous ovarian cancer. Transl Oncol. 2012; **5**: 260-268.

For Peer Review

Figure legends:

Figure 1. Enhancement of visualization of spontaneous ovarian tumors in hens by VEGFR2-targeted ultrasound imaging agents. *(a-b)* Pre-targeted (a) and post-targeted (b, 7 min after the injection of VEGFR2-targeted imaging agents) gray scale image of an ovary. Compared with pre-targeted, remarkable increase in signal intensity was observed in post-targeted imaging (dotted line shows the solid tumor mass). c) Corresponding gross ovarian tumor (dotted line) appears like loafs of meat confirming the prediction of targeted ultrasound molecular imaging. d) Histological sub-type of the corresponding tumor showing endometrioid carcinoma containing back to back tumor glands with sharp luminal lining. Original magnification = 40X. As = ascitic fluid, S=stroma, Tu=tumor.

Figure 2. Detection of spontaneous ovarian tumors at early stage in hens by VEGFR2-targeted ultrasound imaging. A) Pre-targeted ovarian sonogram showing low signal intensity from a suspected small mass in the ovary. B) Corresponding post-targeted sonogram with enhanced visualization and increased signal intensity confirming the presence of a small solid mass in the ovary. C) Gross morphology shows the presence of a tissue mass limited to the ovary accompanied with a little ascites. D) Corresponding histological sub-type of the tumor showing serous carcinoma with a sheath-like structure surrounded by fibromuscular layer and malignant cells containing pleomorphic nuclei. Original magnification = 40X. Legends are similar to those mentioned in figure 1.

Figure 3. Improvement in ultrasound signal intensity by VEGFR2-targeted imaging agent in the ovary of laying hens with or without ovarian tumors. *A*): Compared with pre-targeted imaging, VEGFR2-targeted imaging agents increased ultrasound signal intensities significantly

For Peer Review

(P<0.0001) irrespective of ovarian pathological status. *B*): Compared with normal, the net enhancement of ultrasound signal intensity was significantly (P<0.0001) higher in hens with ovarian tumors at early or late stages. Different letters denote significant differences in ultrasound signal intensities between the pre- or post-targeted imaging within the same or among different stages of OVCA.

Figure 4. Immunohistochemical detection of VEGFR2-expressing microvessels in hen ovaries with or without spontaneous tumors. A) Section of a normal ovary showing few immunoreactive microvessls in the ovarian stroma and theca layer of a stromal follicle. B) Section of an ovary with early stage OVCA. Compared with normal, increased number of immunoreactive VEGFR2-expressing microvessels is seen in the vicinity of the tumor. C) Section of an ovarian tumor at late stage. Many immunoreactive VEGFR2-expressing microvessels are seen in the vicinity of the tumor. Arrows indicate the examples of immunoreactive VEGFR2-expressing microvessels. Original magnification = 40X. G=granulosa layer of the follicle, S= stroma, T= theca layer of the follicle, Tu = tumor. 40X.

Figure 5: Changes in the frequency of VEGFR2-expressing microvessels in the ovaries in hens with or without tumors. The frequency of VEGFR2-expressing microvessels was significantly (P<0.0001) high in the ovaries with early stage ovarian tumors and increased further in hens with late stage OVCA. Different letters denote significant differences in the frequency of VEGFR2-expressing microvessels among different pathological groups.

For Peer Review

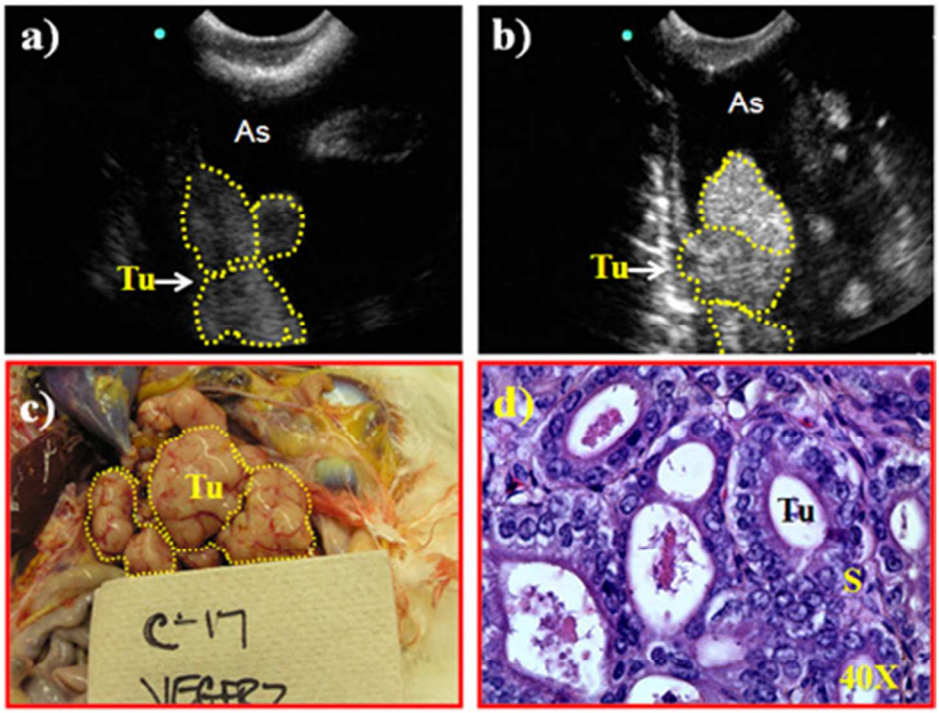

Figure 1

Figure 1. Enhancement of visualization of spontaneous ovarian tumors in hens by VEGFR2-targeted ultrasound imaging agents. (a-b) Pre-targeted (a) and post-targeted (b, 7 min after the injection of VEGFR2-targeted imaging agents) gray scale image of an ovary. Compared with pre-targeted, remarkable increase in signal intensity was observed in post-targeted imaging (dotted line shows the solid tumor mass). c) Corresponding gross ovarian tumor (dotted line) appears like loafs of meat confirming the prediction of targeted ultrasound molecular imaging. d) Histological sub-type of the corresponding tumor showing endometrioid carcinoma containing back to back tumor glands with sharp luminal lining. Original magnification = 40X. As = ascitic fluid, S=stroma, Tu=tumor.
39x33mm (300 x 300 DPI)

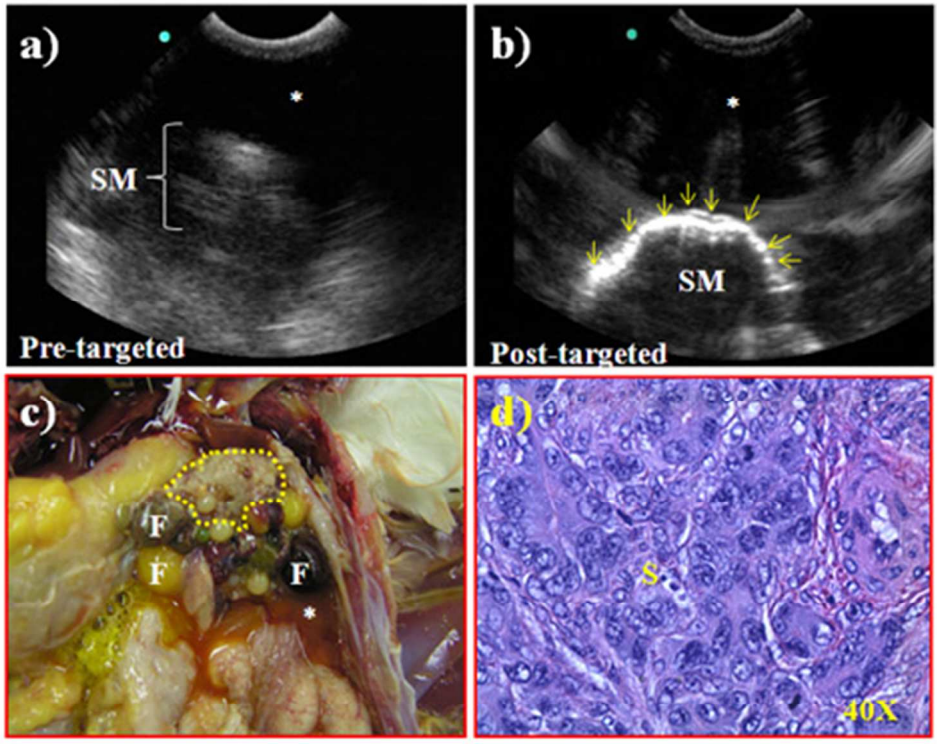

Figure 2

Figure 2. Detection of spontaneous ovarian tumors at early stage in hens by VEGFR2-targeted ultrasound imaging. A) Pre-targeted ovarian sonogram showing low signal intensity from a suspected small mass in the ovary. B) Corresponding post-targeted sonogram with enhanced visualization and increased signal intensity confirming the presence of a small solid mass in the ovary. C) Gross morphology shows the presence of a tissue mass limited to the ovary accompanied with a little ascites. D) Corresponding histological sub-type of the tumor showing serous carcinoma with a sheath-like structure surrounded by fibromuscular layer and malignant cells containing pleomorphic nuclei. Original magnification = 40X. Legends are similar to those mentioned in figure 1.
39x34mm (300 x 300 DPI)

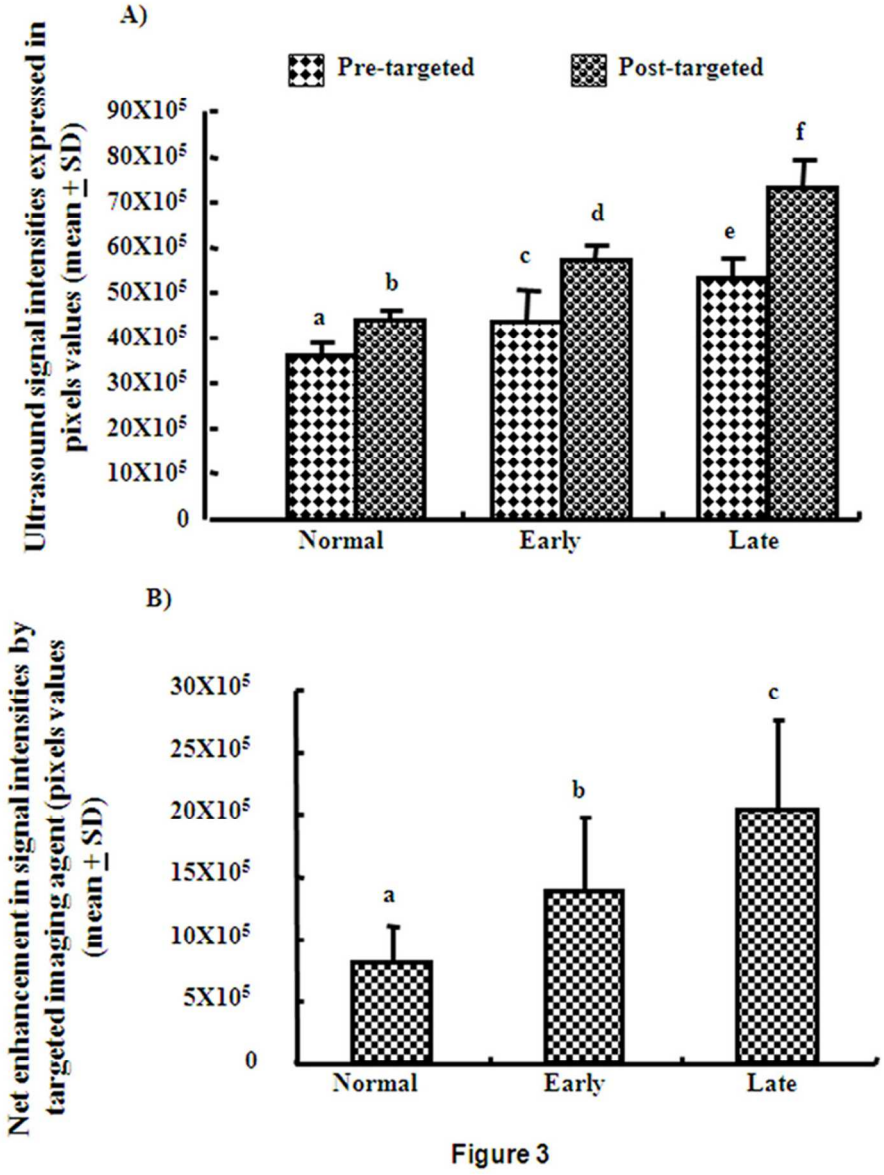

Figure 3

Figure 3. Improvement in ultrasound signal intensity by VEGFR2-targeted imaging agent in the ovary of laying hens with or without ovarian tumors. A): Compared with pre-targeted imaging, VEGFR2-targeted imaging agents increased ultrasound signal intensities significantly (P<0.0001) irrespective of ovarian pathological status. B): Compared with normal, the net enhancement of ultrasound signal intensity was significantly (P<0.0001) higher in hens with ovarian tumors at early or late stages. Different letters denote significant differences in ultrasound signal intensities between the pre- or post-targeted imaging within the same or among different stages of OVCA.
40x54mm (600 x 600 DPI)

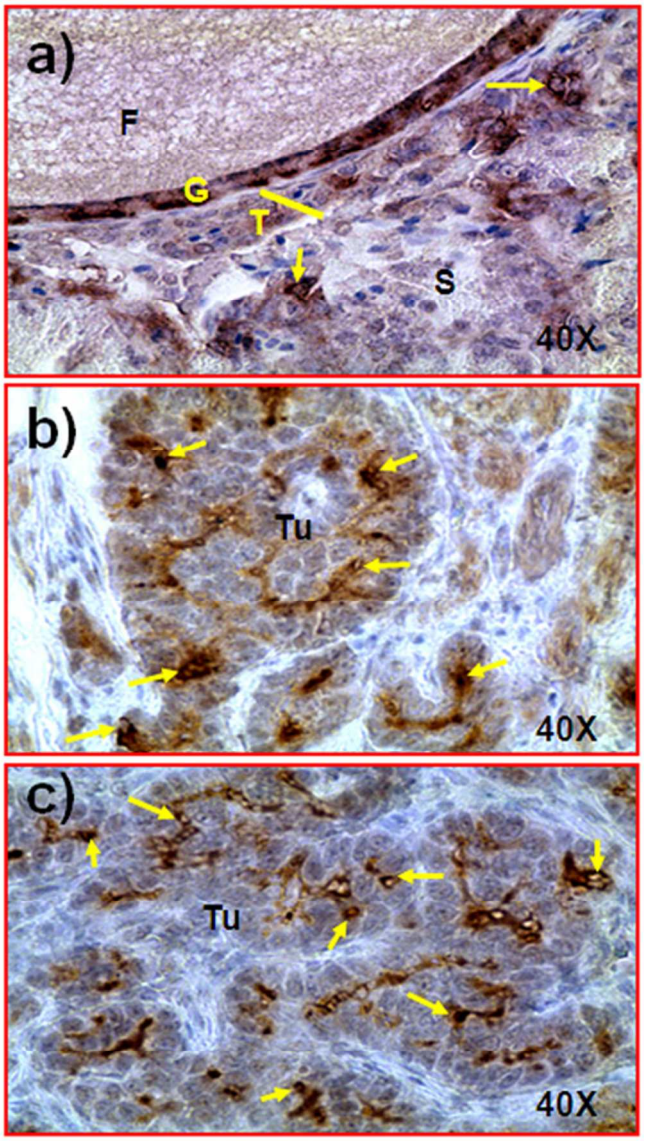

Figure 4

Figure 4. Immunohistochemical detection of VEGFR2-expressing microvessels in hen ovaries with or without spontaneous tumors. A) Section of a normal ovary showing few immunoreactive microvessls in the ovarian stroma and theca layer of a stromal follicle. B) Section of an ovary with early stage OVCA. Compared with normal, increased number of immunoreactive VEGFR2-expressing microvessels is seen in the vicinity of the tumor. C) Section of an ovarian tumor at late stage. Many immunoreactive VEGFR2-expressing microvessels are seen in the vicinity of the tumor. Arrows indicate the examples of immunoreactive VEGFR2-expressing microvessels. Original magnification = 40X. G=granulosa layer of the follicle, S= stroma, T= theca layer of the follicle, Tu = tumor. 40X.
39x73mm (300 x 300 DPI)

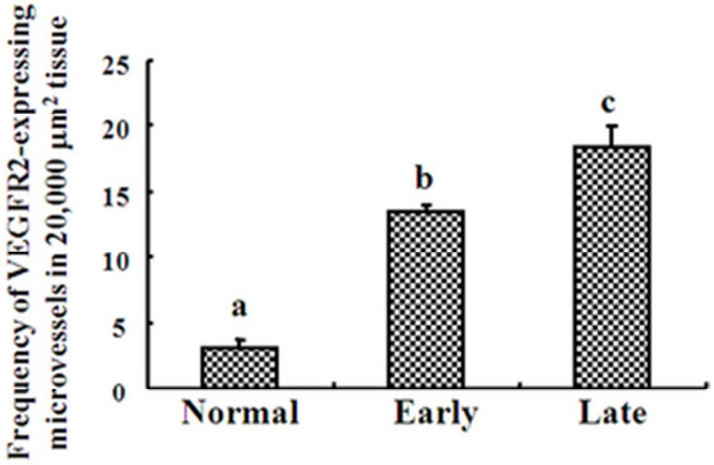

Figure 5

Figure 5: Changes in the frequency of VEGFR2-expressing microvessels in the ovaries in hens with or without tumors. The frequency of VEGFR2-expressing microvessels was significantly ($P<0.0001$) high in the ovaries with early stage ovarian tumors and increased further in hens with late stage OVCA. Different letters denote significant differences in the frequency of VEGFR2-expressing microvessels among different pathological groups.
15x11mm (600 x 600 DPI)

For Review

Interleukin 16 expression changes in association with ovarian malignant transformation

Aparna Yellapa, MS; Pincas Bitterman, MD; Sameer Sharma, MD; Alfred S. Guirguis, MD; Janice M. Bahr, PhD; Sanjib Basu, PhD; Jacques S. Abramowicz, MD; Animesh Barua, PhD

OBJECTIVE: Long-term unresolved inflammation has been suggested as a risk factor for the development of various malignancies. The goal of this study was to examine whether the expression of interleukin (IL)-16, a proinflammatory cytokine, changes in association with ovarian cancer (OVCA) development.

STUDY DESIGN: In an exploratory study, changes in IL-16 expression in association with OVCA development and progression were determined using ovarian tissues and serum samples from healthy subjects (n = 10) and patients with benign (n = 10) and malignant ovarian tumors at early (n = 8) and late (n = 20) stages. In the prospective study, laying hens, a preclinical model of spontaneous OVCA, were monitored (n = 200) for 45 weeks with serum samples collected at 15-week interval. Changes in serum levels of IL-16 relative to OVCA development were examined.

RESULTS: The frequency of IL-16–expressing cells increased significantly in patients with OVCA ($P < .001$) compared to healthy subjects and patients with benign ovarian tumors. The concentration of serum IL-16 was higher in patients with benign tumors ($P < .05$) than in healthy subjects and increased further in patients with early-stage ($P < .05$) and late-stage ($P < .03$) OVCA. Increase in tissue expression and serum levels of IL-16 in patients with early and late stages of OVCA were positively correlated with the increase in ovarian tumor–associated microvessels. Prospective monitoring showed that serum levels of IL-16 increase significantly ($P < .002$) even before ovarian tumors become grossly detectable in hens.

CONCLUSION: This study showed that tissue expression and serum levels of IL-16 increase in association with malignant ovarian tumor development and progression.

Key words: interleukin 16, laying hen model, malignant transformation, ovarian cancer

Cite this article as: Yellapa A, Bitterman P, Sharma S, et al. Interleukin 16 expression changes in association with ovarian malignant transformation. Am J Obstet Gynecol 2014;210:x.ex-x.ex.

Ovarian cancer (OVCA) is a fatal malignancy in women with the highest incidence-to-death ratio among gynecological cancers.[1] The 5-year survival of OVCA patients is >90% when it is detected at an early stage as compared with those detected at late stages.[2,3] Thus, metastasis of OVCA is the main cause of the high death rate of OVCA patients. Nonspecificity of symptoms at early stage makes early detection of OVCA very difficult.[4] Hence, most cases of OVCA are detected at late stages. Circulating levels of CA-125 alone or in combination with transvaginal ultrasound (TVUS) are used for OVCA detection. Although CA-125 is a better prognostic marker than others, it is not specific for early-stage OVCA. On the other hand, the resolution of traditional TVUS is limited for detecting ovarian tumors at early stage. A combination of serum CA-125 and traditional TVUS scan did not improve early detection of OVCA substantially.[5-7] Thus, an effective early detection test for OVCA remains to be established. Furthermore, the pattern of OVCA dissemination is very different from other solid tumors. The tumor usually spreads in a diffuse intraabdominal fashion in addition to systemic circulation and the tumor microenvironment plays critical roles in early OVCA metastasis.[8] Moreover, emerging information suggests that serous OVCA may originate from malignant transformation of precursor lesions in the fimbria of fallopian tube, which later exfoliate to the surface of the ovary.[9,10] In addition, endometriosis has also been suggested as a risk factor for endometrioid ovarian carcinoma.[11,12]

From the Departments of Pharmacology (Ms Yellapa and Drs Sharma and Barua), Pathology (Drs Bitterman and Barua), Obstetrics and Gynecology (Drs Sharma, Guirguis, and Barua), and Preventive Medicine (Biostatistics) (Dr Basu), Rush University Medical Center, Chicago, and Department of Animal Sciences, University of Illinois at Urbana-Champaign, Urbana (Dr Bahr), IL, and Department of Obstetrics and Gynecology, Wayne State University School of Medicine, Detroit, MI (Dr Abramowicz).

Received Sept. 4, 2013; revised Nov. 24, 2013; accepted Dec. 27, 2013.

Supported in part by the Elmer Sylvia and Sramek Foundation (United States) and the US Department of Defense, Ovarian Cancer Research Program, Pilot Award (W81XWH-11-1-0510).

The authors report no conflict of interest.

Presented in oral format at the 80th annual meeting of the Central Association of Obstetricians and Gynecologists, Napa, CA, Oct. 16-19, 2013.

Reprints: Animesh Barua, PhD, Department of Pharmacology, Laboratory for Translational Research on Ovarian Cancer, Room 410, Cohn Bldg., Rush University Medical Center, 1735 W. Harrison St., Chicago, IL 60612. Animesh_Barua@rush.edu.

0002-9378/$36.00
© 2014 Mosby, Inc. All rights reserved.
http://dx.doi.org/10.1016/j.ajog.2013.12.041

Therefore, information on early changes associated with OVCA development as well as factors favoring early metastasis of OVCA is critical to establish an early detection test and to prevent recurrence of OVCA as well as to improve the quality of life of OVCA patients.

The microscopic characteristics of the nucleus of the cell have long been used in pathology to differentiate malignant cells from normal ones[13] and similar to other cancers, malignant nuclear transformation is an early event in OVCA development. Inflammation has been suggested as a risk factor for malignant transformation.[14] Unresolved inflammation leads to hypoxic conditions accompanied by changes in inflammatory cytokines including interleukin (IL)-16.[14,15] Classic members of the immune system including CD8 T cells and monocytes/macrophages are the primary sources of IL-16.[16-18] IL-16 has been reported to be associated with initiation of proinflammatory processes and chemotaxis of immune cells (eg, CD4 T cells) to the site of inflammation[15,19,20] as well as in several malignancies.[21,22] Ovulation has been reported as an inflammatory process and frequent ovulation has been suggested as a risk factor for OVCA.[23] Thus, ovarian tissues are exposed to sustained inflammatory factors including IL-16, a proinflammatory cytokine and it is possible that IL-16 may be associated with malignant ovarian transformation and progression of OVCA. However, information on the involvement of IL-16 in ovarian tumor development is not known.

Tumors require blood supply for their growth and tumor-associated neoangiogenesis is the formation of new vessels from existing ones.[24] Tumor-associated neoangiogenesis is an early event in tumor development preceded by malignant nuclear transformation.[25] Multiple studies have suggested that tumor-secreted factors in association with other components of the tumor microenvironment stimulate the development of tumor-associated microvessels from existing blood vessels. It has been reported that IL-16 stimulates production of proinflammatory and proangiogenic factors IL-15 and IL-8 by members of immune system including $CD4^+$ macrophages.[26-28] Macrophages as well as different subsets of T cells are present in the tumor microenvironment.[29] It is possible that tumor-secreted factors may induce immune cells including macrophages in the tumor microenvironment to produce IL-16, which may stimulate the development of tumor-associated neoangiogenesis. However, no information is available on ovarian tumor–secreted factors and their involvement in the development of tumor-associated angiogenesis.

The goal of this study was to examine the association of IL-16 with the development and progression of OVCA. We hypothesized that the expression of IL-16 by ovarian tissues and its serum concentrations would be increased in association with malignant ovarian transformation and OVCA progression. This hypothesis was tested by 2 objectives: (1) determine the expression of IL-16 in normal ovaries or ovaries with tumor and serum levels of IL-16 in healthy women and OVCA patients; and (2) determine if the concentration of IL-16 increases in serum before the ovarian tumor forms a solid mass and becomes grossly detectable. Because it is difficult to identify patients at early-stage OVCA, access to patient's specimens remains a significant barrier to study alterations associated with early-stage ovarian tumor development. Thus, human specimens were used for the first objective whereas laying hens, a preclinical model of spontaneous OVCA, were used for the second in a prospective study. Laying hens are the only widely available and easily accessible animal that develop OVCA spontaneously with a high incidence rate.[30] The histopathology and expression of several markers of OVCA in hens are similar to those in human beings.[31-34] We have previously reported that the frequency of IL-16–expressing cells and serum levels were significantly higher in OVCA hens than normal hens.[35] However, the period between the increased levels of IL-16 in serum and the tumor mass becoming detectable by ultrasound imaging is not known.

Materials and Methods

Patient specimen

All tissues and serum samples were collected at Rush University Medical Center, Chicago, IL, and Northwest Oncology, Munster, IN. Benign and malignant ovarian tumor tissues were collected from patients who underwent surgery for a suspected ovarian mass. Corresponding blood samples were collected before surgery. Normal serum and ovarian samples were collected from subjects who had a hysterectomy due to nonovarian cause. All specimens were collected under institutional review board–approved protocol and patient's informed consent. Tumor tissues from 28 OVCA patients [n = 8 early stages (4 stage I and 4 stage II), age range, 53–67 years, and n = 20 late stages (10 stage III and 10 stage IV), age range, 42–79 years], patients with benign ovarian tumors (n = 10, age range, 53–85 years), and normal ovaries from subjects who underwent hysterectomy (n = 10, age range, 40–81 years) were used. Staging of the OVCA for each case was performed comprehensively during the primary surgery and later during histopathological examination of ovarian tumor mass as well as omentum, lymph node, and tubal tissues. Histological tumor types were confirmed by board-certified pathologists.

Animals

Commercial strains of 3- to 4-year-old white Leghorn laying hens (*Gallus domesticus*) were reared at the University of Illinois at Urbana-Champaign experimental Poultry Research Farm under standard poultry husbandry practices. The incidence of OVCA in hens of this age group is approximately 20% and is associated with low or complete cessation of egg laying.[30] Hens with normal or low egg-laying rates were scanned by TVUS[36] and 200 hens without any ovarian abnormality were selected. These hens were monitored by traditional TVUS scanning for 45 weeks at 15-week intervals and serum samples were collected at each interval as reported previously. All experimental

procedures were performed according to the institutional animal care and use committee—approved protocol.

Serum samples

Following collection of blood from patients, serum samples were separated by centrifugation (1000*g*, 20 minutes). Blood from all hens was obtained from the brachial vein (wing vein) of all hens at each TVUS scan and processed similarly as mentioned above. Aliquots were made from all serum samples and stored at −80°C until further use.

Staging and histopathology

Patient samples. The diagnosis, tumor types, grading, and staging of tumors were performed by board-certified gynecological pathologists and all relevant clinical information was obtained from the final pathology reports. Each fresh tissue sample (normal or tumor) was divided into 4 portions for protein extraction, total RNA collection, and paraffin and frozen embedding for routine histology and immunohistochemical studies. Samples were classified into 4 groups: normal, benign, malignant early stage, and malignant late stage.

Hen samples. All hens were euthanized at the end of the 45-week monitoring period. Ovarian pathology and tumor staging were performed by gross and histological examination as reported previously.[30] Samples were classified into 3 groups: normal, early (including microscopic), and late stages of OVCA based on gross at euthanasia (gross morphology following euthanasia of hens) and routine histological examination of ovarian tissues as reported previously.[30]

Preparation of ovarian specimen for biochemical analysis

Snap-frozen normal ovaries or ovaries with tumor from patients were homogenized with a Polytron homogenizer (Brinkman Instruments, Westbury, NY) as reported previously[37] and centrifuged, supernatant was collected, protein content of the extract was measured, and they were stored at −80°C after addition of protease inhibitor. In addition, a portion of normal ovaries or ovaries with tumors were used to extract nuclear matrix proteins (NMPs) as reported earlier.[38,39] Furthermore, lysates of ovarian malignant cells (OVCAR3; ATCC, Manassas, VA) were also examined for IL-16 expression by immunoblotting. Total RNA was isolated using TRIzol reagent (Invitrogen, Carlsbad, CA) according to the manufacturer's recommendation. RNA was measured at an optical density (OD) of 260 nm and the purity was evaluated using an OD 260/280-nm absorbance ratio $\geq$1.7 as reported earlier.[40]

Immunoassay

Serum levels of IL-16 were determined by using commercial IL-16 assay kits for human (R&D Systems, Minneapolis, MN) or hen (chicken IL-16 Vetset enzyme-linked immunosorbent assay kit; Kingfisher Biotech, St. Paul, MN) as per the manufacturer's instructions. Briefly, IL-16 standards or serum samples were added to the wells precoated with anti—IL-16 antibodies followed by incubation with detection antibody and streptavidin-HRP. Immunoreactions were developed by 3,3′,5,5′-tetramethylbenzidine substrate and stopped with 0.18 mol/L sulfuric acid. The absorbance for each well was recorded by reading the plates at 450 nm in a plate reader (Thermomax; Molecular Devices, Sunnyvale, CA). Standard curves for humans and hens were generated by plotting the OD values of the standards against their concentrations. Serum IL-16 levels were determined with reference to the standard curve as per manufacturer's instruction using a software program (Gen5, version 2.00; Biotek Instruments Inc, Winooski, VT). All standards and serum samples were run in duplicate.

Immunohistochemistry

Immunohistochemical localization of ovarian IL-16—expressing cells and smooth-muscle actin (SMA)-expressing microvessels was performed using anti-human IL-16 (R&D Systems) and anti-human SMA antibodies (Invitrogen), respectively, in normal ovaries or ovaries with tumor as reported previously.[35] In control staining, the first antibody was replaced with normal mouse IgG and immunoreactions were not found on the control section.

Counting of immunopositive cells or microvessels

The densities of IL-16—expressing cells and anti-SMA-expressing microvessels were counted in the normal ovary or tumor stroma from OVCA patients using a light microscope attached to digital imaging software (MicroSuite, version 5; Olympus Corp, Tokyo, Japan). Three sections per ovary were selected. In each section, 5 regions containing high population of immunopositive microvessels or 5 random areas for IL-16—expressing cells were selected. Frequencies of IL-16—expressing cells or SMA-expressing microvessels in 20,000-μm^2 area were counted at $\times$40 objective and $\times$10 ocular magnification as reported previously.[35] The mean of these counts were considered as the number of IL-16—expressing cells or SMA-expressing microvessels in a 20,000-μm^2 area of a section. The mean of 3 sections was considered as the mean of IL-16—expressing cells or SMA-expressing microvessels in a normal ovary or ovaries with tumor.[35]

One-dimensional Western blot

Immunohistochemical expression of IL-16 protein by normal ovaries, ovaries with tumors, and malignant epithelial cells (OVCAR3) as well as its serum prevalence detected by enzyme-linked immunosorbent assay were confirmed by 1-dimensional Western blot using the same antibodies mentioned above as reported earlier.[32,35] Immunoreactions on the membrane were visualized as a chemiluminescence product (Super Dura West substrate; Pierce, Thermo Fisher Scientific, Rockford, IL) and the image was captured using a Chemidoc XRS (BioRad, Hercules, CA).

Quantitative real-time polymerase chain reaction

IL-16 messenger RNA (mRNA) and miR-125a-5p expression by normal ovaries and ovaries with tumors were assessed by quantitative real-time polymerase chain reaction (qRT-PCR) as reported earlier.[40] For qRT-PCR analyses, human specific

FIGURE 1
IL-16—expression in normal ovaries and ovaries with benign or malignant Tu in patients

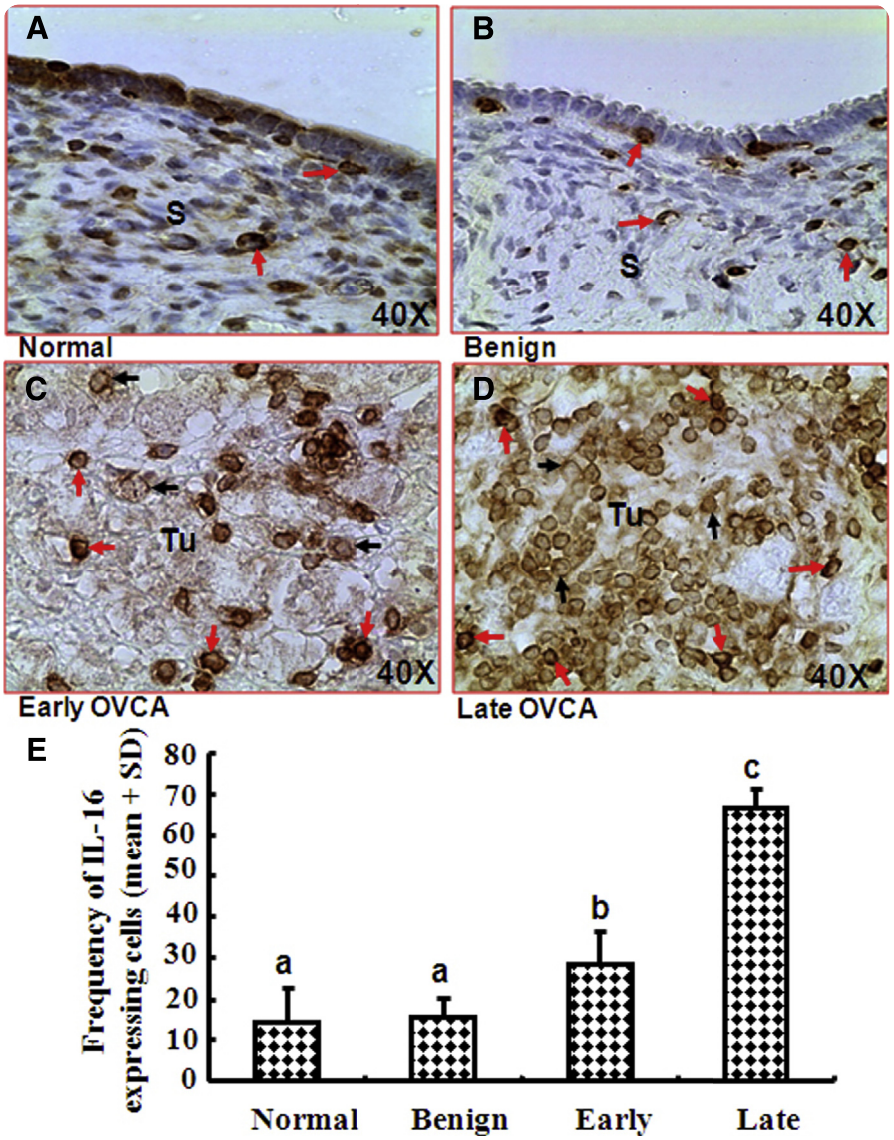

A-D, Immunohistochemical detection of IL-16—expressing cells. **A,** Section of normal ovary showing few IL-16—expressing cells in stroma (S) and surface layer of ovary. **B,** Section of benign ovarian Tu. **C,** Section of early-stage ovarian Tu. **D,** section of late-stage ovarian Tu. *Red arrows*, examples of IL-16—expressing immune phenotype cells. *Black arrows*, examples of malignant cells expressing IL-16. **E,** Changes in frequencies of IL-16—expressing cells in ovary in association with ovarian malignant Tu development and progression. Bars with different letters denote significant differences in frequency of IL-16—expressing cells in ovaries of different pathological groups of patients.

IL, interleukin; *OVCA*, ovarian cancer; *Tu*, tumors.

Yellapa. IL-16 in ovarian cancer development. Am J Obstet Gynecol 2014.

IL-16 primer (QT00075138) and 18S (Svedberg unit) single nucleotide RNA (SnRNA) (QT00199367) as endogenous primer were designed by Qiagen (Foster City, CA). microRNA-125a from the 5' arm (miR-125a-5p) and internal control miR-17-5p were designed by Applied Biosystems (Foster City, CA). The amplification of gene expression by qRT-PCR was analyzed using the differences (δ) in cycle threshold (ΔCt) method with 18S SnRNA and miR-17-5p as an internal control according to the manufacturer's recommendation for IL-16 mRNA and miR-125a-5p, respectively. The $\Delta\Delta$Ct was determined by subtracting ΔCt from each group from the average ΔCt of normal ovary. The differences in IL-16 mRNA or miR-125a-5p expression levels were calculated as the fold change using the formula $2^{-\Delta\Delta Ct}$ as reported earlier.[40]

Statistical analysis

The differences in the frequencies of IL-16—expressing cells and SMA-expressing microvessels among normal ovaries and ovaries with tumor in OVCA patients with early- and late-stage OVCA were assessed by analysis of variance, F tests, and the alternative nonparametric Kruskal-Wallis tests. Then pairwise comparisons between the groups (normal, early-stage OVCA, and late-stage OVCA) were performed by 2-sample *t* tests. Similarly, differences in serum IL-16 levels, IL-16 mRNA, or miR-125a-5p expression were also analyzed. All reported *P* values are 2 sided, and $P < .05$ was considered significant. Statistical analyses were performed with software (SPSS [PASW], version 18; IBM Corp, Armonk, NY).

Results

Expression of IL-16 by human ovarian tumors

All malignant ovarian tumors including early and late stages were papillary serous carcinoma while benign tumors were serous cystadenomas or cystadenofibromas. The morphology of IL-16—expressing cells detected in the stroma of normal ovaries or in the microenvironment of ovarian tumors varied from rounded (T-cell-like) to irregular-shaped macrophage-like cells (Figure 1, A-D). In some cases, these IL-16—expressing cells were localized in the stroma of a tumor in close proximity with tumor cells detached from the core tumor. Occasionally, malignant epithelial cells were also stained for IL-16 (Figure 1, *black arrows*). There were significant differences in the frequencies of IL-16—expressing cells among healthy subjects and patients with early- and late-stage OVCA ($P < .0001$). The frequency of IL-16—expressing cells in the stroma of

ovarian tumors in patients with early-stage OVCA was significantly higher (mean ± SEM, 28.55 ± 3.55 cells/20,000-μm^2 area) ($P < .01$) than that of normal healthy subjects (mean ± SEM, 15.33 ± 3.54 cells/20,000-μm^2 area) (Figure 1, E). The frequency of IL-16–expressing cells increased further in OVCA patients with late-stage OVCA (mean ± SEM, 66.64 ± 2.12 cells/20,000-μm^2 area) ($P < .0001$). However, significant differences were not observed in the frequencies of IL-16–expressing cells between normal ovaries and ovaries with benign tumors (mean ± SEM, 15.87 ± 2.34 cells/20,000-μm^2 area). Thus, expression of IL-16 in the ovary increases in association with OVCA development and progression.

Immunoblotting for IL-16 protein in ovarian tissues

Immunohistochemical observations for IL-16 expression by homogenates of normal whole ovaries or malignant ovarian tissues as well as malignant cells were confirmed by 1-dimensional Western blot using whole ovarian homogenates. Moderate to intense immunoreactive band of approximately 60-65 kDa were detected in whole ovarian homogenates from malignant ovaries (Figure 2, A). In addition, compared with normal ovarian NMPs, a strong immunoreactive band of similar size was also detected in the homogenates from malignant tumors for NMPs. The patterns of IL-16 expression in lysates of malignant epithelial cells (OVCAR3) were similar to that of ovarian malignant tumor tissues (data not shown). These results confirm the immunohistochemical detection of IL-16 expression by ovarian tumors and malignant cells.

Changes in IL-16 gene expression in relation to OVCA development

Compared with normal ovaries, qRT-PCR showed strong signal amplification for IL-16 mRNA in specimens from patients with early- and late-stage OVCA (Figure 2, B). In contrast, qRT-PCR analysis showed that, compared with normal ovaries, the expression of miR-125a-5p was significantly decreased in malignant ovarian tumors at early stage (4-fold) and decreased further as the tumor progressed to late stages (10-fold) (Figure 2, C). Thus, gene expression data for IL-16 support the immunohistochemical observation that the expression of IL-16 increases in association with OVCA development and progression, and this enhanced expression is associated with the down-regulation of miR-125a-5p, an inhibitor of IL-16 mRNA expression.

FIGURE 2
Changes in IL-16 protein and gene expressions as well as its regulator miRNA in association with ovarian cancer development and progression

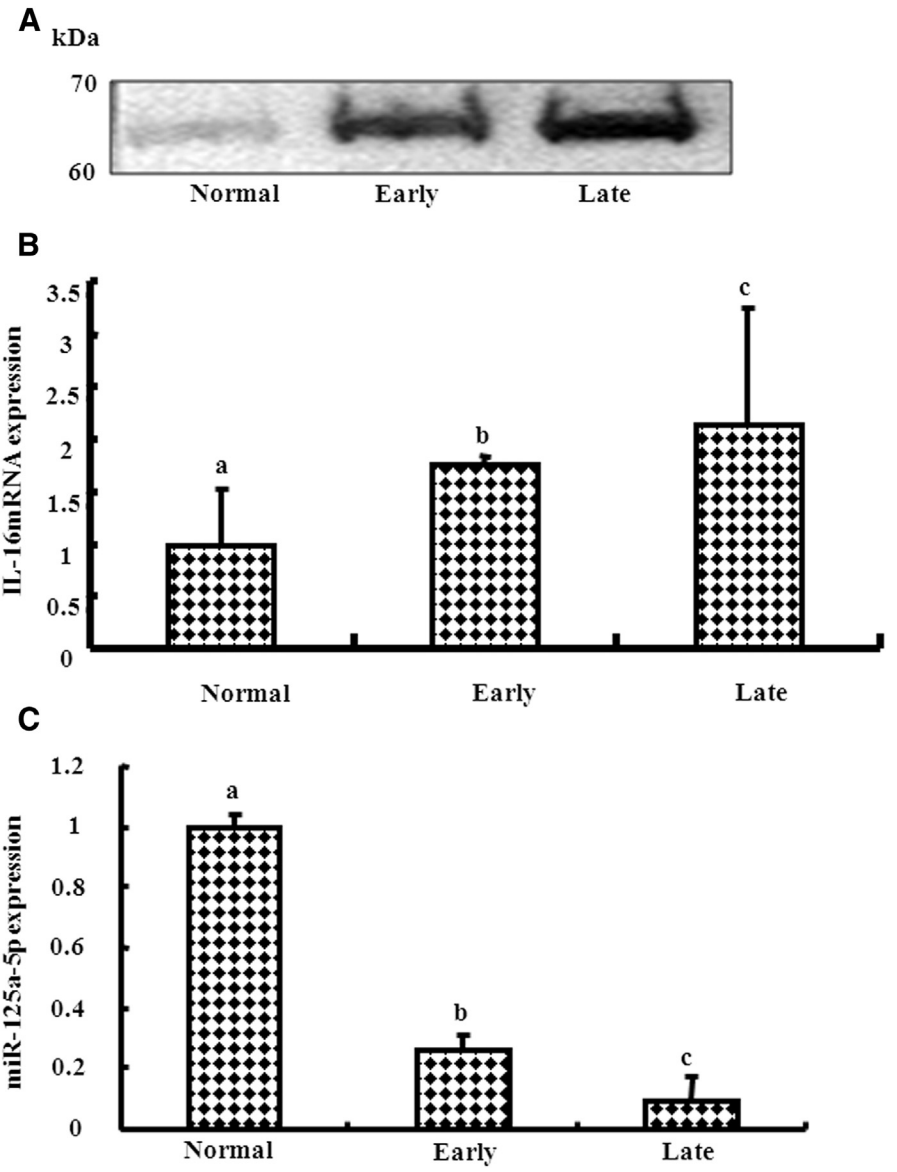

A, Immunoblotting for IL-16 protein expression by normal ovarian homogenates or homogenates of ovaries with early- and late-stage tumors. **B,** IL-16 messenger RNA (mRNA) expression in ovarian tumors at early and late stages. **C,** Expression of miRNA-125a-5p, regulator of IL-16 gene expression. Bars with different letters denote significant differences between normal ovaries or ovaries with tumors.

IL, interleukin; *miRNA*, microRNA; *mRNA*, messenger RNA.

Yellapa. IL-16 in ovarian cancer development. Am J Obstet Gynecol 2014.

FIGURE 3
Changes in population of SMA-expressing ovarian MVs in association with ovarian Tu development and progression

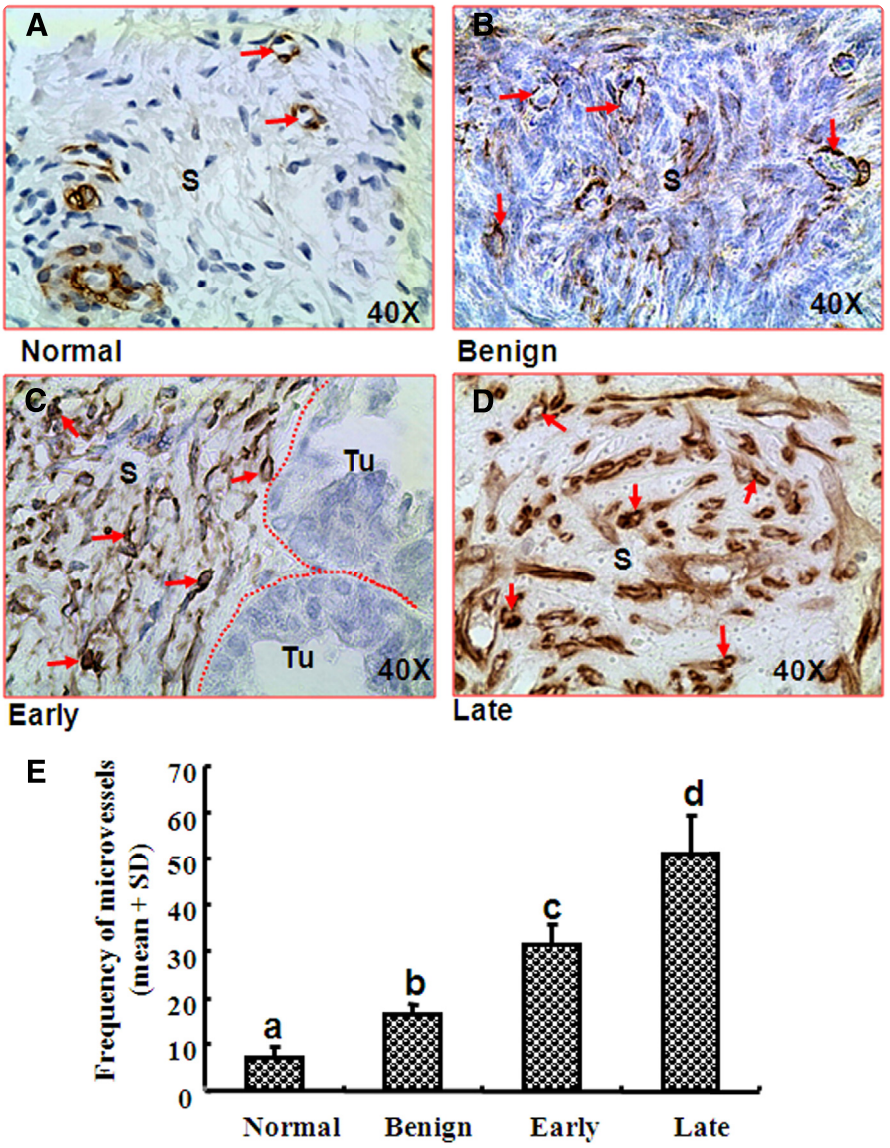

A-D, I immunohistochemical detection of SMA-expressing MVs. **A,** Section of normal ovary. **B,** Section of benign ovarian Tu. **C,** Section of ovarian malignant Tu at early stage. **D,** Section of ovarian Tu at late stage. *Arrows* indicate examples of SMA-expressing MVs. **A-D,** Frequency of SMA-expressing ovarian MVs in normal ovary and ovaries with benign and malignant Tu. Bars with different letters denote significant differences between normal ovaries or ovaries with Tu.

MVs, microvessels; *S,* stroma; *SMA,* smooth-muscle actin; *Tu,* tumors.

Yellapa. IL-16 in ovarian cancer development. Am J Obstet Gynecol 2014.

Serum levels of IL-16

The mean concentration of serum IL-16 (mean ± SEM) was 147.61 ± 10.63 pg/mL in healthy subjects. Compared with healthy females, the mean concentration of serum IL-16 was significantly higher ($P < .001$) in patients with benign tumors (2-fold) (mean ± SEM, 217.9 ± 25.36 pg/mL) and increased 4-fold in early-stage OVCA (mean ± SEM, 307.61 ± 28.42 pg/mL) ($P < .0001$) and 5.5-fold in patients with late-stage OVCA (mean ± SEM, 948.54 ± 202.6 pg/mL) ($P < .0001$). Significant differences were not observed in serum IL-16 levels between patients with early- and late-stage OVCA. Furthermore, similar to those observed for malignant ovarian homogenates, immunoblots of serum samples from patients with early- as well as late-stage OVCA showed a strong band of 60-65 kDa for IL-16 (data not shown). Similarly as observed in normal ovarian tissue homogenates, a weak immunoreactive band for IL-16 was observed in serum of healthy subjects. Overall, these results suggest that the concentration of IL-16 in serum was significantly higher in patients with early- and late-stage OVCA than normal subjects or patients with benign tumors.

Frequency of tumor-associated angiogenic microvessels

Mature or immature blood vessels expressing SMA were localized in healthy ovaries as well as ovaries with tumors. Mature blood vessels were characterized by the presence of a thick, continuous, and complete wall surrounding the vessels. In contrast, immature SMA-expressing vessels were leaky, incomplete, discontinuous, and surrounded by a thin vessel wall. This leakiness is a characteristic feature of tumor-associated microvessels that leak ascitic fluid to the tumor microenvironment. Whereas very few SMA-expressing microvessels were localized in the stroma of normal ovaries, many SMA-expressing microvessels were localized in the stroma and in the vicinity of malignant of tumors (Figure 3, A-D). There were significant differences in the frequencies of SMA-expressing microvessels among healthy subjects and patients with benign and malignant ovarian tumors ($P < .0001$). The mean frequency of SMA-expressing microvessels (mean ± SEM) in healthy subjects was 7.4 ± 0.93 in 20,000 μm^2 of tissue and it was 2-fold higher in patients with benign ovarian tumors (mean ± SEM, 16.4 ± 0.92 in 20,000 μm^2 of tissue) ($P < .0001$). In contrast, the frequencies of SMA-expressing microvessels increased remarkably (>4-fold) in patients with early-stage OVCA (mean ± SEM, 31.4 ± 1.913 in 20,000 μm^2 of tissue) ($P < .0001$) and increased approximately 7-fold in patients with

late-stage OVCA (mean ± SEM, 51.17 ± 3.26 in 20,000 μm^2 of tissue) ($P < .001$) (Figure 3, E).

Frequency of SMA-expressing microvessels was positively correlated with the frequency of IL-16–expressing cells (r = 0.60 and 0.67, for early and late stages of OVCA, respectively), and serum IL-16 levels (r = 0.69 and 0.93 for early and late stages of OVCA, respectively). Thus, the frequency of tumor-associated microvessels increases in association with OVCA development and progression similar to those of IL-16–expressing cells and serum levels of IL-16.

Changes in serum IL-16 levels in association with ovarian tumor development in a prospective study in laying hens

Changes in serum concentrations of IL-16 relative to the development of OVCA were examined by monitoring laying hens for 45 weeks with TVUS scan at 15-week intervals. No TVUS-detectable ovarian abnormality was present in any of the selected hens at the initial scan. All hens were euthanized at the end of the study period (45 weeks) and the stages of the OVCA in hens that developed ovarian tumors were determined. Final diagnosis including tumor subtypes was made by routine histology. Serum from all hens with OVCA, namely, 17 hens at early stage including microscopic carcinoma and tumors limited to the ovaries (7 serous, 6 endometrioid, and 4 mucinous adenocarcinoma), 12 hens with tumors metastasized beyond ovaries (4 serous, 4 endometrioid, and 4 mucinous adenocarcinoma), as well as 10 normal hens were used in this study (Figure 4). The levels of serum IL-16 were not significantly different among all hens at the start of the prospective monitoring. Although serum IL-16 levels were observed in all hens as they aged with the progression of the study, the rates of increase were remarkably high in hens that developed OVCA at the end of the 45 weeks of prospective monitoring. The serum IL-16 level (mean ± SEM) in hens with normal ovaries at the end of the 45 weeks of monitoring was 372.00 ± 87.12 pg/mL. The serum IL-16 level (mean ± SEM) was significantly higher (640.01 ± 207.66 pg/mL) ($P < .05$) in hens with early-stage OVCA (including microscopic carcinoma and tumors limited to the ovary) with no metastasis at 45 weeks of monitoring. Compared with normal hens, the serum IL-16 levels increased further (986.53 ± 71.78 pg/mL) ($P < .0002$) in hens that developed tumors and OVCA metastasized to the peritoneal organs at 45 weeks (at third scan). Thus, serum concentration of IL-16 in hens with early-stage OVCA is much higher than a cutoff value (mean of normal + 2 × SEM of normal = 372 + 2 × 87.12 = 546.24 pg/mL) (Figure 5). Hence a cutoff value of serum IL-16 level (mean of normal + 2 × SEM of normal hens) may indicate malignant transformation in the ovary. Thus, these results suggest that serum IL-16 levels increase in association with OVCA development even before the tumor forms a solid mass detectable by traditional TVUS scanning.

FIGURE 4
Spontaneous ovarian cancer development in laying hens

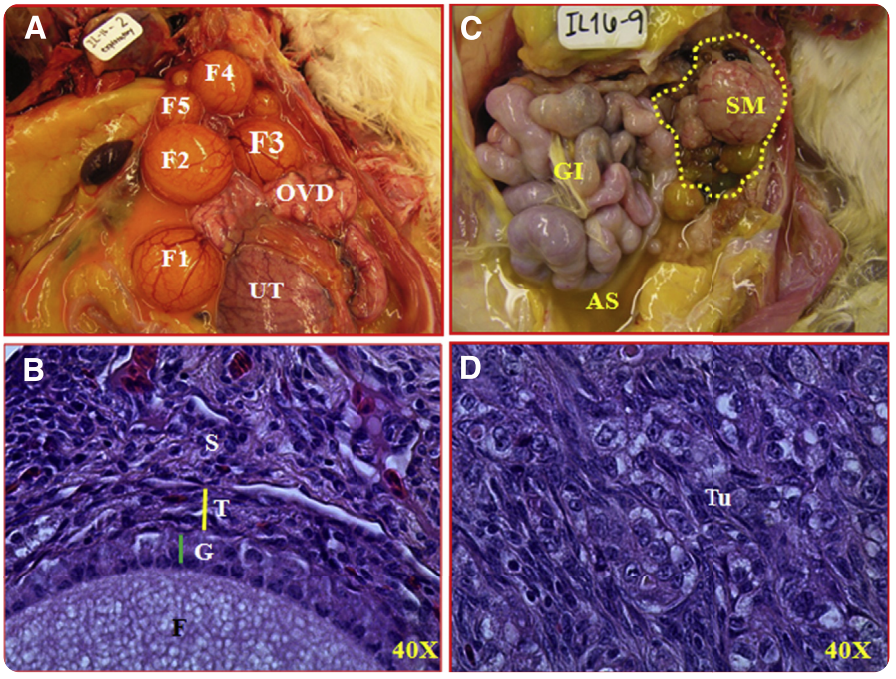

A, Fully functional ovary in laying hen showing hierarchy of preovulatory follicles (F1-4). **B,** Section of normal ovary showing follicle (F) embedded in ovarian stroma (S) and composed of theca (T) and granulosa (G) layers. **C,** Ovarian malignant tumor (Tu) in hen showing solid mass (SM) in ovary (*dotted circle*), coiled intestine (GI) accompanied with profuse ascites (AS). **D,** Section of serous ovarian adenocarcinoma in hen.

OVD, oviduct; *UT,* uterus.

Yellapa. IL-16 in ovarian cancer development. Am J Obstet Gynecol 2014.

Comment

This study demonstrated an association of IL-16, a proinflammatory and proangiogenic cytokine, with the development and progression of OVCA. The results of this study showed that an increase in tissue expression and serum concentrations of IL-16 were associated with ovarian tumor development. This study also showed that the enhancement in IL-16 expression was positively correlated with the increase in the frequency of tumor-associated angiogenic microvessels. In addition, this study further showed that ovarian tumor–associated increase in IL-16 expression was accompanied with the decreased expression of miR-125a-5p, a putative tumor suppressor microRNA and a regulator of IL-16 gene expression. Thus, these results suggest that IL-16 may be a potential indicator of

FIGURE 5
Prospective changes in serum IL-16 levels in association with malignant ovarian transformation and progression of ovarian cancer in hens

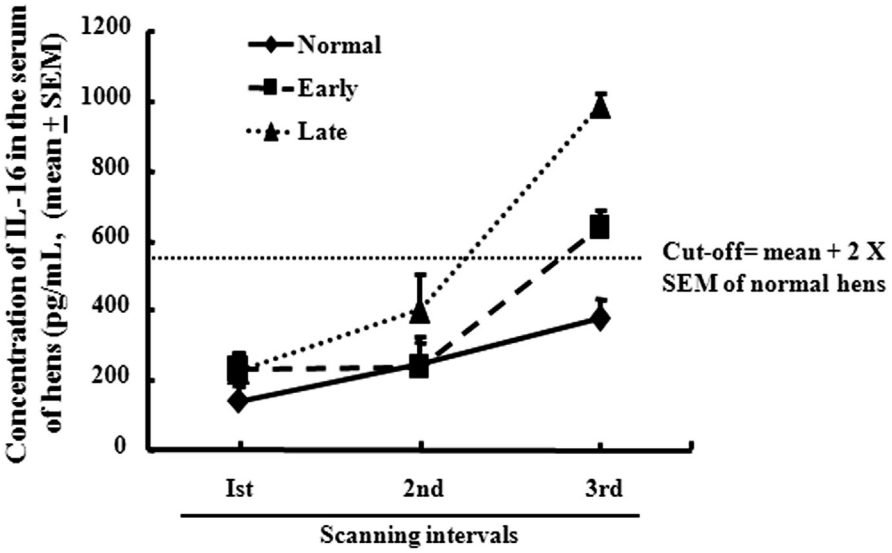

Horizontal dotted line denotes cutoff value (equal to mean of normal hens with 2 × SEM), which may be used as diagnostic level of serum IL-16 indicative of ovarian malignant transformation.

IL, interleukin.

Yellapa. IL-16 in ovarian cancer development. Am J Obstet Gynecol 2014.

ovarian malignant transformation as well as a surrogate marker of ovarian tumor—associated neoangiogenesis.

Although extensively studied, the precise mechanism of malignant transformation and early metastasis of OVCA, an aggressive heterogeneous malignancy in women, is not well understood. Moreover, fimbrial (of fallopian tube) origin of OVCA, as proposed recently, makes early detection more complex. Cytokines have been suggested to be involved in the local regulation of normal ovarian functions including follicular development (eg, transforming growth factor β, tumor necrosis factor α, IL-1, and IL-11) while others have been implicated to play a protumor role in OVCA (eg, IL-6, IL-8, IL-10).[41] Although IL-16 has been reported to stimulate the synthesis of other cytokines with protumor roles (IL-8 and IL-15),[27,28] its association with OVCA development and progression in human beings has not been reported. In the present study, compared with normal ovaries, the frequency of IL-16—expressing cells was significantly high in patients with early-stage and late-stage OVCA. Immunohistochemical detection of IL-16 expression was confirmed by immunoblotting as well as gene expression analysis. Thus, these results suggest that IL-16 may be associated with OVCA development and progression. However, the reason for this enhanced expression of IL-16 in ovarian tumors including whether it is involved in OVCA development or it is a product of malignant ovarian transformation is not known. IL-16 has been reported to be increased in several chronic inflammatory conditions such as asthma,[42,43] rheumatoid arthritis,[44] inflammatory bowel disease,[45] peritoneal fluid of women with endometriosis,[46] and in patients with multiple myeloma.[47] As part of the reproductive system, ovarian surface epithelium and fimbria of fallopian tube are constantly exposed to inflammatory cytokines including those associated with ovulation and long-term unresolved inflammation may lead to malignant transformation of these tissues.[14] Thus, increased IL-16 in patients with OVCA may suggest that IL-16 may play potential roles in ovarian malignant transformation due to its association with the long-term unresolved inflammatory processes in the ovary including ovulation. Specific mechanism(s) by which IL-16 facilitates ovarian malignant transformation is not known.

It is possible that IL-16 may facilitate ovarian malignant transformation and OVCA progression through 2 mechanisms. First, IL-16 may be involved in abnormal cell growth and proliferation during malignant transformation. This study showed, compared with normal ovaries, a strong immunoreactivity for IL-16 in NMPs extracted from ovarian tumors of patients with early- and late-stage OVCA. The nucleus of the cell is the primary site of malignant transformation. Thus, it is possible that IL-16 expressed by ovarian malignant cells might have translocated to the nucleus of the cells. Such translocation of IL-16 following enzymatic cleavage has been reported earlier.[48] However, the function of this nuclear translocated IL-16 is not known. It is assumed that the nuclear-translocated IL-16 may function as a transforming nuclear oncoprotein as reported for IL-1a.[49] This assumption is based on the fact that IL-16 and IL-1a have some common features. Both are processed by the same family (caspase) of enzymes, neither is secreted as a mature cytokine, and their remaining prodomains translocate to the nucleus following the processing by caspase enzyme. Second, IL-16 is a target of miR-125a-5p, a tumor suppressive microRNA.[50,51] This study showed that the expression of miR-125a-5p was down-regulated significantly as the tumor developed and progressed to advanced stages. Thus, in the context of malignant transformation, decreased miR-125a-5p might be a reason for increased IL-16 expression.

Furthermore, this study showed that there was an increase in serum IL-16 levels in association with OVCA development and progression. However, the sources of serum IL-16 are not fully reported and published information in this regard is very limited. Immune cells including CD8 T cells and a subset of macrophages are the traditional sources of secretory IL-16.[16–18] This study

showed increased serum IL-16 levels were positively correlated with the frequency of IL-16–expressing cells, which were rounded T-cell-like or larger irregular-shaped macrophage-like cells. Moreover, malignant cells also occasionally expressed IL-16. This observation is supported by the immunoblotting results of OVCAR3 ovarian malignant cells. Hence, in addition to the immune cells, malignant ovarian cells may also be a source of secretory IL-16, which might have contributed to the enhanced level of serum IL-16 in OVCA patients. These findings are in agreement with previous findings that bronchial epithelium in human beings is a source of a secretory IL-16.[17,43] Thus, in addition to traditional sources (members of immune system), ovarian malignant epithelial cells are also a source of IL-16 in patients with OVCA.

The role of increased secreted IL-16 including IL-16 secreted by tumor cells in OVCA development and progression is not known. It is possible that secreted IL-16 may stimulate establishment of ovarian tumor–associated neoangiogenesis. In this study serum IL-16 levels and the frequencies of SMA-expressing microvessels were positively correlated in patients with early and late stages of OVCA. IL-16 is reported to be a proangiogenic cytokine that stimulates angiogenesis through secretion of IL-15 and stimulation of IL-8 production.[27,28] On the other hand, secreted IL-16 may also be used as a surrogate marker of ovarian tumor development. Previously, we have reported that compared with normal hens, expression of IL-16 was high in OVCA hens. However, the period between the increased IL-16 concentration in serum and the formation of tumor mass detectable by ultrasound imaging was not known. The current (prospective) study showed that ovarian tumors in hens become detectable by ultrasound imaging within 30-45 weeks after the increase in serum IL-16 levels. Furthermore, serum levels and expression of IL-16 by benign ovarian tumors in patients were significantly lower than that of the malignant ovarian tumors both at early as well as late stages. Serum IL-16 levels were reported to be significantly lower in patients with benign prostatic hyperplasia than patients with prostate cancer.[52] Thus, it is possible that secreted IL-16 in patients with OVCA may be an indicator of ovarian malignant transformation and may stimulate angiogenesis as the tumor continues to grow.

Taken together, this study offers new insights on the possible roles of IL-16 in the development and progression of OVCA. IL-16 may be involved in ovarian tumor progression by stimulating abnormal cell growth and proliferation, enhancing tumor-associated neoangiogenesis and may be a surrogate marker of ovarian malignant transformation. Small sample size and lack of stratification of IL-16 expression with regard to racial differences are 2 limitations of this study. However, our preclinical prospective study with laying hens, a spontaneous model of OVCA, suggests a protumor role of IL-16 and its increase in serum levels in association with OVCA development. Moreover, the age ranges of patients including those with benign and malignant tumors as well as subjects with normal ovaries were similar. Thus, there might have been less variation in serum IL-16 levels due to non-OVCA factors (like differences in age and race of patients).

Therefore, a further study with larger cohorts will be necessary to confirm the role of IL-16 in OVCA development and progression.

In conclusion, the results of this study showed that the frequencies of ovarian IL-16–expressing cells and corresponding serum levels increased significantly in association with the development and progression of OVCA. This study also revealed that enhanced IL-16 expression and increased serum levels were positively correlated with the frequency of tumor-associated microvessels. Furthermore, our prospective study in hens, a preclinical model of spontaneous OVCA, showed that serum IL-16 level increases even before the tumor forms a solid tissue mass of a detectable size. ■

ACKNOWLEDGMENTS

We thank Chet and Pam Utterback, Doug Hilgendorf, Chelsie Parr, and staff of the University of Illinois at Urbana-Champaign Poultry Research Farm for maintenance of the hens. We also thank Heather Lopez Lope, Sergio Abreu Machado, and Syed Tahir Abbas Shah, graduate students, Department of Animal Sciences, University of Illinois at Urbana-Champaign, for helping in hen tissue collection.

REFERENCES

1. Siegel RD, Naishadham D, Jemal A. Cancer statistics, 2012. CA Cancer J Clin 2012;62:10-29.
2. Ries LA. Ovarian cancer: survival and treatment differences by age. Cancer 1993;71(Suppl):524-9.
3. Goodman MT, Correa CN, Tung KH, et al. Stage at diagnosis of ovarian cancer in the United States, 1992-1997. Cancer 2003;97(Suppl):2648-59.
4. Holschneider CH, Berek JS. Ovarian cancer: epidemiology, biology, and prognostic factors. Semin Surg Oncol 2000;19:3-10.
5. Moore RG, Bast RC Jr. How do you distinguish a malignant pelvic mass from a benign pelvic mass? Imaging, biomarkers, or none of the above. J Clin Oncol 2007;25:4159-61.
6. Bosse K, Rhiem K, Wappenschmidt B, et al. Screening for ovarian cancer by transvaginal ultrasound and serum CA125 measurement in women with a familial predisposition: a prospective cohort study. Gynecol Oncol 2006;103:1077-82.
7. Menon U, Gentry-Maharaj A, Jacobs I. Ovarian cancer screening and mortality. JAMA 2011;306:1544-5.
8. Yigit R, Massuger LF, Figdor CG, Torensma R. Ovarian cancer creates a suppressive microenvironment to escape immune elimination. Gynecol Oncol 2010;117:366-72.
9. Vang R, Shih IM, Kurman RJ. Fallopian tube precursors of ovarian low- and high-grade serous neoplasms. Histopathology 2013;62:44-58.
10. Kuhn E, Kurman RJ, Shih IM. Ovarian cancer is an imported disease: fact or fiction? Curr Obstet Gynecol Rep 2012;1:1-9.
11. Heidemann LN, Hartwell D, Heidemann CH, Jochumsen KM. The relation between endometriosis and ovarian cancer—a review. Acta Obstet Gynecol Scand 2014;93:20-31.
12. Buis CC, van Leeuwen FE, Mooij TM, Burger CW. Increased risk for ovarian cancer and borderline ovarian tumors in subfertile women with endometriosis. Hum Reprod 2013;28:3358-69.
13. Zink D, Fischer AH, Nickerson JA. Nuclear structure in cancer cells. Nat Rev Cancer 2004;4:677-87.
14. Maccio A, Madeddu C. Inflammation and ovarian cancer. Cytokine 2012;58:133-47.
15. Cruikshank WW, Kornfeld H, Center DM. Interleukin-16. J Leukoc Biol 2000;67:757-66.
16. Chupp GL, Wright EA, Wu D, et al. Tissue and T-cell distribution of precursor and mature IL-16. J Immunol 1998;161:3114-9.
17. Wu DM, Zhang Y, Parada NA, et al. Processing and release of IL-16 from $CD4^+$ but not

CD8$^+$ T cells is activation dependent. J Immunol 1999;162:1287-93.
18. Elssner A, Doseff AI, Duncan M, Kotur M, Wewers MD. IL-16 is constitutively present in peripheral blood monocytes and spontaneously released during apoptosis. J Immunol 2004;172:7721-5.
19. Lim KG, Wan HC, Bozza PT, et al. Human eosinophils elaborate the lymphocyte chemoattractants. IL-16 (lymphocyte chemoattractant factor) and RANTES. J Immunol 1996;156:2566-70.
20. Center DM, Kornfeld H, Cruikshank WW. Interleukin-16. Int J Biochem Cell Biol 1997;29:1231-4.
21. Kovacs E. The serum levels of IL-12 and IL-16 in cancer patients: relation to the tumor stage and previous therapy. Biomed Pharmacother 2001;55:111-6.
22. Bellomo G, Allegra A, Alonci A, et al. Serum levels of interleukin-16 in lymphoid malignancies. Leuk Lymphoma 2007;48:1225-7.
23. Tone AA, Virtanen C, Shaw P, Brown TJ. Prolonged postovulatory proinflammatory signaling in the fallopian tube epithelium may be mediated through a BRCA1/DAB2 axis. Clin Cancer Res 2012;18:4334-44.
24. Folkman J. What is the evidence that tumors are angiogenesis dependent? J Natl Cancer Inst 1990;82:4-6.
25. Ramakrishnan S, Subramanian IV, Yokoyama Y, Geller M. Angiogenesis in normal and neoplastic ovaries. Angiogenesis 2005;8:169-82.
26. Mathy NL, Scheuer W, Lanzendorfer M, et al. Interleukin-16 stimulates the expression and production of pro-inflammatory cytokines by human monocytes. Immunology 2000;100:63-9.
27. Angiolillo AL, Kanegane H, Sgadari C, Reaman GH, Tosato G. Interleukin-15 promotes angiogenesis in vivo. Biochem Biophys Res Commun 1997;233:231-7.
28. Simonini A, Moscucci M, Muller DW, et al. IL-8 is an angiogenic factor in human coronary atherectomy tissue. Circulation 2000;101:1519-26.
29. Balkwill F, Charles KA, Mantovani A. Smoldering and polarized inflammation in the initiation and promotion of malignant disease. Cancer Cell 2005;7:211-7.
30. Barua A, Bitterman P, Abramowicz JS, et al. Histopathology of ovarian tumors in laying hens: a preclinical model of human ovarian cancer. Int J Gynecol Cancer 2009;19:531-9.
31. Barua A, Yellapa A, Bahr JM, et al. Expression of death receptor 6 by ovarian tumors in laying hens, a preclinical model of spontaneous ovarian cancer. Transl Oncol 2012;5:260-8.
32. Khan MF, Bahr JM, Yellapa A, et al. Expression of leukocyte inhibitory immunoglobulin-like transcript 3 receptors by ovarian tumors in laying hen model of spontaneous ovarian cancer. Transl Oncol 2012;5:85-91.
33. Hales DB, Zhuge Y, Lagman JA, et al. Cyclooxygenases expression and distribution in the normal ovary and their role in ovarian cancer in the domestic hen (*Gallus domesticus*). Endocrine 2008;33:235-44.
34. Ansenberger K, Zhuge Y, Lagman JA, et al. E-cadherin expression in ovarian cancer in the laying hen, *Gallus domesticus*, compared to human ovarian cancer. Gynecol Oncol 2009;113:362-9.
35. Yellapa A, Bahr JM, Bitterman P, et al. Association of interleukin 16 with the development of ovarian tumor and tumor-associated neoangiogenesis in laying hen model of spontaneous ovarian cancer. Int J Gynecol Cancer 2012;22:199-207.
36. Barua A, Bitterman P, Bahr JM, et al. Detection of tumor-associated neoangiogenesis by Doppler ultrasonography during early-stage ovarian cancer in laying hens: a preclinical model of human spontaneous ovarian cancer. J Ultrasound Med 2010;29:173-82.
37. Barua A, Bradaric MJ, Kebede T, et al. Anti-tumor and anti-ovarian autoantibodies in women with ovarian cancer. Am J Reprod Immunol 2007;57:243-9.
38. Barua A, Qureshi T, Bitterman P, et al. Molecular targeted imaging of vascular endothelial growth factor receptor (VEGFR)-2 and anti-NMP autoantibodies detect ovarian tumor at early stage. Cancer Res 2012;72(Suppl). Abstract nr 2455. doi: 1538-7445.AM2012-2455.
39. Yu E, Lee H, Oh W, Yu B, Moon H, Lee I. Morphological and biochemical analysis of antinuclear matrix protein antibodies in human sera. J Korean Med Sci 1999;14:27-33.
40. Penumatsa K, Edassery SL, Barua A, Bradaric MJ, Luborsky JL. Differential expression of aldehyde dehydrogenase 1a1 (ALDH1) in normal ovary and serous ovarian tumors. J Ovarian Res 2010;3:28.
41. Nash MA, Ferrandina G, Gordinier M, Loercher A, Freedman RS. The role of cytokines in both the normal and malignant ovary. Endocr Relat Cancer 1999;6:93-107.
42. Laberge S, Ernst P, Ghaffar O, et al. Increased expression of interleukin-16 in bronchial mucosa of subjects with atopic asthma. Am J Respir Cell Mol Biol 1997;17:193-202.
43. Arima M, Plitt JR, Stellano C, Schwiebert LM, Schleimer RP. The expression of lymphocyte chemoattractant factor (LCF) in human bronchial epithelial cells. J Allergy Clin Immunol 1996;97:443.
44. Cho ML, Jung YO, Kim KW, et al. IL-17 induces the production of IL-16 in rheumatoid arthritis. Exp Mol Med 2008;40:237-45.
45. Seegert D, Rosenstiel P, Pfahler H, Pfefferkorn P, Nikolaus S, Schreiber S. Increased expression of IL-16 in inflammatory bowel disease. Gut 2001;48:326-32.
46. Koga K, Osuga Y, Yoshino O, et al. Elevated interleukin-16 levels in the peritoneal fluid of women with endometriosis may be a mechanism for inflammatory reactions associated with endometriosis. Fertil Steril 2005;83:878-82.
47. Atanackovic D, Hildebrandt Y, Templin J, et al. Role of interleukin 16 in multiple myeloma. J Natl Cancer Inst 2012;104:1005-20.
48. Zhang Y, Kornfeld H, Cruikshank WW, Kim S, Reardon CC, Center DM. Nuclear translocation of the N-terminal prodomain of interleukin-16. J Biol Chem 2001;276:1299-303.
49. Stevenson FT, Turck J, Locksley RM, Lovett DH. The N-terminal propiece of interleukin 1 alpha is a transforming nuclear oncoprotein. Proc Natl Acad Sci U S A 1997;94:508-13.
50. Nam EJ, Yoon H, Kim SW, et al. MicroRNA expression profiles in serous ovarian carcinoma. Clin Cancer Res 2008;14:2690-5.
51. Nishida N, Mimori K, Fabbri M, et al. MicroRNA-125a-5p is an independent prognostic factor in gastric cancer and inhibits the proliferation of human gastric cancer cells in combination with trastuzumab. Clin Cancer Res 2011;17:2725-33.
52. Zhang L, Sun SK, Shi LX, Zhang X. Serum cytokine profiling of prostate cancer and benign prostatic hyperplasia using recombinant antibody microarray [in Chinese]. Zhonghua Nan Ke Xue 2010;16:584-8.

ORIGINAL ARTICLE

Dietary Supplementation of *Ashwagandha* (*Withania somnifera*, Dunal) Enhances NK Cell Function in Ovarian Tumors in the Laying Hen Model of Spontaneous Ovarian Cancer

Animesh Barua[1], Michael J. Bradaric[2], Pincas Bitterman[1], Jacques S. Abramowicz[1], Sameer Sharma[1], Sanjib Basu[1], Heather Lopez[3], Janice M. Bahr[3]

[1]Rush University Medical Center, Chicago, IL, USA;
[2]Chicago State University, Chicago, IL, USA;
[3]University of Illinois at Urbana-Champaign, Urbana, IL, USA

Keywords
Dietary supplement, immune response, NK cells, prevention, spontaneous animal model

Correspondence
Animesh Barua, Laboratory for Translational Research on Ovarian Cancer, Department of Pharmacology, Room # 410, Cohn Building, Rush University Medical Center, 1735 W. Harrison St., Chicago IL 60612, USA.
E-mail: Animesh_Barua@rush.edu

Submission July 15, 2013;
accepted October 5, 2013.

Citation
Barua A, Bradaric MM, Bitterman P, Abramowicz JS, Sharma S, Basu S, Lopez H, Bahr JM. Dietary supplementation of *Ashwagandha* (*Withania somnifera*, Dunal) enhances NK cell function in ovarian tumors in the laying hen model of spontaneous ovarian cancer. Am J Reprod Immunol 2013; 70: 538–550

doi:10.1111/aji.12172

Problem
Ovarian cancer (OVCA) disseminates in a distinct pattern through peritoneal metastasis and little is known about the immunosuppression in the tumor microenvironment. Our goal was to determine changes in NK cell population during OVCA development and the effects of *Ashwagandha* (*Withania somnifera,* Dunal) supplementation on NK cell localization in laying hens with OVCA.

Methods
Frequency of NK cells in ovarian tumors at early and late stages in 3- to 4-year-old hens (exploratory study) as well as in hens supplemented with dietary *Ashwagandha* root powder for 90 days (prospective study) was examined.

Results
The population of stromal NK cells but not the intratumoral NK cells increased with OVCA development and progression. *Ashwagandha* supplementation decreased the incidence and progression of OVCA. Both the stromal and intratumoral NK cell population increased significantly ($P < 0.0001$) in *Ashwagandha* supplementated hens.

Conclusion
The results of this study suggest that the population of stromal and tumorinfiltrating NK cells is increased by dietary *Ashwagandha* supplementation. Thus, *Ashwagandha* may enhance antitumor function of NK cells. This study may be useful for a clinical study to determine the effects of dietary *Ashwagandha* on NK cell immune function in patients with ovarian cancer.

Introduction

Ovarian cancer (OVCA) is a lethal gynecological malignancy and ranked as the second highest (after breast cancer) cause of death of women due to gynecological cancers in the USA.[1] Despite the notable improvements in cytoreductive surgeries and chemotherapeutics, the rate of death of OVCA patients remains very high. Due to the lack of an effective early detection test, OVCA in most cases is detected at late stages. Resistance to current chemotherapeutics and high rate of recurrence

© 2013 John Wiley & Sons Ltd

contribute to the poor prognosis of OVCA.[2,3] Ovarian cancer differs from other malignancies in its specific dissemination pattern.[4] The tumor typically spreads in a diffuse intra-abdominal fashion rather than through systemic circulation. Thus, factors including members of immune system in the tumor microenvironment play critical roles in tumor progression or inhibition of tumor growth.

Tumor development, in general, elicits immune responses by both innate and adaptive immune cells.[5–7] Natural killer (NK) cells are a component of the innate immune system and have the ability to both lyse target cells and provide an early source of immunoregulatory cytokines.[8] NK cells are not major histocompatibility complex (MHC) restricted and eliminate cells harboring endogenous antigens that are not recognized by cytotoxic lymphocytes and kill virus infected cells.[9] In addition, NK cells kill neoplastic cells following stimulation by its receptor, natural killer receptor 2 group D (NKG2D), an NK cell activating receptor.[10–12] Therefore, they are considered to play an important role in immunosurveillance against cancer. However, despite the presentation of antigens by ovarian malignant cells, which should induce immune-mediated rejection, spontaneous rejection of an established tumor is rare.[4] This lack of immune response is not only due to the inefficiency of the immune system but also because of the tumor induced immune suppression that protects the tumor from eradication.[4] Although the proportion of NK cell in peripheral blood lymphocytes in OVCA patients is 12–13%, it constitutes only 7–8% of tumor infiltrating lymphocytes.[13] Numerous studies on NK cells against the tumors of several organs are available but very little is known about the antitumor activities of NK cells in OVCA. During early stages, the number of OVCA cases with tumor-infiltrating NK cells was less than those of late stages.[14] Activation of NKG2D is one of the earlier steps in NK cell-mediated antitumor immune response. NKG2D recognizes the malignant cells by identifying its ligand MHC class I chain-related protein A (MICA) or B (MICB) expressed on the surface of the tumor cells.[14] But, as the tumor progresses, it evades antitumor activity of NK cells by secreting MICA into the circulation, which binds with the circulatory NKG2D receptors making it ineffective against tumor cells.[15] However, little is known about the tumor-induced evasion of NK cell function in the context of ovarian cancer. In addition, the mechanism and the factors modulating MICA expression are also not well understood.

Conventional immunotherapies to enhance antitumor immunity have met with little success.[5, 16] Development of new strategies to promote immune responses against malignancies is critical in overcoming or to supplement the limited efficacy of conventional therapies. Majority of all chronic illnesses and diseases in human are linked to lifestyle and dietary habits.[17,18] Dietary supplementation of natural products including herbal elements has long been used in traditional medicine for the prevention and treatment of many human diseases.[19,20] *Ashwagandha* (*Withania somnifera* Dunal, common name: Winter Cherry) is a medicinal plant belonging to the Solanacea family. It has been safely used in traditional medicine for the treatment of a variety of human diseases.[21] Although studies have reported various biological and biochemical properties of *Ashwagandha* including antioxidative, anti-inflammatory and antistressor, very few studies have been performed on the immunomodulatory roles of *Ashwagandha*. Furthermore, compared with other common herbs (e.g., turmeric and its derivative curcumin), information on the anti-OVCA activities of *Ashwagandha* is very limited and those available were based on either cell lines or rodent models of induced ovarian carcinoma. Rodents do not develop OVCA spontaneously and the histopathologies of induced OVCA in rodents do not resemble the spontaneous OVCA in humans.[22] Difficulties in identifying and access to patients at the early stage of OVCA hinder the ability to study efficacy of *Ashwagandha* against OVCA and developing interventional strategies for its prevention. Recently, we and others have shown that laying hens are the only widely available and easily accessible animals that develop OVCA spontaneously with a high incidence rate and histopathologies remarkably similar to human OVCA.[23] Chicken NK cell activities including characteristics, regulation, and role in poultry diseases have been described in detail.[24–29] Avian NK cell biology has strong similarities to that of mammalian.[9] Therefore, the goals of this pilot study were to examine (i) whether dietary *Ashwagandha* supplementation reduces ovarian tumor incidence and progression and (ii) whether dietary *Ashwagandha* supplementation changes the frequency of NK cells in the ovaries of hens with or without ovarian cancer.

© 2013 John Wiley & Sons Ltd

Materials and methods

Animals

Commercial strains of 3- to 4-year-old White Leghorn laying hens (*Gallus domesticus*) were used. The incidence of OVCA in hens of this age group is approximately 15–20% and is associated with partial or complete cessation of egg laying.[23,30,31] In the exploratory study, archived tissue samples of normal hens (n = 15), or hens with early stage (n = 15, 5 for each of serous, endometrioid, and mucinous types) and late stage (n = 15, 5 for each of serous, endometrioid, and mucinous types) OVCA were examined. All experimental procedures were performed according to the institutional animal care and use committee (IACUC) approved protocol. For prospective study with *Ashwagandha* supplementation, hens (n = 90) with low egg laying rates and with or without ovarian tumors at early stage detected by transvaginal ultrasound (TVUS) scanning were selected as reported previously [23,31] and described briefly below. All hens including control and supplemented with *Ashwagandha* were reared in individual cages under similar standard poultry husbandry practices with *ad libitum* access to feed and water.

Ultrasound Imaging of Hen Ovaries

TVUS imaging of hen ovaries was performed as reported previously [23,31] using an instrument equipped with a 5- to 7.5-MHz endovaginal transducer (MicroMaxx, SonoSite, Inc, Bothell, WA, USA). Gray scale morphologic evaluation of the ovaries was performed with attention to the number of developing hierarchical follicles, echogenicity as well as bilaterality, septations, papillary projections when a solid mass was present with or without accompanied ascites. Large pre-ovulatory hierarchical follicles appeared as dark circular or oval and can be distinguished from cystic follicles by the presence of a concentric ring at the center of each follicle on gray scale sonography. Approximately 5 or 6 large preovulatory hierarchical follicles were seen in a fully functional ovary. Normal ovaries in hens with reduced ovarian function contained 2 or 3 large preovulatory hierarchical follicles. Hens with early stage of OVCA had a solid tissue mass limited to a part of the ovary with no or minimal accompanied ascites and contained 1 or 2 large preovulatory hierarchical follicles. Hens with late stage OVCA contained a large solid tissue mass with papillary or septal projections accompanied by profuse ascites in the peritoneal cavity without any large preovulatory hierarchical follicle.

After morphologic evaluation by gray scale, tumor associated blood flow was examined using color Doppler ultrasound imaging. Once blood flow was detected, it was shown as either 'peripheral' (color signals in the wall or periphery of a follicle) or 'central' (blood flow detected in septa, papillary projections in solid tissue mass). Normal hens with multiple developing hierarchical follicles showed blood flow around areas of small growing follicles and along the follicular walls of large preovulatory follicles in Doppler sonography. Tumor in the ovary showed confluent blood flow at the center of the solid mass.

Ashwagandha Supplementation

Hens were divided into 3 groups including control, 1% *Ashwagandha* (1 g/kg body weight)- and 2% *Ashwagandha* (2 g/kg body weight)-supplemented groups. All hens were selected by transvaginal ultrasound and each group had 30 hens (5 with ovarian tumors at early stage and 25 with normal ovaries). All animals were provided with *ad libitum* access to food and water. In *Ashwagandha* treated groups, hens were supplemented with *Ashwagandha* root powder commercially available for human consumption (Organic India USA, Boulder, CO, USA) mixed with their basal ration for 90 days. Control hens (n = 30) were fed basal ration only. Hens were maintained in individual cages, egg laying and mortality (if any) were recorded daily.

Tissue Collection and Processing

Collection of serum samples

Blood was obtained from brachial veins of all hens before the start of feed supplementation and at 30-day interval and prior to euthanasia (90th day of the experiment, centrifuged ($1000 \times g$, 20 min)), serum samples were separated, and aliquots were stored at −80°C until further use.

Gross ovarian morphology and histopathology

Ovarian pathology and tumor staging were performed by gross observation at euthanasia and by histological examination as reported previously.[23] Briefly, emphasis was given on location of tumors, the presence or absence of metastasis and peritoneal

© 2013 John Wiley & Sons Ltd

ascites. In early stages of OVCA, tumors were confined to the ovary, appeared firm and resembled cauliflower-like nodules with no or minimal ascites. In late stage OVCA, tumors were metastasized to both abdominal and peritoneal organs including small and large intestine, mesentery, undersurface of the diaphragm and surface of the liver, oviduct with moderate to profuse ascites.

Each normal ovary or ovary with tumor was divided into four portions for protein extraction, total RNA collection, paraffin, and frozen sections for routine histology and immunohistochemical studies as reported previously.[32] All samples collected from each group (with or without supplementation) were subdivided into normal, hens with early and late stage OVCA based on gross and histopathological diagnosis of ovarian tissues as reported previously.[23] Paraffin sections from ovaries with tumor or ovaries that appeared normal without any grossly detectable tumor were stained with hematoxylin & eosin and examined under a light microscope. The presence or absence of malignant cells in the section and their histological types were determined as reported earlier.[23]

Preparation of Ovarian Specimen for Biochemical Analysis

Snap-frozen ovarian cortical specimen from normal ovaries and tumor specimen from ovaries with tumor were homogenized with a Polytron homogenizer (Brinkman Instruments, Westbury, NY, USA) as reported previously,[7,23] centrifuged, supernatant was collected, protein content of the extract was measured and stored at −80°C until further use.

Immunohistochemistry

Immunoreactive NK cells were localized and MICA expression was determined in paraffin sections from normal or malignant ovaries by immunohistochemistry using mouse anti-chicken NK-cell antibodies (purchased from the Developmental Studies Hybridoma Bank, Iowa city, IA[33]) and Rabbit anti-MICA antibodies (Abcam, Cambridge, MA, USA), respectively. Sections were then examined under a light microscope attached to a digital imaging software (MicroSuite, version 5; Olympus Corporation, Tokyo, Japan). The population of immunoreactive NK cells were determined from three sections per ovary and 5 regions of interest (ROI, 20,000 μm^2/region) per section selected randomly as reported earlier.[34,35] The mean of NK cell frequencies in 5 ROIs was considered as the mean of each section, and the mean of 3 sections was considered as the mean of each ovary. The mean of all ovaries in each group of hen was considered as the mean frequency of NK cells in that group (with or without *Ashwagandha* supplementation). The intensity of the MICA immunostaining by normal ovaries or ovaries with tumor in serial sections was measured similarly using a computer-assisted software program (MicroSuite version 5; Olympus Corporation) and recorded as pixel values in 20,000 μm^2 of the section as reported previously.[36] The mean of pixel values for each group of hens was determined similarly as mentioned above for the mean frequency of NK cells.

One-Dimensional (1D) Western Blot

Expression of MICA proteins by normal ovarian surface epithelium (OSE) or ovarian tumor epithelium was determined by Western blotting as reported earlier[37,38] using primary and secondary antibodies mentioned above. Based on immunohistochemical staining results, representative samples of OSE homogenates from normal or ovarian tumors were used in immunoblotting. Immunoreactions on the membrane were visualized as a chemiluminescence product (Super Dura West substrate; Pierce, Thermo Fisher Scientific, Rockford, IL, USA), and the image was captured using a Chemidoc XRS (BioRad, Hercules, CA, USA). No immune reaction was observed in negative controls when protein samples were omitted.

Statistical Analysis

The differences in the frequencies of immunoreactive NK cells among the three treatment groups [control (unsupplemented), 1% and 2% *Ashwagandha* supplementation] were assessed by ANOVA *F*-test and the alternative nonparametric Kruskal–Wallis test. Comparisons among group pairs were performed by two-sample *t* tests and alternative Mann–Whitney tests. Similar methods were used to compare normal, early and late stage OVCA or their subsets. Differences in the staining intensity for MICA expression among different groups of hens were also analyzed similarly. All reported *P* values are 2 sided, and $P < .05$ was considered significant. Descriptive summaries were reported, especially in cases when the group sizes were small for inferential comparisons. Statistical analyses were performed

© 2013 John Wiley & Sons Ltd

with SPSS (PASW), version 18 software (SPSS Inc., Chicago, IL, USA).

Results

Effects of *Ashwagandha* Supplementation on the Incidence and Progression of Ovarian Tumors in Hens

Gross morphology

Hens with pre-existing ovarian tumor at early stage: In the control group (without *Ashwagandha* supplementation), all hens ($n = 5$) with pre-existing ovarian tumors at early stages progressed to the late stages with the tumor metastasized to abdominal organs accompanied with profuse ascites. In the 1% *Ashwagandha* treated group, 4 of 5 hens with pre-existing ovarian tumors at early stage progressed to late stages and the tumor remained limited to the ovary in one hen. In the 2% *Ashwagandha* treated group, tumors remained limited to the ovary in 4 of 5 hens with pre-existing ovarian tumors, whereas the tumor progressed to late stage in one hen (Fig. 1a–b). Thus, 2% dietary *Ashwagandha* supplementation reduced tumor progression in hens.

Hens without pre-existing ovarian tumors: Of the 4 of 25 hens in the control group developed ovarian tumors with solid tissue masses limited to the ovaries, and these hens were grouped as hens with early stage OVCA. No abnormality was detected in the remaining 21 hens, and they were grouped as normal hens. In the 1% *Ashwagandha* treated group, 2 of 25 hens had an ovarian tumor mass at early stage. In the 2% *Ashwagandha* treated group, a solid tissue mass limited to a part of the ovary was found in 1 of 25 hens (early stage), and remaining 24 hens were normal (Fig. 1c). Thus, incidence of ovarian tumor development is reduced in hens supplemented with 2% dietary *Ashwagandha*.

Histopathology (Prospective Study)

Hens with pre-existing ovarian tumors

Of the 5 hens in the control group in which tumor progressed to late stages, 2 were serous, 1 endometrioid, 1 mucinous, whereas 1 was a mixed (seromucinous) ovarian carcinoma. In the 1% *Ashwagandha* supplemented group, of the 5 hens with tumors, 1 was at early stage (1 serous) and 4 late stage of OVCA (1 serous, 2 endometrioid and 1 mucinous). In the 2% *Ashwagandha* supplemented group, of the 5 hens with tumors, 4 were at early stage (1 serous, 2 endometrioid, and 1 mucinous) and 1 was at late stage OVCA (serous) (Fig. 1d).

Hens without pre-existing ovarian tumors

Of the 4 hens that developed OVCA during the study period in the control group, 2 were serous and

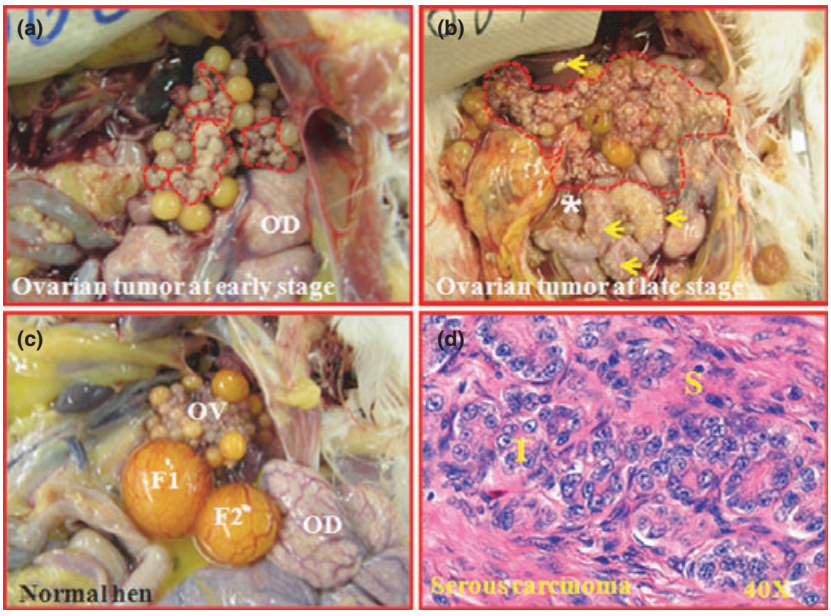

Fig. 1 Effects of 2% dietary *Ashwagandha* supplementation on the progression of spontaneous ovarian tumors in hens. (a) Ovarian cancer (OVCA) at an early stage in a hen. Tumor is limited to the ovary (red dotted area). (b) Ovarian cancer at late stage in a hen. Tumor (red dotted area) metastasized to other organs (arrows) with accompanied ascites (*). (c) Normal hen ovary showing preovulatory follicles (F1 and F2) and oviduct (OD). (d) Section of a serous carcinoma from a hen in control group showing tumor cells with large pleomorphic nucleus. 40X. *F* = Follicle, S = Stroma, Tu = Tumor.

© 2013 John Wiley & Sons Ltd

2 were endometrioid carcinomas. In the 1% *Ashwagandha* supplemented group, 2 hens developed ovarian tumors (early stage), which were serous carcinomas. In the 2% *Ashwagandha* supplemented group, 1 hen developed an ovarian tumor (early stage) which was a serous carcinoma.

Localization of Immunopositive NK Cells

Exploratory study: Changes in NK cell population in association with ovarian tumor development and progression

Enumeration of NK cells was separated by their localization as intratumoral (infiltrating into tumor nests) or intrastromal (stroma of the tumor) (Table I). Compared with the ovarian stroma in normal hens (Fig. 2a), more NK cells were observed in the ovarian stroma of hens with early stage (Fig. 2b) and late stage OVCA (Fig. 2c). The frequency of NK cells in the stroma of normal hens was 2.76 ± 0.83 (mean ± SD, in 20,000 μm^2 area of tissue) (Fig. 3). The frequency of NK cells was significantly ($P < 0.0001$) high in the stroma of hens with early stage OVCA (4.84 ± 1.31 in 20,000 μm^2 area of tissue) and increased further in the stroma of hens with late stage OVCA (7.2 ± 0.65 in 20,000 μm^2 area of tissue) ($P < 0.0001$) (Fig. 3). The mean frequency of intratumoral NK cells in hens with early stage OVCA was 3.76 ± 1.05 in 20,000 μm^2 area of tissue. Although compared with hens with early stage OVCA, the frequency of intratumoral NK cells was higher in hens with late stage OVCA (4.28 ± 0.98 in 20,000 μm^2 area of tissue); however, the differences were not significant (Fig. 3).

Prospective study: Changes in NK cell population relative to dietary Ashwagandha *supplementation*

NK cell population in hens without or with pre-existing ovarian tumors and supplemented with dietary *Ashwagandha* is mentioned in Table II. Differences in NK cell population were not observed in normal hens supplemented with or without dietary *Ashwagandha*. In the prospective study without pre-existing tumors, hens which developed OVCA in 2% *Ashwagandha* supplemented group had more stromal and intratumoral NK cells than those developed OVCA in 1% *Ashwagandha* supplemented group (Fig. 4a,b). However, differences in NK cell population among different histological subtypes of OVCA within the similar dose of *Ashwagandha* supplementation (1 or 2%) were not observed. The frequency

Table I Frequencies of ovarian NK cells in normal hens or hens with ovarian cancer (OVCA)

		Histological subtypes							
	Normal	Serous		Endometrioid		Mucinous		All subtypes	
OVCA Stages	Stroma	Stroma	Tumor	Stroma	Tumor	Stroma	Tumor	Stroma	Tumor
Normal ($n = 15$)	2.76 ± 0.83	–	–	–	–	–	–	–	–
Early ($n = 15$)		5.16 ± 1.52^{NS}	4.04 ± 1.02^{NS}	4.72 ± 1.17^{NS}	3.68 ± 1.07^{NS}	4.64 ± 1.15^{NS}	3.56 ± 1.04^{NS}	4.84 ± 1.31*	3.76 ± 1.05^{NS}
Late ($n = 15$)		7.40 ± 0.5^{NS}	4.64 ± 1.04^{NS}	7.20 ± 0.65^{NS}	4.20 ± 0.96^{NS}	7.00 ± 0.71^{NS}	4.00 ± 0.87^{NS}	7.20 ± 0.64**	4.28 ± 0.98^{NS}

*Indicates significant differences ($P < 0.01$) in NK cell numbers between normal and early stage OVCA.
**Indicates significant differences at ($P < 0.01$) in NK cell numbers between early and late stage OVCA.
NS indicates no significant difference in NK cell number among different subtypes of tumor within the same stage of OVCA (early or late) as well as between the intra-tumoral NK cell (all subtypes) population of early and late stages OVCA.

© 2013 John Wiley & Sons Ltd

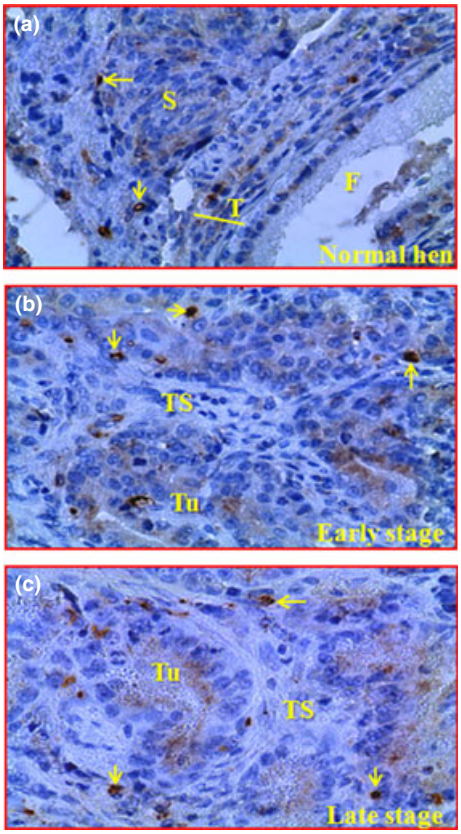

Fig. 2 Localization of immunoreactive NK cells in the ovary of hens with or without ovarian tumors (exploratory study). (a) Section of a normal ovary showing few immunoreactive NK cells in the stroma (S) and follicular theca (T). (b and c) Sections of ovarian tumors at early and late stages, respectively. Immunoreactive NK cells are localized in the tumor stroma (TS) with a few in intratumoral (Tu) spaces. Arrows indicate examples of immunoreactive NK cells. 20X.

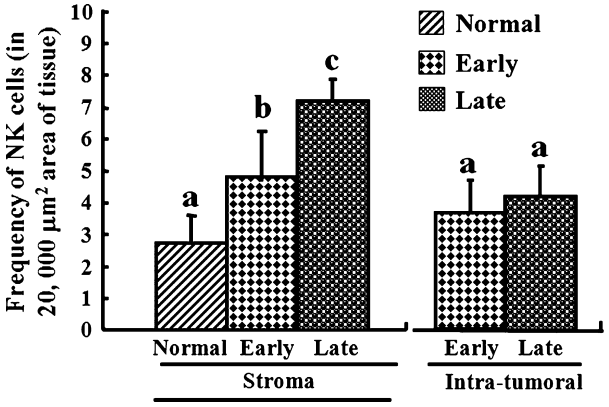

Fig. 3 Changes in NK cell population in association with ovarian cancer (OVCA) tumor development and progression in hens (exploratory study). The frequency of NK cells was significantly higher in the tumor stroma in OVCA hens at early and late stages than in the stroma of normal hens. Differences in intratumoral NK cell population were not significant between the early and late stages of OVCA. Different letters denote significant differences ($P < 0.0001$) within the same group of tissue (stroma or intratumor).

of NK cells in the stroma of OVCA hens in the control group was (mean ± S.D.) 5.19 ± 1.10 in 20,000 μm^2 area of tissue and increased significantly ($P < 0.0001$) to 7.40 ± 1.43 cells in 20,000 μm^2 area of tissue in OVCA hens supplemented with 1% dietary *Ashwagandha* (Fig. 4 bottom panel). The frequency of NK cells increased further to 10.20 cells in 20,000 μm^2 area of tissue area in OVCA hens supplemented with 2% dietary *Ashwagandha*. Similarly, compared with OVCA hens in control group (4.23 ± 1.11), the frequency of intratumoral NK cells increased significantly ($P < 0.01$) to 6.50 ± 1.18 cells in 20,000 μm^2 area of tissue in OVCA hens supplemented with 1% dietary *Ashwagandha*. The population of intratumoral NK cells increased further to 8.20 cells in 20,000 μm^2 area of tissue in OVCA hens supplemented with 2% dietary *Ashwagandha*. (Fig. 4 bottom panel). Thus, dietary *Ashwagandha* supplementation enhanced localization of NK cells in hens with OVCA.

Changes in MICA Expression by Dietary *Ashwagandha* Supplementation

Expression of MICA was not detected in normal epithelium. Intense staining for MICA by malignant cells was observed in hens with OVCA in the control group (Fig. 5a). In contrast, the staining for MICA by malignant cells was weak in hens supplemented with 2% dietary *Ashwagandha* (Fig. 5c). However, a weak to moderate staining for MICA was observed in OVCA hens supplemented with 1% dietary *Ashwagandha* (Fig. 5b). Compared with control hens with OVCA [(205.06 ± 39.16) X10^4 pixels/20,000 μm^2 of tissue], the intensity of MICA expression by malignant epithelium was significantly ($P < 0.01$) decreased in OVCA hens supplemented with 1% dietary *Ashwagandha* [(145.18 ± 22.76) X10^4 pixels/20,000 μm^2 of tissue] and decreased further in hens supplemented with 2% dietary *Ashwagandha* (77.22 × 10^4 pixels/20,000 μm^2 of tissue) (Fig. 6a). Significant differences in MICA expression among hens of different histological subtypes treated with 1% *Ashwagandha* was not observed.

MICA expression in representative samples from OVCA hens in control, 1%- and 2%-*Ashwagandha*

© 2013 John Wiley & Sons Ltd

Table II Changes in the population of ovarian NK cells in normal hens or hens with ovarian cancer (OVCA) supplemented with or without dietary *Ashwagandha*

Prospective study: NK cells in hens with pre-existing tumors

	Histological subtypes							
	Serous		Endometrioid		Mucinous		All subtypes	
OVCA Stages	Stroma	Tumor	Stroma	Tumor	Stroma	Tumor	Stroma	Tumor
Early:	All hens with pre-existing early OVCA in (control) untreated group progressed to late stage OVCA							
Control								
1% ASH ($n = 1$)	8.20	7.40	ND	ND	ND	ND	8.20	7.40
2% ASH ($n = 4$)	10.40 ± 1.14^{NS}	8.40 ± 0.55^{NS}	10.30 ± 1.34^{NS}	8.10 ± 0.88^{NS}	10.00 ± 1.58^{NS}	8.00 ± 1.00^{NS}	10.25 ± 1.29**	8.15 ± 0.81**
Late:	8.10 ± 0.88^{NS}	5.80 ± 1.03^{NS}	7.80 ± 1.79^{NS}	5.40 ± 1.34^{NS}	7.20 ± 0.84^{NS}	4.80 ± 1.30^{NS}	7.80 ± 1.15	$4.85 + 0.88$
Control ($n = 5$)								
1% ASH ($n = 4$)	11.20 ± 0.83^{NS}	9.40 ± 0.89^{NS}	10.50 ± 1.35^{NS}	8.40 ± 0.84^{NS}	10.20 ± 0.84^{NS}	8.20 ± 1.48^{NS}	10.60 ± 1.14*	8.60 ± 1.10*
2% ASH ($n = 1$)	12.60	10.00	ND	ND	ND	ND	12.60	10.00

Prospective study: Hens without pre-existing tumors

		Histological subtypes							
	Normal	Serous		Endometrioid		Mucinous		All subtypes	
OVCA Stages	Stroma	Stroma	Tumor	Stroma	Tumor	Stroma	Tumor	Stroma	Tumor
Normal:	2.96 ± 1.32^{NS}	–	–	–	–	–	–	–	–
Control ($n = 21$)									
1% ASH ($n = 23$)	3.16 ± 0.80^{NS}		–		–	–	–	–	–
2% ASH ($n = 24$)	3.4 ± 0.87^{NS}		–		–	–	–	–	–
Early:		5.30 ± 1.12^{NS}	4.30 ± 1.34^{NS}	5.09 ± 1.05^{NS}	4.18 ± 0.87^{NS}	ND	ND	5.19 ± 1.10	4.23 ± 1.11
Control ($n = 4$)									
1% ASH ($n = 2$)		7.40 ± 1.43	6.50 ± 1.18	ND	ND	ND	ND	7.40 ± 1.43*	6.50 ± 1.18*
2% ASH ($n = 1$)		10.20	8.20	ND	ND	ND	ND	10.20	8.20
Late:	None of the hens had late stage OVCA								

*Indicates significant differences ($P < 0.01$) in NK cell numbers between control and 1% ASH supplemented group.

**Indicates significant differences at ($P < 0.01$) in NK cell numbers between 1% and 2% ASH supplemented group.

NS indicates no significant difference in NK cell number among different subtypes of tumor within the same stage of OVCA (early or late) and same dose of ASH supplementation (1% or 2%) as well as among normal hens with or without ASH supplementation.

ND, Not detected.

© 2013 John Wiley & Sons Ltd

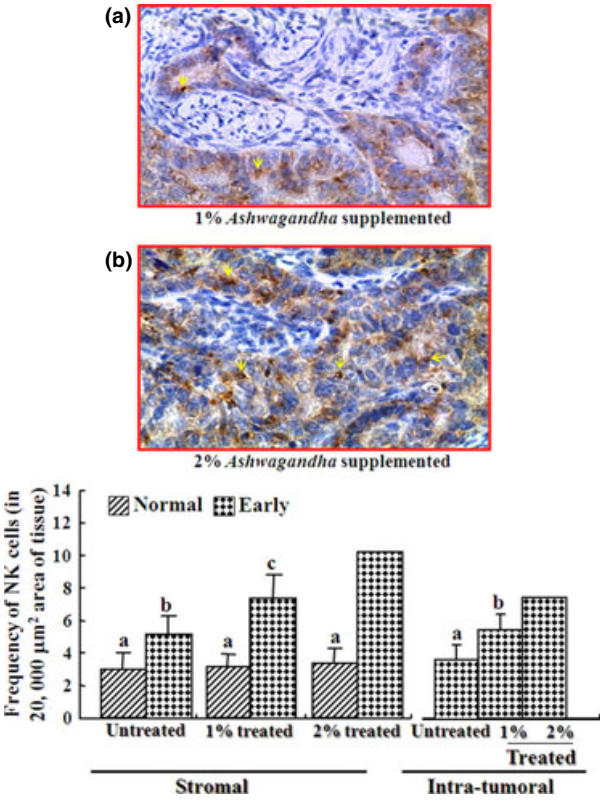

Fig. 4 Changes in NK cell population in ovarian tumors at early stage due to dietary *Ashwagandha* supplementation. (a,b) Compared with 1% *Ashwagandha* supplemented hens (a), more immunoreactive NK cells are seen in 2% *Ashwagandha* supplemented hens (b). Arrows indicate examples of immunoreactive NK cells. 20X. Bottom panel: Differences in NK cell frequencies were not observed in normal (healthy) hens supplemented with or without *Ashwagandha*. Compared with OVCA hens in control group (hens without pre-existing tumor group), the frequencies of stromal and intratumoral NK cells were significantly ($P < 0.0001$) higher in 1% *Ashwagandha* supplemented hens and increased further in 2% *Ashwagandha* supplemented hens. Different letters denote significant differences among dietary supplementations.

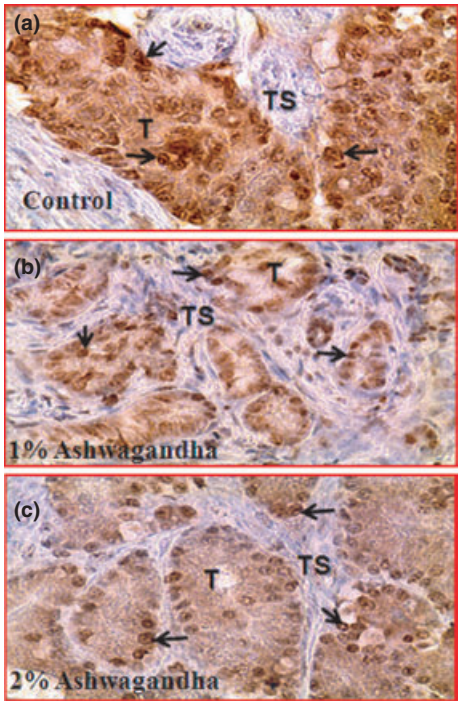

Fig. 5 Changes in MHC class I chain-related protein A (MICA, ligand of NKG2D receptors) expression in ovarian tumors at early stage in hens supplemented with or without dietary *Ashwagandha*. (a) Section of an ovarian tumor at early stage in control hens showing intense expression of MICA. (b–c) Sections of ovarian tumors at early stages in hens supplemented with 1% - and 2%-*Ashwagandha*, respectively. Compared with control hens, MICA expression was relatively weak in hens supplemented with 1% *Ashwagandha* (b) and decreased further in hens supplemented with 2% *Ashwagandha* (c). T = tumor; TS = tumor stroma. Arrows indicate examples of immunoreactive MICA-expressing tumor cells. 20X.

treated groups were examined by immunoblotting. A protein band of approximately 75 kDa was detected with strong immunoreactivity in control hens with OVCA, whereas a weak immunoreactive band was observed in OVCA hens supplemented with 1% or 2% *Ashwagandha* (Fig. 6b).

Discussion

This is the first report to show that dietary supplementation with *Ashwagandha*, a medicinal herb, reduced the incidence and progression of ovarian tumors in hens, a spontaneous pre-clinical model of human ovarian cancer. This study showed that *Ashwagandha* supplementation increased the frequency of NK cells in tumor vicinity. This increase in NK cell population was associated with the decrease in the expression of MICA by the tumor.

Medicinal plants including herbs have long been used in traditional medicine for the prevention and treatment of many chronic and acute human diseases. *Ashwagandha* has been reported to exert cytotoxic effects against a variety of human tumor cell lines.[39–43] In this study, ovarian tumors at early stage did not progress to later stages in 4 of 5 (80%) OVCA hens supplemented with 2% dietary *Ashwagandha*. In contrast, all tumors metastasized to distant organs in hens (with pre-existing ovarian tumors at early stage) without *Ashwagandha* supplementation. However, 1% *Ashwagandha*

American Journal of Reproductive Immunology **70** (2013) 538–550
© 2013 John Wiley & Sons Ltd

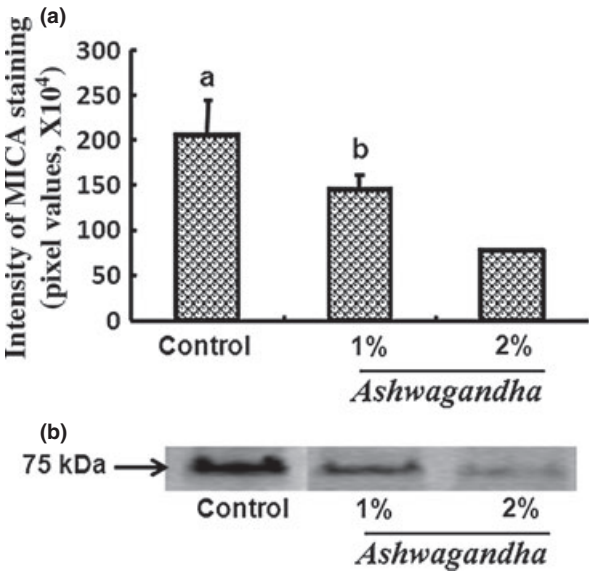

Fig. 6 (a) Changes in the intensity of MICA expression by *Ashwagandha* supplementation in hens with ovarian cancer (OVCA) at early stage. Compared with control group, the intensity of MICA expression was significantly decreased in 1% *Ashwagandha* supplemented hens and 2% decreased further in *Ashwagandha* supplemented hens ($P < 0.01$). Different letters denote significant differences among different dietary groups. (b) Immunoblotting confirmed the decrease in MICA protein expression by *Ashwagandha* supplementation. An immunoreactive band of approximately 75 kDa was detected in all hens. The band for MICA was strongest in control hens compared with hens supplemented with 1%- and 2%-*Ashwagandha*.

supplementation was not found as effective as 2% *Ashwagandha* in the prevention of tumor progression and metastasis. In addition, compared with control and 1% *Ashwagandha* supplementation, the rate of OVCA incidence was lowest in 2% *Ashwagandha* supplemented hens. Thus, 2% dietary supplementation with *Ashwagandha* was found to be more preventive of tumor progression and reduction in tumor incidence than 1% *Ashwagandha* supplementation in hens. Antitumor effects of *Ashwagandha* have also been reported against several other tumors.[39,44,45] The mechanism(s) of this antiproliferative effect of *Ashwagandha* on tumor progression is not fully understood. Herbal preparations have been reported to enhance both specific and non-specific immunity. It is possible that *Ashwagandha* may exert its antitumor effects by stimulating immune function against developing ovarian tumors.

NK cells are a member of innate immune system and provide rapid responses to virally infected cells and developing tumors.[46] NK cells play critical roles in tumor immunosurveillance by directly inducing the death of tumor cells even with the absence of surface adhesion-molecules and antigenic peptides. In this study, the frequency of stromal but not intratumoral immunoreactive NK cells increased significantly with the development and progression of OVCA. In contrast, *Ashwagandha* supplementation prevented tumor progression in 4 of 5 OVCA hens (prospective study in hens with pre-existing early stage OVCA), and these hens had significantly high population of NK cells as compared with untreated OVCA hens. In addition, *Ashwagandha* supplementation increased NK cell population in OVCA hens irrespective of their tumor subtypes and significant differences in NK cell population among different histological subtypes were not observed. Thus, these results indicate that NK cell may play dualistic roles including a protumor role (a negative prognosis factor) leading to tumor progression as well as an antitumor role (a positive prognostic) involving the prevention of tumor metastasis. Several reports have mentioned a dualistic role of NK cells in the context of various cancers.[47–49] Intratumoral NK cells exerts its protumoral immunosuppressive roles by secreting CCL22 and recruiting T regulatory cells.[49] On the other hand, when activated with IL-2, IL-12, and IL18, NK cells have been reported to enhance cytotoxic activity against tumors.[48,50] *Ashwagandha* treatment was reported to enhance NK cell functions in mice.[51] Enhanced secretion of IL-12 was reported in mouse upon oral administration of root extract of *Ashwagandha*.[52] Thus, it is possible that *Ashwagandha* might have prevented or reduced the availability of factor(s) involved in immunosuppression or enhanced the secretion factors stimulating antitumor functions of NK cells in the tumor microenvironment irrespective of tumor subtypes.

In the present study, compared with OVCA hens in control group, MICA expression decreased significantly in OVCA hens supplemented with 2% *Ashwagandha* suggesting that *Ashwagandha* treatment might have reduced or prevented tumor-associated stress as well as production and secretion of MICA. Studies have reported that tumor escapes antitumor immune responses by secreting/producing immunosuppressive agents. It is established that the lysis of tumor cells by NK cells is mediated by receptors including natural killer group 2, member D (NKG2D).[53] NKG2D recognizes a number of ligands including MICA, which are typically expressed by tumor cells. MICA expression is associated with cellular stresses

© 2013 John Wiley & Sons Ltd

including those induced by a developing tumor.[54] To evade killing by NK cells, the tumor sheds/secretes MICA into the circulation. Secreted MICA binds with circulatory NK cells expressing NKG2D; thus, making NK cells less available to kill tumor cells.[14] *Ashwagandha* has been reported to reduce stress by enhancing antioxidant functions.[55] Tumors require oxygen and nutrients for their growth and progression, which creates a stressful condition (tumor-associated stress) in the tumor microenvironment. Supplementation *of hens with Ashwagandha*, an anti-stress natural product, might have reduced tumor-associated stress. Thus, reduced stress might have decreased shedding of MICA (a marker of cellular stress) from the surface of tumor cells into the circulation. Decreased MICA levels in circulation may result in more NK cells with free NKG2D receptor available to infiltrate into the vicinity of the tumor and bind with their ligand expressed on the surface of tumor cells in *Ashwagandha* supplemented hens.

Overall, this study suggests that low influx of NK cells in response to developing ovarian tumors in control hens may be related to the increased shedding of MICA and subsequent high MICA levels in the circulation as reported previously.[56] *Ashwagandha* supplementation of hens with tumors had increased influx of NK cells into the vicinity of the tumor, possibly, by decreasing the expression and shedding of MICA, a marker of cellular stress. The findings of the present study suggest several translational significances. Our understanding regarding the mechanism and role of tumor-induced immunosuppression in the context of spontaneous OVCA is very limited, in part, due to the lack of an animal model that develops spontaneous OVCA. Because of the difficulty in detecting OVCA at an early stage, access to patient specimens to study and develop an effective antitumor immunotherapy is difficult and time consuming. Similarities between the spontaneous OVCA development and histological subtypes in humans and hens, risk factors (e.g., incessant ovulation), expression of several molecular markers of OVCA and above all similar patterns of tumor dissemination suggest a high probability that results obtained from this study may form a foundation for a clinical study. More importantly, the development and functions of avian innate and adoptive immune functions are similar to mammals.[9] Thus, the antitumor immunoenhancing properties of *Ashwagandha* may also be effective in humans. Taken together, information on the NK cell population and its influx into the tumor vicinity by dietary *Ashwagandha* supplementation will aid in the development of anti-OVCA immunotherapies based on natural products. Alternatively, *Ashwagandha* may also be used in combination with currently available chemotherapeutics to enhance the tumoricidal ability of the later drugs. Thus, the results of the present study will lay the foundation for clinical studies.

This study did not examine the effects of *Ashwagandha* in hens with clear cell ovarian carcinoma. Spontaneous incidence of all four histological subtypes of epithelial OVCA including clear cell carcinoma in laying hens was reported earlier.[23] However, similar to humans, the rate of incidence of clear cell OVCA in hens is also very low. Thus, lack of information on NK cell population in clear cell OVCA due to small number of sample size is a limitation of this study. In conclusion, this study showed that dietary supplementation of *Ashwagandha*, increased the influx of NK cells and prevented the severity of ovarian cancer by inhibiting tumor progression in hens, a pre-clinical model of spontaneous OVCA.

Acknowledgements

The authors declare no conflict of interest. This research was supported (in part) by the Department of Defense Ovarian Cancer Research Program under award # W81XWH-11-1-0510 and the Elmer Sylvia and Sramek Foundation (USA). We thank Chet and Pam Utterback, Doug Hilgendorf and Chelsie Parr, staff of the University of Illinois at Urbana-Champaign Poultry Research Farm, for maintenance of the hens.

References

1 American CS (2013). "Cancer Facts & Figures 2013"http://www.cancer.org/research/cancerfactsstatistics/cancerfactsfigures2013/index.
2 Goodman MT, Correa CN, Tung KH, Roffers SD, Cheng Wu X, Young JL Jr, Wilkens LR, Carney ME, Howe HL: Stage at diagnosis of ovarian cancer in the United States, 1992-1997. *Cancer* 2003; 97 (10 Suppl):2648–2659.
3 Ries LA: Ovarian cancer. Survival and treatment differences by age. *Cancer* 1993; 71(2 Suppl):524–529.
4 Yigit R, Massuger LF, Figdor CG, Torensma R: "Ovarian cancer creates a suppressive microenvironment to escape immune elimination." *Gynecol Oncol* 2010; 117:366–372.
5 Zou W: Regulatory T cells, tumour immunity and immunotherapy. *Nat Rev Immunol* 2006; 6:295–307.

© 2013 John Wiley & Sons Ltd

6 Schreiber RD, Old LJ, Smyth MJ: Cancer immunoediting: integrating immunity's roles in cancer suppression and promotion. *Science* 2011; 331:1565–1570.

7 Barua A, Edassery SL, Bitterman P, Abramowicz JS, Dirks AL, Bahr JM, Hales DB, Bradaric MJ, Luborsky JL: Prevalence of antitumor antibodies in laying hen model of human ovarian cancer. *Int J Gynecol Cancer* 2009; 19:500–507.

8 Robertson MJ, Ritz J: Biology and clinical relevance of human natural killer cells. *Blood* 1990; 76:2421–2438.

9 Erf GF: Cell-mediated immunity in poultry. *Poult Sci* 2004; 83:580–590.

10 Tsukerman P, Stern-Ginossar N, Gur C, Glasner A, Nachmani D, Bauman Y, Yamin R, Vitenshtein A, Stanietsky N, Bar-Mag T, Lankry D, Mandelboim O: MiR-10b downregulates the stress-induced cell surface molecule MICB, a critical ligand for cancer cell recognition by natural killer cells. *Cancer Res* 2012; 72:5463–5472.

11 Raulet DH: Roles of the NKG2D immunoreceptor and its ligands. *Nat Rev Immunol* 2003; 3:781–790.

12 Moretta A, Bottino C, Vitale M, Pende D, Cantoni C, Mingari MC, Biassoni R, Moretta L: Activating receptors and coreceptors involved in human natural killer cell-mediated cytolysis. *Annu Rev Immunol* 2001; 19:197–223.

13 Santin AD, Hermonat PL, Ravaggi A, Bellone S, Roman JJ, Smith CV, Pecorelli S, Radominska-Pandya A, Cannon MJ, Parham GP: Phenotypic and functional analysis of tumor-infiltrating lymphocytes compared with tumor-associated lymphocytes from ascitic fluid and peripheral blood lymphocytes in patients with advanced ovarian cancer. *Gynecol Obstet Invest* 2001; 51:254–261.

14 Li K, Mandai M, Hamanishi J, Matsumura N, Suzuki A, Yagi H, Yamaguchi K, Baba T, Fujii S, Konishi I: Clinical significance of the NKG2D ligands, MICA/B and ULBP2 in ovarian cancer: high expression of ULBP2 is an indicator of poor prognosis. *Cancer Immunol Immunother* 2009; 58:641–652.

15 Salih HR, Rammensee HG, Steinle A: Cutting edge: down-regulation of MICA on human tumors by proteolytic shedding. *J Immunol* 2002; 169:4098–4102.

16 Whiteside TL: Immune suppression in cancer: effects on immune cells, mechanisms and future therapeutic intervention. *Semin Cancer Biol* 2006; 16:3–15.

17 Reddy L, Odhav B, Bhoola KD: Natural products for cancer prevention: a global perspective. *Pharmacol Ther* 2003; 99:1–13.

18 Block G, Patterson B, Subar A: Fruit, vegetables, and cancer prevention: a review of the epidemiological evidence. *Nutr Cancer* 1992; 18:1–29.

19 Govindarajan R, Vijayakumar M, Pushpangadan P: Antioxidant approach to disease management and the role of 'Rasayana' herbs of Ayurveda. *J Ethnopharmacol* 2005; 99:165–178.

20 Aggarwal BB, Kumar A, Bharti AC: "Anticancer potential of curcumin: preclinical and clinical studies."*Anticancer Res* 2003; 23:363–398.

21 Mishra LC, Singh BB, Dagenais S: Scientific basis for the therapeutic use of *Withania somnifera* (*Ashwagandha*): a review. *Altern Med Rev* 2000; 5:334–346.

22 Rodriguez-Burford C, Barnes MN, Berry W, Partridge EE, Grizzle WE: Immunohistochemical expression of molecular markers in an avian model: a potential model for preclinical evaluation of agents for ovarian cancer chemoprevention. *Gynecol Oncol* 2001; 81: 373–379.

23 Barua A, Bitterman P, Abramowicz JS, Dirks AL, Bahr JM, Hales DB, Bradaric MJ, Edassery SL, Rotmensch J, Luborsky JL: Histopathology of ovarian tumors in laying hens: a preclinical model of human ovarian cancer. *Int J Gynecol Cancer* 2009; 19: 531–539.

24 Sharma JM, Okazaki W: Natural killer cell activity in chickens: target cell analysis and effect of antithymocyte serum on effector cells. *Infect Immun* 1981; 31:1078–1085.

25 York JJ, Sonza S, Fahey KJ: Immunogenic glycoproteins of infectious laryngotracheitis herpesvirus. *Virology* 1987; 161:340–347.

26 Myers TJ, Schat KA: Natural killer cell activity of chicken intraepithelial leukocytes against rotavirus-infected target cells. *Vet Immunol Immunopathol* 1990; 26:157–170.

27 Davison TF "Cell-mediated immunity: effector functions." In Poultry Immunology, Poultry Science Symposium Series. Vol 24. TF Davison, TR Morris, LN Payne, (ed). Abingdon, UK, Carfax Publishing Company, 1996, pp 115–134.

28 Gobel TW, Chen CH, Cooper MD: Expression of an avian CD6 candidate is restricted to alpha beta T cells, splenic CD8 + gamma-delta (gd) T cells and embryonic natural killer cells. *Eur J Immunol* 1996; 26:1743–1747.

29 Gobel TW, Kaspers B, Stangassinger M: NK and T cells constitute two major, functionally distinct intestinal epithelial lymphocyte subsets in the chicken. *Int Immunol* 2001; 13:757–762.

30 Fredrickson TN: Ovarian tumors of the hen. *Environ Health Perspect* 1987; 73:35–51.

31 Barua A, Abramowicz JS, Bahr JM, Bitterman P, Dirks A, Holub KA, Sheiner E, Bradaric MJ, Edassery SL, Luborsky JL: Detection of ovarian tumors in chicken by sonography: a step toward early diagnosis in humans? *J Ultrasound Med* 2007; 26:909–919.

32 Barua A, Bitterman P, Bahr JM, Bradaric MJ, Hales DB, Luborsky JL, Abramowicz JS: Detection of tumor-associated neoangiogenesis by Doppler ultrasonography during early-stage ovarian cancer in laying hens: a preclinical model of human spontaneous ovarian cancer. *J Ultrasound Med* 2010; 29:173–182.

33 Jansen CA, van de Haar PM, van Haarlem D, van Kooten P, de Wit S, van Eden W, Viertlbock BC, Gobel TW, Vervelde L: Identification of new populations of chicken natural killer (NK) cells. *Dev Comp Immunol* 2010; 34:759–767.

34 Barua A, Yoshimura Y, Tamura T: The effects of age and sex steroids on the macrophage population in the ovary of the chicken, Gallus domesticus. *J Reprod Fertil* 1998; 114:253–258.

35 Yellapa A, Bahr JM, Bitterman P, Abramowicz JS, Edassery SL, Penumatsa K, Basu S, Rotmensch J, Barua A: Association of interleukin 16 with the development of ovarian tumor and tumor-associated neoangiogenesis in laying hen model of spontaneous ovarian cancer. *Int J Gynecol Cancer* 2012; 22:199–207.

36 Khan MF, Bahr JM, Yellapa A, Bitterman P, Abramowicz JS, Edassery SL, Basu S, Rotmensch J, Barua A: Expression of Leukocyte Inhibitory Immunoglobulin-like Transcript 3 Receptors by Ovarian Tumors in Laying Hen Model of Spontaneous Ovarian Cancer. *Transl Oncol* 2012; 5:85–91.

37 Barua A, Yellapa A, Bahr JM, Abramowicz JS, Edassery SL, Basu S, Rotmensch J, Bitterman P: Expression of death receptor 6 by ovarian tumors in laying hens, a preclinical model of spontaneous ovarian cancer. *Transl Oncol* 2012; 5:260–268.

38 Yellapa A, Bahr JM, Bitterman P, Abramowicz JS, Edassery SL, Penumatsa K, Basu S, Rotmensch J, Barua A: "Association of interleukin 16 with the development of ovarian tumor and tumor-associated neoangiogenesis in laying hen model of spontaneous ovarian cancer." *Int J Gynecol Cancer* 2012; 22:199–207.

39 Devi PU: *Withania somnifera* Dunal (*Ashwagandha*): potential plant source of a promising drug for cancer chemotherapy and radiosensitization. *Indian J Exp Biol* 1996; 34:927–932.

© 2013 John Wiley & Sons Ltd

40 Hsieh PW, Huang ZY, Chen JH, Chang FR, Wu CC, Yang YL, Chiang MY, Yen MH, Chen SL, Yen HF, Lubken T, Hung WC, Wu YC: Cytotoxic withanolides from Tubocapsicum anomalum. *J Nat Prod* 2007; 70:747–753.
41 Abdeljebbar LH, Benjouad A, Morjani H, Merghoub N, El Haddar S, Humam M, Christen P, Hostettmann K, Bekkouche K, Amzazi S: Antiproliferative effects of withanolides from Withania adpressa. *Therapie* 2009; 64:121–127.
42 Lee SW, Pan MH, Chen CM, Chen ZT: Withangulatin I, a new cytotoxic withanolide from Physalis angulata. *Chem Pharm Bull (Tokyo)* 2008; 56:234–236.
43 He QP, Ma L, Luo JY, He FY, Lou LG, Hu LH: Cytotoxic withanolides from Physalis angulata L. *Chem Biodivers* 2007; 4: 443–449.
44 Devi PU, Sharada AC, Solomon FE: Antitumor and radiosensitizing effects of *Withania somnifera* (*Ashwagandha*) on a transplantable mouse tumor, Sarcoma-180. *Indian J Exp Biol* 1993; 31:607–611.
45 Devi PU, Sharada AC, Solomon FE, Kamath MS: In vivo growth inhibitory effect of *Withania somnifera* (*Ashwagandha*) on a transplantable mouse tumor, Sarcoma 180. *Indian J Exp Biol* 1992; 30:169–172.
46 Vivier E, Raulet DH, Moretta A, Caligiuri MA, Zitvogel L, Lanier LL, Yokoyama WM, Ugolini S: Innate or adaptive immunity? The example of natural killer cells. *Science* 2011; 331:44–49.
47 Wong JL, Mailliard RB, Moschos SJ, Edington H, Lotze MT, Kirkwood JM, Kalinski P: Helper activity of natural killer cells during the dendritic cell-mediated induction of melanoma-specific cytotoxic T cells. *J Immunother* 2011; 34:270–278.
48 Wong JL, Berk E, Edwards RP, Kalinski P: IL-18-Primed Helper NK Cells Collaborate with Dendritic Cells to Promote Recruitment of Effector CD8 + T Cells to the Tumor Microenvironment. *Cancer Res* 2013; 73:4653–4662.
49 Mailloux AW, Young MR: NK-dependent increases in CCL22 secretion selectively recruits regulatory T cells to the tumor microenvironment. *J Immunol* 2009; 182:2753–2765.
50 Bhat J, Damle A, Vaishnav PP, Albers R, Joshi M, Banerjee G: In vivo enhancement of natural killer cell activity through tea fortified with Ayurvedic herbs. *Phytother Res* 2010; 24:129–135.
51 Davis L, Kuttan G: Effect of Withania somnifera on cell mediated immune responses in mice. *J Exp Clin Cancer Res* 2002; 21:585–590.
52 Malik F, Singh J, Khajuria A, Suri KA, Satti NK, Singh S, Kaul MK, Kumar A, Bhatia A, Qazi GN: A standardized root extract of Withania somnifera and its major constituent withanolide-A elicit humoral and cell-mediated immune responses by up regulation of Th1-dominant polarization in BALB/c mice. *Life Sci* 2007; 80: 1525–1538.
53 Terunuma H, Deng X, Dewan Z, Fujimoto S, Yamamoto N: Potential role of NK cells in the induction of immune responses: implications for NK cell-based immunotherapy for cancers and viral infections. *Int Rev Immunol* 2008; 27:93–110.
54 Ljunggren HG: Cancer immunosurveillance: NKG2D breaks cover. *Immunity* 2008; 28:492–494.
55 Soman S, Korah PK, Jayanarayanan S, Mathew J, Paulose CS: Oxidative stress induced NMDA receptor alteration leads to spatial memory deficits in temporal lobe epilepsy: ameliorative effects of Withania somnifera and Withanolide A. *Neurochem Res* 2012; 37:1915–1927.
56 Salih HR, Antropius H, Gieseke F, Lutz SZ, Kanz L, Rammensee HG, Steinle A: Functional expression and release of ligands for the activating immunoreceptor NKG2D in leukemia. *Blood* 2003; 102:1389–1396.

© 2013 John Wiley & Sons Ltd

Cancer Research: April 15, 2012; Volume 72, Issue 8, Supplement 1
doi: 10.1158/1538-7445.AM2012-2455
Proceedings: AACR 103rd Annual Meeting 2012-- Mar 31-Apr 4, 2012; Chicago, IL
© 2012 American Association for Cancer Research

Poster Presentations - Imaging in Animal Models

Abstract 2455: Molecular targeted imaging of vascular endothelial growth factor receptor (VEGFR)-2 and anti-NMP autoantibodies detect ovarian tumor at early stage

Animesh Barua[1], Talha Qureshi[1], Pincas Bitterman[1], Janice M. Bahr[2], Sanjib Basu[1], Seby L. Edassery[1], and Jacques S. Abramowicz[1]

[1]Rush Univ. Medical Ctr., Chicago, IL

[2]University of Illinois, Urbana_Champaign, IL

Background: Although several serum markers of ovarian cancer (OVCA) have been suggested, none can detect OVCA at early stage specifically because of the lack of a corresponding marker in the ovary. Ovarian malignant cellular transformation is an early event followed by tumor-associated neoangiogenesis (TAN). Malignant cellular transformation results in shedding of nuclear matrix proteins (NMPs) in circulation and anti-NMP autoantibody production. VEGFR-2, an ovarian TAN marker, may also be an imaging marker for early OVCA detection. Thus VEGFR-2 in association with anti-NMP antibodies may constitute an early detection test for OVCA. Objectives: The goal of this study was to examine (i) whether VEGFR-2 targeted ultrasound imaging detects ovarian TAN vessels and (ii) whether the frequency of TAN vessels is associated with serum anti-NMP antibodies at early stage of OVCA in laying hens model of human OVCA. Materials and Methods: Mature White Leghorn laying hens with normal or low egg laying rates or no egg laying were scanned by transvaginal ultrasound before and after intravenous injection with VEGFR-2 targeted microbubbles. All images were archived and analyzed offline. Serum samples were collected, hens were euthanized, ovarian tissues were processed for paraffin or frozen sections and NMP extraction. Ovarian tumors were confirmed by gross morphology and routine histology. Sera were tested for anti-NMP antibodies and VEGFR-2 levels by immunoassay and 1- and 2D-Western blot (WB). The frequencies of VEGFR-2 expressing TAN vessels were determined by immunohistochemistry (IHC). Results: VEGFR-2 targeted microbubbles bounded with ovarian tumors and appeared as a ring of irregular shape on the ovarian surface. Compared with non-targeted, VEGFR-2 targeted imaging increased the visualization of TAN vessels remarkably. VEGFR-2 expressing TAN vessels confirmed targeted ultrasound imaging predictions. Serum levels of VEGFR-2 were higher in OVCA hens than in normal hens and associated with the frequencies of ovarian TAN vessels. None of the hens with normal egg laying rates was positive for anti-NMP antibodies. Immunoreactive tumor antigens (NMP) of 50-60kDa were detected by 2D-WB. The frequencies of VEGFR-2 expressing TAN vessels were higher in hens with serum anti-NMP antibodies than in normal hens. Conclusion: VEGFR-2 targeted ultrasound imaging enhanced the visualization of ovarian TAN vessels remarkably. The intensity of targeted imaging was associated with serum VEGFR-2 levels and anti-NMP antibodies. Thus, VEGFR-2 targeted imaging together in association with serum anti-NMP antibodies may improve OVCA detection at early stage. These results will form a foundation for a clinical study. Support: DOD-(OC0100192), Elmer and Sylvia Sramek Foundation, NCI-POCROC (P50 CA83636).

Citation Format: {Authors}. {Abstract title} [abstract]. In: Proceedings of the 103rd Annual Meeting of the American Association for Cancer Research; 2012 Mar 31-Apr 4; Chicago,

IL. Philadelphia (PA): AACR; Cancer Res 2012;72(8 Suppl):Abstract nr 2455. doi:1538-7445.AM2012-2455

Cancer Research: April 15, 2013; Volume 73, Issue 8, Supplement 1
doi: 10.1158/1538-7445.AM2013-4642
Proceedings: AACR 104th Annual Meeting 2013; Apr 6-10, 2013; Washington, DC
© 2013 American Association for Cancer Research

Poster Presentations - Biomarkers of Drug Response

Abstract 4642: GRP78 in association with VEGFR-2 detects early stage ovarian cancer.

Doungkamol Alongkronrusmee[1], Pincas Bitterman[1], Jacques S. Abramowicz[1], Janice M. Bahr[2], Sanjib Basu[1], Salvatore Grasso[1], Sameer Sharma[1], Jacob Rotmensch[1], and Animesh Barua[1]

[1]Rush University Medical Center, Chicago, IL;
[2]University of Illinois at Urbana-Champaign, Urbana-Champaign, IL.

Background: The lack of an effective early detection test makes ovarian cancer (OVCA) a fatal malignancy of women. Changes in cellular metabolic processes during ovarian malignant transformation lead to the endoplasmic reticular (ER) and mitochondrial stress. Glucose-regulated protein of 78kDa (GRP78) is a marker of ER stress. Tumor-associated ER stress causes relocalization of GRP78 from ER to cell surface with an increase in its serum levels. Secreted GRP78 also stimulates tumor associated neoangiogenesis (TAN). Vascular endothelial growth factor receptor-2 (VEGFR-2) is a marker of ovarian TAN. Thus GRP78 represents a marker of ovarian malignant transformation and in association with VEGFR-2 may constitute an early detection test for OVCA. However, information on OVCA related changes in GRP78 expression and its association with ovarian TAN is unknown.

Objectives: The goals of this study were to examine (i) whether GRP78 expression increases during malignant changes in the ovary and (ii) whether the frequency of TAN vessels is associated with ovarian tumor-associated GRP78 expression at early stage of OVCA in the laying hen, a spontaneous model of human OVCA.

Materials and Methods: 3-4 years old White Leghorn laying hens with normal (n=25) or ovarian tumors (n=30) were selected by contrast enhanced transvaginal ultrasound scanning. Serum samples were collected, hens were euthanized, and ovarian tissues were processed for routine histology or immunohistochemistry (IHC) and protein extraction. Ovarian tumors were confirmed by gross morphology and microscopy. Expression of GRP78 by ovarian malignant cells and VEGFR-2 by TAN vessels was determined by IHC. IHC observations were confirmed by immunoproteomic studies.

Results: As compared with normal ovaries (n=25), the intensity of GRP78 expression was significantly ($p<0.001$) higher in hens with early stage OVCA (n=12) and increased further in hens with late stage OVCA (n=18) ($p<0.05$). GRP78 expression was higher in hens with serous OVCA followed by endometrioid OVCA and was least in hens with mucinous and clear cell OVCA irrespective of their stages of OVCA. A band of approximately 80kDa was observed for GRP78 in all ovaries examined and the patterns of expression were similar to that of IHC. The frequency of VEGFR-2 expressing TAN vessels was significantly ($p<0.001$) higher in OVCA hens than in normal hens. Increase in the frequency of VEGFR-2 expressing TAN vessels was positively correlated with the intensity of GRP78 expression.

Conclusion: The results of this study suggest that increase in the GRP78 expression is associated with ovarian malignant transformation, and this enhanced expression may stimulate ovarian tumor-associated neoangiogenesis. Thus GRP78 in combination with VEGFR-2 may constitute an early detection test for OVCA. These results will constitute a foundation for a clinical study to establish an early detection test for OVCA. Support: DOD Award # W81XWH-11-1-0510.

Citation Format: Doungkamol Alongkronrusmee, Pincas Bitterman, Jacques S. Abramowicz, Janice M. Bahr, Sanjib Basu, Salvatore Grasso, Sameer Sharma, Jacob Rotmensch, Animesh Barua. GRP78 in association with VEGFR-2 detects early stage ovarian cancer. [abstract]. In: Proceedings of the 104th Annual Meeting of the American Association for Cancer Research; 2013 Apr 6-10; Washington, DC. Philadelphia (PA): AACR; Cancer Res 2013;73(8 Suppl):Abstract nr 4642. doi:10.1158/1538-7445.AM2013-4642

Animesh Barua

From: Konrad, Natalie [natalie.konrad@aacr.org]
Sent: Wednesday, August 21, 2013 1:29 PM
To: Animesh Barua
Subject: Advances in Ovarian Cancer Research: Poster Session A Notice

August 21, 2013

Poster Session Information: Advances in Ovarian Cancer Research: From Concept to Clinic conference
September 18-21, 2013, Miami, Florida

Temporary Abstract Number #136197_2
Title: Association of interleukin 16 with early metastasis of ovarian tumors

Dear Dr. Barua:

Your above-referenced abstract has been scheduled for presentation in a Poster Session at the Advances in Ovarian Cancer Research: From Concept to Clinic conference and will be published in the Program and Proceedings. Presentation information pertaining to your abstract is below:

Session Title: Poster Session A
Session Date and Start Time: Thursday, September 19, 4:30 p.m. – 6:30 p.m.
Session Location: Met Ballrooom 2-4, Met Ballroom 5-7
Poster Board Number: A64

Please note that poster boards are 4 feet high and 8 feet wide (122 cm. x 244 cm.). Pushpins will be available in the poster session room. Please set up your poster during the first coffee break on September 19 from 10:10 a.m. – 10:30 a.m. There will be additional viewing time from 12:30 p.m. – 7:00 p.m. Please remove your poster at 7:00 p.m. on Thursday, September 19. We are not responsible for unclaimed posters.

Posters must be placed on assigned boards. If you move your poster to another board, you may be marked as a no-show. If there is a problem with your assignment, please contact the AACR staff onsite. Presenters must stand by their posters for at least 90 minutes during the session. Please note that there is a light reception during this poster session.

For additional information about the conference, visit the conference home page:
www.aacr.org/page32086.aspx

PLEASE NOTE: The deadline for hotel reservations at the reduced conference rate is Monday, August 26. Room reservations may be made after the Monday, August 26 deadline, but they are subject to availability and group room rates are not guaranteed.

Housing Information
www.aacr.org/page32160.aspx

Abstract Reprinting
The AACR will be reprinting the printed Program and Proceedings from this conference as an online-only supplement to Clinical Cancer Research after the conference. The abstracts from the meeting will be searchable, freely available, and archived. We need to collect your permission to publish, use, and/or reuse your abstract. To grant or deny permission to reprint your abstract as it will appear in the printed Program and Proceedings book, please complete the one question

survey at the following link. Please note if you submitted 2 abstracts, you must do this for both abstracts. You will need to enter your abstract title which is included above:

Link: http://www.surveymonkey.com/s/Ovarian13

Thank you for your participation in the 2013 AACR Conference on Advances in Ovarian Cancer Research: From Concept to Clinic.

Sincerely,

Margaret Foti, Ph.D., M.D. (h.c.)
Chief Executive Officer
American Association for Cancer Research

PLEASE NOTE: This document is your **official notice** of acceptance and scheduling. No separate letter will be mailed.

Please note that this e-mail and any files transmitted with it may be privileged, confidential, and protected from disclosure under applicable law. This information is intended only for the person or entity to which it is addressed and may contain confidential or privileged material. Any review, retransmission, dissemination, or other use of, or taking of any action in reliance upon, this information by persons or entities other than the intended recipient is prohibited. If you received this in error, please contact the sender and delete the material from any computer.

Association of interleukin 16 with early metastasis of ovarian tumors

Aparna Yellapa, Pincas Bitterman, Jacques Abramowicz, Janice Bahr, Sameer Sharma, Sanjib Basu and Animesh Barua

Introduction: Ovarian cancer (OVCA) differs from other malignancies in its specific dissemination pattern that the tumor typically spreads in a diffuse intra-abdominal fashion rather than systemic circulation. Interactions among different cell types and their secretory products in the tumor microenvironment may contribute to the tumor development and metastasis. Interleukin 16 (IL-16) is a chemoattractant and pro-angiogenic cytokine involved in multiple immunopathobiological processes. IL-16 is expressed by several cell types including CD8 T cells and macrophages and occasionally by malignant cells. IL-16 expression is reported to be increased in several tumors including OVCA. Thus, IL-16 may be involved in the development and metastasis of ovarian tumors, if so, how IL-16 enhances tumor metastasis is not known. CD9, a member of tetraspanin family, has been implicated in the regulation of cell proliferation, invasion and motility. Emerging studies reported CD9 as a receptor for IL-16.

Objectives: The goal of this study was to determine (1) whether IL-16 is associated with ovarian tumor metastasis in the vicinity of tumors including the omentum and (2) if so, to determine how IL-16 is associated with ovarian tumor metastasis. In this study we examined association of IL-16 and its receptor (CD9) expression with respect to ovarian tumor development and progression. The association of CD8+T cells and IL-16 expression during tumor initiation was examined in laying hens, an animal model of spontaneous OVCA.

Methods: Experiment-1: Tumor specimen from patients with serous OVCA (10 early and 20 late stages), serous benign ovarian tumors (n=10) and normal (n=5, from patients underwent hysterectomies for non-ovarian disease) and omental tissues (n= 5, each of OVCA and benign) were used. Changes in IL-6 and CD9 expression in tumor tissues (ovaries and omentum) were examined by immunohistochemistry, proteomics and by quantitative polymerase chain reaction (qPCR). Experiment-II: Laying hens with normal ovaries (n=10) or microscopic OVCA (n=10) were examined for CD8 T cells and IL-16 expressing cells as mentioned above. The correlation between the IL-16 and CD8+ T cells were examined. In addition, to examine the effects of IL-16 on CD9 expression, normal ovarian surface epithelial (OSE) cells were treated with recombinant IL-16 protein.

Results: Compared with normal ovaries and benign tumors, the frequencies of IL-16 expressing cells were significantly high in early stage OVCA ($P<0.01$) and increased further in late stage OVCA. Compared with primary ovarian tumors, the population of IL-16 expressing cells was remarkably high in omental tissues containing tumor ($P<0.01$). Similarly, compared with normal, intense staining was observed for CD9 expression both in malignant ovarian and omental tissues. CD9 staining intensities were positively correlated with the increased frequency of IL-16

expressing cells. Recombinant IL-16 treatment of OSE enhanced CD9 expression suggesting the stimulatory effects of IL-16 on CD9 expression. Compared with normal hens, frequency of CD8+ T cells increased significantly in hens with microscopic OVCA. Similarly, compared with normal hens, the population of IL-16 expressing cells increased significantly in hens with microscopic OVCA. The frequency of IL-16 expressing cells was positively correlated with the frequency of CD8+ T cells.

Conclusions: The results of the present study suggest that increased IL-16 expression may be associated with enhanced CD9 expression which may be a factor for ovarian tumor progression and metastasis to the omental tissues. Increased CD8+ T cells in the tumor vicinity suggests that CD8+ T cells may be a source of enhanced IL-16 expression in developing ovarian tumors.

Support: DOD award # W81XWH-11-1-0510